

ผลของตัวกรองรังสีที่มีต่อปริมาณรังสีเฉลี่ยที่ตอม่านน้ำนมและคุณภาพของภาพ โดยเครื่องถ่ายภาพรังสี  
เต้านมระบบดิจิทัล



บทคัดย่อและแฟ้มข้อมูลฉบับเต็มของวิทยานิพนธ์ตั้งแต่ปีการศึกษา 2554 ที่ให้บริการในคลังปัญญาจุฬาฯ (CUIR)  
เป็นแฟ้มข้อมูลของนิสิตเจ้าของวิทยานิพนธ์ ที่ส่งผ่านทางบัณฑิตวิทยาลัย

The abstract and full text of theses from the academic year 2011 in Chulalongkorn University Intellectual Repository (CUIR)  
are the thesis authors' files submitted through the University Graduate School.

วิทยานิพนธ์นี้เป็นส่วนหนึ่งของการศึกษาตามหลักสูตรปริญญาวิทยาศาสตรมหาบัณฑิต  
สาขาวิชาอาชีวเวชศาสตร์ ภาควิชารังสีวิทยา  
คณะแพทยศาสตร์ จุฬาลงกรณ์มหาวิทยาลัย  
ปีการศึกษา 2559  
ลิขสิทธิ์ของจุฬาลงกรณ์มหาวิทยาลัย

Effect of filter on average glandular dose and image quality in digital mammography

Miss Chatsuda Songsaeng



A Thesis Submitted in Partial Fulfillment of the Requirements  
for the Degree of Master of Science Program in Medical Imaging  
Department of Radiology  
Faculty of Medicine  
Chulalongkorn University  
Academic Year 2016  
Copyright of Chulalongkorn University

Thesis Title	Effect of filter on average glandular dose and image quality in digital mammography
By	Miss Chatsuda Songsaeng
Field of Study	Medical Imaging
Thesis Advisor	Associate Professor Anchali Krisanachinda, Ph.D.

---

Accepted by the Faculty of Medicine, Chulalongkorn University in Partial Fulfillment of the Requirements for the Master's Degree

..... Dean of the Faculty of Medicine  
(Professor Suttipong Wacharasindhu, M.D.)

**THESIS COMMITTEE**

..... Chairman  
(Jenjeera Prueksadee, M.D.)

..... Thesis Advisor  
(Associate Professor Anchali Krisanachinda, Ph.D.)

..... External Examiner  
(Professor Franco Milano, Ph.D.)

ฉัตรสุดา ส่องแสง : ผลของตัวกรองรังสีที่มีต่อปริมาณรังสีเฉลี่ยที่ต่อมน้ำนมและคุณภาพของภาพ โดยเครื่องถ่ายภาพรังสีเต้านมระบบดิจิทัล (Effect of filter on average glandular dose and image quality in digital mammography) อ.ที่ปริกษาวิทยานิพนธ์หลัก: รศ. ดร.อัญชลี กฤษณจินดา, 104 หน้า.

จุดประสงค์หลักของการศึกษานี้ เพื่อศึกษาผลของตัวกรองรังสีที่มีต่อปริมาณรังสีเฉลี่ยที่ต่อมน้ำนมและคุณภาพของภาพโดยเครื่องถ่ายภาพรังสีเต้านมระบบดิจิทัล ในการศึกษาจะใช้หุ่นจำลองเต้านม ACR และ BR 12 ที่ความหนาต่างกัน เพื่อศึกษาปริมาณรังสีเฉลี่ยที่ต่อมน้ำนมและคุณภาพของภาพโดยศึกษาค่าอัตราส่วนความคมชัดต่อสัญญาณรบกวน(CNR) และค่าอัตราส่วนสัญญาณจริงต่อสัญญาณรบกวน(SNR) ในตัวกรองรังสีต่างชนิดกัน การศึกษานี้จะเก็บข้อมูลย้อนหลังจากผู้ป่วยที่เข้ารับการถ่ายภาพรังสีเต้านมจำนวน 200 คนแบ่งเป็นผู้ป่วยที่ถ่ายภาพรังสีเต้านมที่ใช้เป่าหลอดที่ทำด้วยทั้งสแตนเลสและฟิลเตอร์ชนิดโรเดียมจำนวน 100 คน และผู้ป่วยที่ถ่ายภาพรังสีเต้านมที่ใช้เป่าหลอดที่ทำด้วยทั้งสแตนเลสและฟิลเตอร์ชนิดซิลเวอร์จำนวน 100 คน ในปัจจัยต่างๆได้แก่ ความหนาของเต้านมที่บีบอัด แรงแบบบีบอัด ปริมาณรังสีเฉลี่ยที่ต่อมน้ำนม ค่ากิโลโวลต์สูงสุด ค่ามิลลิแอมแปร์วินาที ทำการบันทึกข้อมูลและเปรียบเทียบระหว่างฟิลเตอร์สองชนิด ผลการทดลองในหุ่นจำลองพบว่า ที่ความหนาที่เท่ากัน เมื่อใช้ระบบเออีซี การเพิ่มค่า กิโลโวลต์จะทำให้ค่า CNR และ SNR ลดลง แต่เมื่อใช้ค่าที่ตั้งเอง เมื่อค่า กิโลโวลต์คงที่ และเพิ่มค่ามิลลิแอมแปร์วินาที ค่า CNR และ SNR จะเพิ่มขึ้น ผลการศึกษาจะสอดคล้องกันทั้งตัวกรองรังสี สองชนิด โรเดียม และซิลเวอร์ ผลการทดลองในผู้ป่วยพบว่า ปริมาณรังสีเฉลี่ยที่ต่อมน้ำนมของเป่าหลอดที่ทำด้วยทั้งสแตนเลสและฟิลเตอร์ชนิดโรเดียมมีค่าเท่ากับ 1.26 มิลลิเกรย์ ค่าเฉลี่ยของความหนาของเต้านมที่บีบอัด มีค่าเท่ากับ 54.18 มิลลิเมตร ค่าเฉลี่ยของแรงแบบบีบอัดมีค่าเท่ากับ 13.24 ปอนด์ ค่าเฉลี่ยกิโลโวลต์เท่ากับ 29.68 ค่าเฉลี่ยของมิลลิแอมแปร์วินาทีที่มีค่าเท่ากับ 106.75 ปริมาณรังสีเฉลี่ยที่ต่อมน้ำนมของเป่าหลอดที่ทำด้วยทั้งสแตนเลสและฟิลเตอร์ชนิดซิลเวอร์มีค่าเท่ากับ 1.79 มิลลิเกรย์ ค่าเฉลี่ยของความหนาของเต้านมที่บีบอัด มีค่าเท่ากับ 81 มิลลิเมตร ค่าเฉลี่ยของแรงแบบบีบอัดมีค่าเท่ากับ 14.15 ปอนด์ ค่าเฉลี่ยของกิโลโวลต์เท่ากับ 31.79 ค่าเฉลี่ยของมิลลิแอมแปร์วินาทีที่มีค่าเท่ากับ 113.34 สรุปผลการทดลองในหุ่นจำลอง จะให้ปริมาณรังสีเฉลี่ยอยู่ในช่วง 0.82 ถึง 1.15 มิลลิเกรย์ เป่าหลอดที่ทำด้วยทั้งสแตนเลสและฟิลเตอร์ชนิดซิลเวอร์ โดยจะให้ปริมาณรังสีเฉลี่ยที่ต่อมน้ำนมอยู่ในช่วง 1.28 ถึง 2.97 มิลลิเกรย์ สำหรับความหนาของเต้านมตั้งแต่ 40 ถึง 60 มิลลิเมตรควรเลือกใช้เป่าหลอดที่ทำด้วยทั้งสแตนเลสและฟิลเตอร์ชนิดโรเดียมและสำหรับความหนาของเต้านมที่มีค่ามากกว่า 70 มิลลิเมตร ควรเลือกใช้เป่าหลอดที่ทำด้วยทั้งสแตนเลสและฟิลเตอร์ชนิดซิลเวอร์เพื่อลดปริมาณรังสีให้แก่ผู้ป่วยและคงคุณภาพของภาพที่ดี สรุปผลการทดลองของผู้ป่วย ในโรงพยาบาลจุฬาลงกรณ์สภากาชาดไทย ในปี 2559 ถึง 2560 พบว่าปริมาณรังสีเฉลี่ยที่ต่อมน้ำนมของเป่าหลอดที่ทำด้วยทั้งสแตนเลสและฟิลเตอร์ชนิดโรเดียมมีค่าเท่ากับ 1.26 มิลลิเกรย์ ที่ความหนาเฉลี่ยของเต้านม 54.18 มิลลิเมตร ปริมาณรังสีเฉลี่ยที่ต่อมน้ำนมของเป่าหลอดที่ทำด้วยทั้งสแตนเลสและฟิลเตอร์ชนิดซิลเวอร์มีค่าเท่ากับ 1.79 มิลลิเกรย์ ที่ความหนาเฉลี่ยของเต้านม 81 มิลลิเมตร ในการศึกษาพบว่าผู้ป่วยที่เข้ารับการถ่ายภาพรังสีเต้านม ได้รับปริมาณรังสีเกินปริมาณรังสีอ้างอิง 3 มิลลิเกรย์ คิดเป็น 2.5%

ภาควิชา รังสีวิทยา

ลายมือชื่อนิสิต .....

สาขาวิชา ฉายาเวชศาสตร์

ลายมือชื่อ อ.ที่ปรึกษาหลัก .....

ปีการศึกษา 2559

# # 5974114330 : MAJOR MEDICAL IMAGING

KEYWORDS: DIGITAL MAMMOGRAPHY / AVERAGE GLANDULAR DOSE / TUNGSTEN RHODIUM TARGET FILTER / TUNGSTEN SILVER TARGET FILTER

CHATSUDA SONGSAENG: Effect of filter on average glandular dose and image quality in digital mammography. ADVISOR: ASSOC. PROF. ANCHALI KRISANACHINDA, Ph.D., 104 pp.

The purpose of this study is to determine the average glandular dose, AGD and the image quality in phantom and patient for different target-filters (W/Rh and W/Ag) of the digital mammography system. The ACR mammography phantom and BR 12 phantom were used to determine the AGD and the image quality, the contrast to noise ratio (CNR) and the signal to noise ratio (SNR) of various target filters in different phantom thickness. A retrospective mammography study includes 200 patients which 100 patients were examined using the W/Rh target-filter and 100 different patients using W/Ag target-filter. The compressed breast thickness (CBT, mm), compression force (lbs), average glandular dose (AGD, mGy), peak kilovoltage (kVp) and tube current time (mAs) were recorded and compared between W/Rh and W/Ag target. The result in the phantom study, at the same thickness, the CNR and SNR values were decreased with increasing tube voltages in AEC technique. At the manual technique, when the tube voltage was constant and tube current time was increasing, CNR and SNR were increased. This was agreeable for both W/Rh and W/Ag target-filters. In patient study, the mean AGD, CBT, CF, kVp, mAs of W/Rh were 1.26 mGy, 54.18 mm, 13.24 lbs., 29.68 and 106.75 respectively in CC view. The mean AGD, CBT, CF, kVp, mAs of W/Ag was 1.79 mGy, 81 mm, 14.15 lbs., 31.79 and 113.34 respectively. At 40 mm CBT, the optimal tube output for W/Rh range from 27 to 29 kVp and mAs range from 58 to 129, the AGD range from 0.82 to 1.15 mGy. The optimal tube output for W/Ag range from 30 to 35 kVp and mAs range from 145 to 200, the AGD range from 1.28 to 2.97 mGy. For compress breast thickness range from 40 mm to 60 mm, the W/Rh target-filter should be chosen and the CBT greater than 70 mm, the W/Ag target-filter is appropriate in order to compensation between good image quality and dose reduction. Conclusion in patient study, the determination of patient dose in King Chulalongkorn Memorial Hospital in 2016-2017 revealed that the mean AGD was 1.26 mGy, the mean CBT was 54.18 mm for W/Rh. The mean AGD was 1.79 mGy, the mean CBT was 81 mm for W/Ag. In our study, 2.5% of the patients received the average glandular dose over the diagnostic reference level of 3 mGy per view.

Department: Radiology

Student's Signature .....

Field of Study: Medical Imaging

Advisor's Signature .....

Academic Year: 2016

## ACKNOWLEDGEMENTS

I would like to greatly thank Associate Professor Anchali Krisanachinda, Ph.D., Department of Radiology, Faculty of Medicine, Chulalongkorn University, my advisor for her support, instruction, care and polish my English language in this research.

I would like to greatly thank Associate Professor Sivalee Suriyapee, Department of Radiology, Faculty of Medicine, Chulalongkorn University, my teacher for her advice and comments in the research.

My sincere thanks to Professor Franco Milano, who is the external examiner of the thesis, for his help in the experiment, kind suggestion, constructive comments in the experiments and English language improvement in this research.

I would like to deeply thank Jenjeera Prueksadee, M.D., Department of Radiology, Faculty of Medicine, Chulalongkorn University for her advice and comment in the research.

I would like to thank the staff at Breast Imaging Center, Department of Radiology, King Chulalongkorn Memorial Hospital for their helps in data collection.

I am thankful for all teachers, lecturers and staff in the Master of Science Program in Medical Imaging, Faculty of Medicine, Chulalongkorn University for their unlimited teaching of knowledge in Medical Imaging.

Finally, this is dedicated to my father and mother, Arun and Sunee Songsaeng for the moral and spiritual compass instilled me.

## CONTENTS

	Page
THAI ABSTRACT .....	iv
ENGLISH ABSTRACT.....	v
ACKNOWLEDGEMENTS.....	vi
CONTENTS.....	vii
LIST OF TABLES .....	x
LIST OF ABBREVIATIONS.....	xv
CHAPTER 1 .....	1
INTRODUCTION .....	1
1.1 Background and rationale.....	1
1.1.1 Theory .....	1
1.1.2 Breast cancer .....	2
1.1.3 Breast dosimetry.....	4
1.1.4 Mammography .....	5
1.1.5 Image quality in digital mammography. ....	7
1.2 Research objectives .....	7
CHAPTER 2 .....	8
LITERATURE REVIEW .....	8
CHAPTER 3 .....	15
RESEARCH METHODOLOGY.....	15
3.1 Research design .....	15
3.2 Research question .....	15
3.3 Research Design Model.....	15
3.4 Conceptual framework.....	16
3.5 The Sample .....	17
3.5.1 Target population .....	17
3.5.1.1 Inclusion criteria.....	17
3.5.1.2 Exclusion criteria.....	17
3.5.2 Sample population.....	17

	Page
3.5.3 Sample .....	17
3.6 Materials .....	18
3.7 Methods .....	22
3.7.1 Phantom study .....	22
3.7.2 Patients study.....	25
3.8 Sample size .....	25
3.9 Measurement Variable.....	26
3.10 Statistical analysis.....	26
3.11 Data Collection .....	26
3.12 Data analysis .....	27
3.13 Outcome.....	27
3.14 Expected benefits and application .....	27
3.15 Ethic consideration .....	28
CHAPTER 4 .....	29
RESULTS .....	29
4.1 Image quality evaluation: the phantom study .....	29
4.1.1 Image quality evaluation for different thickness of mammography phantom.....	29
4.2 Patient information and technique factor.....	42
CHAPTER5 .....	75
DISCUSSION AND CONCLUSION .....	75
5.1 Discussion.....	75
5.1.1 Image quality evaluation: the phantom study.....	75
5.1.1.1 Image quality evaluation for different thickness of mammography phantom.....	75
5.1.1.2 The average glandular dose in phantom study .....	76
5.1.2 The patient study: .....	76
5.1.3 The optimization of the dose and image quality; .....	77
5.2 Conclusion .....	78



	Page
5.3 Limitations.....	79
APPENDICES .....	80
REFERENCES .....	102
VITA.....	104



## LIST OF TABLES

Table	Pages
<b>4. 1</b> The CNR, SNR and AGD using W/Rh target-filter in phantom of different thickness when varying kVp for AEC technique. ....	30
<b>4. 2</b> The CNR, SNR and AGD using W/Rh target-filter in phantom of different thickness when increasing kVp, mAs for manual technique.....	30
<b>4. 3</b> The CNR, SNR and AGD using W/Ag target-filter in phantom of various thicknesses when varying kVp for AEC technique. ....	31
<b>4. 4</b> The CNR, SNR and AGD using W/Ag target-filter in phantom of different thickness when varying kVp, mAs for manual technique. ....	31
<b>4. 5</b> The scatter plot shows the correlation between the AGD and mAs ( $R^2 = 0.98$ ) of patient study in W/Rh.....	43
<b>4. 6</b> The scatter plot shows the correlation between the AGD and mAs ( $R^2 = 0.89$ ) of patient study in W/Ag.....	44
<b>4. 7</b> The parameters of W/Rh in 100 patients in right cranio-caudal view (RCC).....	45
<b>4. 8</b> The parameters of W/Rh in 100 patients in right medio-lateral view (RMLO). ....	48
<b>4. 9</b> The parameters of W/Rh in 100 patients in left .....	51
<b>4. 10</b> The parameters of W/Rh in 100 patients in left medio-lateral view (LMLO).....	54

<b>4. 11</b> The parameters of W/Ag in 100 patients in right cranio-caudal view (RCC).....	57
<b>4. 12</b> The parameters of W/Ag in 100 patients in right medio-lateral view (RMLO).....	60
<b>4. 13</b> The parameters of W/Ag in 100 patients in left cranio-caudal view (LCC).....	63
<b>4. 14</b> The parameters of W/Ag in 100 patients in left medio-lateral view (LMLO).....	66



## LIST OF FIGURES

<b>Figure</b>	<b>Page</b>
1. 1 The female breast structure[1] .....	2
1. 2 The breast structures showing cancer starting from cells of the breast [1] .....	3
1. 3 Spectra of Mo/Mo (30 $\mu$ m), Mo/Rh (25 $\mu$ m), W/Rh (50 $\mu$ m), and W/Ag (50 $\mu$ m) at 28kVp.....	6
3. 1 The research design model. ....	15
3. 2 The framework.....	16
3. 3 The framework.....	16
3. 4 Digital Mammography system: Hologic Selenia dimension.....	18
3. 5 Mammography phantom image Quality Evaluation: ACR breast phantom model RMI 156.....	19
3. 6 Location of the test objects in the RMI 156 breast phantom .....	20
3. 7 Phantom BR12, 1 and 2 cm thickness .....	21
3. 8 ACR phantom 4 cm thickness in CC view.....	23
3. 9 ACR and BR12 phantom 5 cm thickness in CC view.....	23
3. 10 ACR and BR12 phantom 6 cm thickness in CC view.....	23
3. 11 ACR and BR12 phantom 7 cm thickness in CC view.....	24

<b>Figure</b>	<b>Page</b>
<b>4. 1</b> The CNR in ACR and BR12 phantoms when varying kVp in W/Rh for AEC technique .....	32
<b>4. 2</b> The CNR in ACR and BR12 phantoms when varying kVp for W/Ag in AEC technique.....	32
<b>4. 3</b> The SNR in ACR and BR12 phantoms when varying kVp for W/Rh in AEC technique .....	33
<b>4. 4</b> The SNR in ACR and BR12 phantoms when varying kVp for W/Ag in AEC technique.....	33
<b>4. 5</b> The CNR vs mAs in ACR and BR12 phantoms for W/Rh in AEC technique.....	34
<b>4. 6</b> The CNR vs mAs in ACR and BR12 phantoms when varying phantom thickness for W/Ag in AEC technique. ....	34
<b>4. 7</b> The SNR vs mAs in ACR and BR12 phantoms when varying thickness for W/Rh in AEC technique.....	35
<b>4. 8</b> The SNR vs mAs in ACR and BR12 phantoms when varying thickness for W/Ag in AEC technique. ....	35
<b>4. 9</b> The CNR in ACR and BR12 phantoms when varying mAs for W/Rh in manual technique .....	36
<b>4. 10</b> The CNR in ACR and BR12 phantoms when varying mAs for W/Ag in manual technique .....	36
<b>4. 11</b> The SNR in ACR and BR12 phantoms when varying mAs for W/Rh in manual technique .....	37

<b>4. 12</b> The SNR in ACR and BR12 phantoms when varying mAs for W/Ag in manual technique. ....	37
<b>4. 13</b> The AGD in ACR and BR12 phantoms when varying kVp for W/Rh in AEC technique. ....	38
<b>4. 14</b> The AGD in ACR and BR12 phantoms when varying kVp .....	39
<b>4. 15</b> The AGD vs mAs in ACR and BR12 phantoms when varying thickness for W/Rh in AEC technique. ....	39
<b>4. 16</b> The AGD vs mAs in ACR and BR12 phantoms when varying thickness for W/Ag in AEC technique. ....	40
<b>4. 17</b> The AGD in ACR and BR12 phantoms when varying mAs for W/Rh in manual technique .....	40
<b>4. 18</b> The AGD in ACR and BR12 phantoms when varying mAs for W/Ag in manual technique .....	41

## LIST OF ABBREVIATIONS

<b>Abbreviation</b>	<b>Terms</b>
ACR	The American College of Radiology
AEC	Automatic Exposure Control
Ag	Silver
AGD	Average Glandular Dose
ALARA	As Low As Reasonably Achievable
BRCA	Breast Cancer
CBT	Compressed Breast Thickness
CC	Cranio Caudal
CF	Compression Force
cm	Centimeter
DICOM	Digital Imaging Communications in Medicine
ESAK	Entrance Surface Air Kerma
ESD	Entrance Skin Dose
ESE	Entrance Skin Exposure
FDA	Food and Drug Administration
FFDM	Full Field Digital Mammography
HVL	Half-Value Layer
lbs.	Pounds
ICRU	International Commission on Radiation Units and Measurements
Ka	Air kerma
kVp	Kilo-voltage peak
LCIS	Lobular carcinoma in situ
mAs	Milliamperere seconds
MGD	Mean Glandular Dose
mGy	Milligray
MLO	Mediolateral Oblique
mm	Millimeter
Mo	Molybdenum
MQSA	Mammography Quality Standard Act
mrad	Millirad
MTF	Modulation Transfer Function

<b>Abbreviation</b>	<b>Terms</b>
NCI	National Cancer Institute
N	Newton
PMMA	Polymethylmethacrylate
QA	Quality Assurance
QC	Quality Control
R	Roentgen
Rh	Rhodium
S	Second
SD	Standard deviation
SID	Source to Image Distance
SPSS	Statistical Package for the Social Sciences
TEC	Tissue Exposure Control
TLD	Thermoluminescent Dosimeter
W	Tungsten



# CHAPTER 1

## INTRODUCTION

### 1.1 Background and rationale

Breast cancer remains a leading cause of cancer death among women in many parts of the world. No one knows the exact causes of the breast cancer. Today, breast cancer, like other forms of cancer, is considered to be a result of damage to DNA. This mechanism may occur from several known or hypothesized factors such as exposure to ionizing radiation, or viral mutagenesis. Some factors lead to an increased rate of mutation (exposure to estrogens) and decreased repair genes.

Mammography is the most effective method to produce a high sensitivity image, based on x-ray attenuated through the image receptor and absorbed as a latent image on the recording devices. Most standard mammography includes two views per breast, the craniocaudal (CC) and mediolateral oblique (MLO) views. Mammography requires the highest quality of imaging techniques and the finest detail over a wide spectrum of object contrast in order to successfully identify cancer growth in their stages of development. The estimation of the absorbed dose to the breast is an important part of the quality control of the mammographic examination. Minimizing radiation risk is important in general as manifested by (ALARA) principle. Radiation risk is a factor in the benefit-risk ratio of mammography. To quantify the risk from radiation in mammography, the average glandular dose (AGD) is used. AGD is determined. The Food and Drug Administration (FDA), American College of Radiologist (ACR) and Mammography Quality Standards Act (MQSA) have established the limit for AGD in order to minimize the risk to the glandular tissue.

#### 1.1.1 Theory

##### 1.1.1.1 The breasts

The breasts sit on the chest muscles that cover the ribs. Each breast is made of 15 to 20 lobes, which contain many smaller lobes. Lobules contain groups of tiny glands that can produce milk. Milk flows from the lobules through thin tubes called ducts to nipple. The nipple is in the

center of dark area of skin called duct of nipple. The nipple is in the center of a dark area of skin called the areola. Fat fills the spaces between the lobules and ducts as shown in Figure 1.1

The breasts also contain lymph vessels lead to small, round organs called lymph nodes. Groups of lymph nodes are near the breast in the axilla, above the collarbone, in the chest behind the breastbone, and in many other parts of body. The lymph nodes trap bacteria, cancer cells, or other harmful substances.

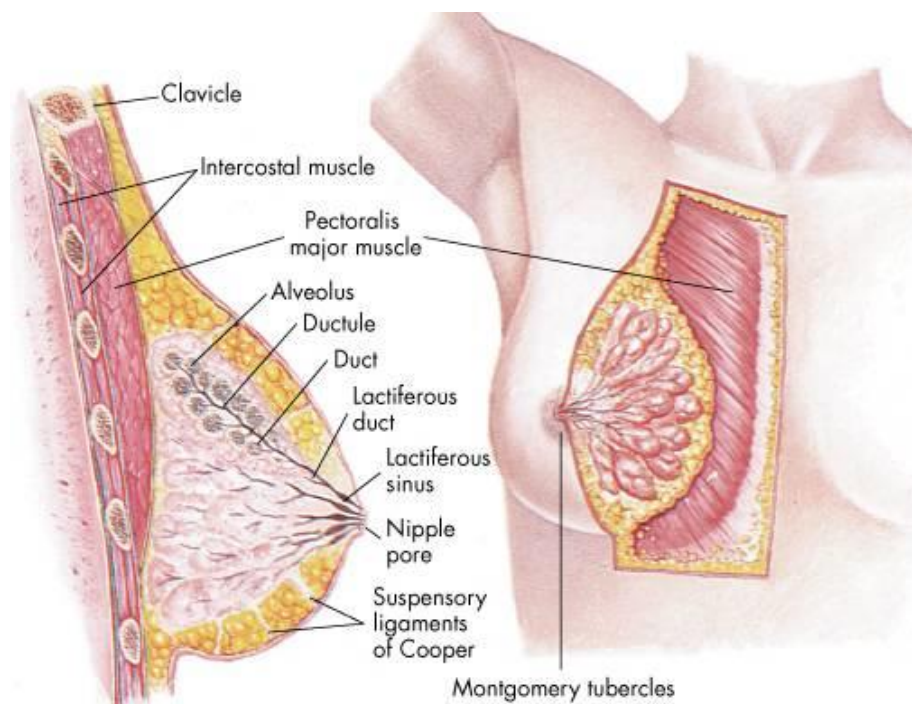


**Figure1. 1** The female breast structure[1]

### 1.1.2 Breast cancer

Breast cancer is a malignant tumor that starts from cells of the breast. The disease occurs mostly in the women, but men can get breast cancer too. Most breast cancers begin in the cells that line the ducts (ductal cancer), some begin in the lobules (lobular cancer), and the rest in other tissues as shown in Figure 1.2.

If the breast cancer cells reach the underarm lymph nodes and continue to grow, they cause the nodes swell. Once cancer cells have reached these nodes they are more likely spreading to other organs of the body such as bones, liver, lung and brain.

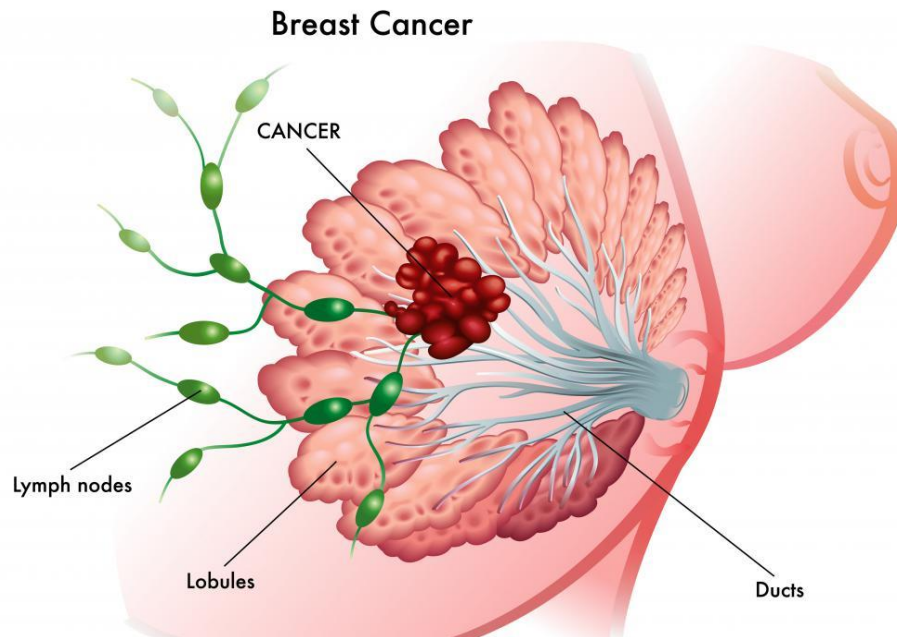


**Figure1. 2** The breast structures showing cancer starting from cells of the breast [1]

#### 1.1.2.1 Symptoms

Early breast cancer can in some cases be painful. Usually breast cancer is discovered before any symptoms are present, either on mammography or by feeling a breast lump. A lump under the arm or above the collarbone that does not go away may be present. Other possible symptoms include breast discharge, nipple inversion and changes in the skin overlying the breast.

#### 1.1.2.2 Diagnosis

The diagnosis of breast cancer is established by the pathological examination of removed breast tissue. Such tissue is generally obtained at the time of surgical treatment. A number of procedures have been devised to obtain tissue or cells prior to the treatment for histological or cytological examination. Such procedures include fine-needle aspiration, nipples aspirates, ductal lavage, core needle biopsy, and local surgical biopsy. Most of these diagnostic steps, however, have some limitations as they may not yield enough tissue or miss the cancer, while the surgical biopsy already becomes an invasive procedure. Imaging tests are used to detect metastasis and include chest x-ray, bone scan, CT, MRI, and PET scanning. Carbohydrate antigen 15.3, Ca 15.3 epithelial mucin is a tumor marker determined in blood test, which can be used to follow up disease activity.

### 1.1.2.3 Treatment

The mainstay of breast cancer treatment is surgery when the tumor is localized, with possible adjuvant hormonal therapy (with tamoxifen or an aromatase inhibitor), chemotherapy, and/or radiotherapy. At present, the treatment recommendations after surgery (adjuvant therapy) follow a pattern, which may be adapted as every two years a worldwide conference takes place in St. Gallen, Switzerland to discuss the actual results of worldwide multi center studies. Depending on clinical criteria, age, type of cancer, size, metastasis, the patients are roughly divided according to the high risk and the low risk cases, which follow different rules for therapy. Treatment possibilities include Radiation Therapy, Chemotherapy, Hormone Therapy, and Immune Therapy.

### 1.1.3 Breast dosimetry

#### 1.1.3.1 Average Glandular dose (AGD) [2]

AGD is a universal term used in the field of diagnostic breast imaging that provides a means of characterizing the carcinogenic risk associated with diagnostic mammograms. This term represents the average absorbed radiation dose to the most radiosensitive tissues (glandular tissues) of the female breast. The AGD to the female breast from diagnostic mammograms is contingent on properties and qualities of both the x-ray beam and the breast tissue itself. The two most important characteristics of the breast tissue are the thickness of the breast and the tissue composition of the breast. Glandular breast tissues are more susceptible to radiation induce carcinogenesis than adipose and skin tissue. Additionally, it takes more x-ray exposure to penetrate denser (glandular) breast tissue than fatty (adipose) breast tissue and more exposure to penetrate a thicker breast than thinner breast. The characteristics of x-ray beam also influence the absorbed dose to breast tissue. The x-ray beam characteristics that are of particular importance to AGD determination are the beam quality (HVL) and the target materials (anode) of the x-ray tube. The HVL is the indirect measure of the energies of the photons from the x-ray beam and is determined by the amount of material required to reduce the x-ray beam intensity by 50%. Both of these properties are important in the determination of AGD, because both influence the energy spectrum of the photons in the mammography beam. The estimation of the absorbed dose to the breast is an important part of the quality control of the mammography examination. Knowledge of breast dose is essential for the design and

performance assessment of mammographic imaging systems. The approved ACR methodology for AGD determination entails a direct measurement of collisional air Kerma ( $K_a$ ) and its conversion to absorbed dose through the use of calculated conversion factors.

It is also possible to measure the average glandular [3] doses for a series of breast examinations on each mammography system. To do this, the breast thickness under compression is measured, and the tube voltage, and tube loading delivered are recorded. From a knowledge of the output of the X-ray set for the kV and target and filter material used, this tube loading may be used to estimate average glandular dose using the following formula:

$$D = Kgcs$$

Where;

$K$  = the entrance surface air kerma calculated (in the absence of scatter) at the upper surface of the breast.

$g$  = the factor corresponds to a glandularity of 50% [AppendixA].

$c$  = the factor corrects for any difference in breast composition from 50% glandularity [AppendixA].

$s$  = the factor  $s$  corrects for differences due to the choice of X-ray spectrum as noted earlier [AppendixA].

#### 1.1.4 Mammography

Mammography is the process of using low-dose X-ray to examine the human breast. It is used as a diagnostic as well as screening tool. Goal of mammography is early detection of breast cancer, typically through detection of characteristic of the masses and micro-calcifications. Mammography is believed to reduce mortality of breast cancer.

The risk of breast cancer for asymptomatic women under 35 years is not high enough to warrant the risk of radiation exposure. For this reason, and because the radiation sensitivity of breast in women under 35 years is possibly greater than that older women, screening mammography is not recommended in women under 40 years old. However, if there is a significant risk of cancer in particular patient, mammography may still be important. In 2003, molybdenum target and molybdenum or rhodium filters were designed. Currently, tungsten-rhodium and tungsten-silver target-filters were used in the last development, resulting in reduction of

the average glandular dose and the entrance surface air kerma. Spectrum suit for various breast thicknesses

Optimal energy band and breast thickness

- 14-18 keV 2 cm
- 17-21 keV 4 cm
- 19-23 keV 6 cm
- 20.5-23.5 keV 8 cm

K-edge Rhodium

- 20.2 - 22.8 keV.

The characteristics of the new digital detectors use anode filter combinations W/Rh, W/Ag which has some advantages for imaging dense or thick breasts. The breast doses associated with these combinations (Rh/Rh, W/Rh, W/Ag, W/Al) are lower than those delivered with Mo/Mo or Mo/Rh (reduce the dose values above 20%) (Young 2006, Dance 2000, Riabi 2010). The threshold value for breast thickness where the spectrum changed depends on the AEC calibration. The correct selection of the X-ray beam will strongly influence the dose and image quality.

Typical x-ray spectrum are reported in figure 1.3

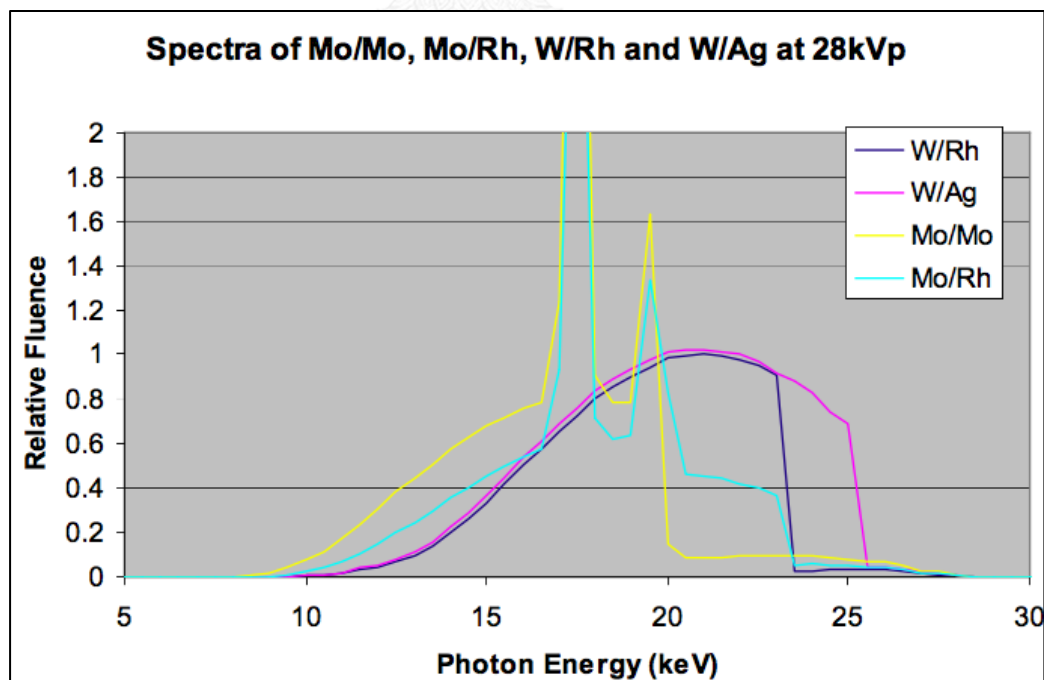


**Figure1. 3** Spectra of Mo/Mo (30 $\mu$ m), Mo/Rh (25 $\mu$ m), W/Rh (50 $\mu$ m), and W/Ag (50 $\mu$ m) at 28kVp[3]

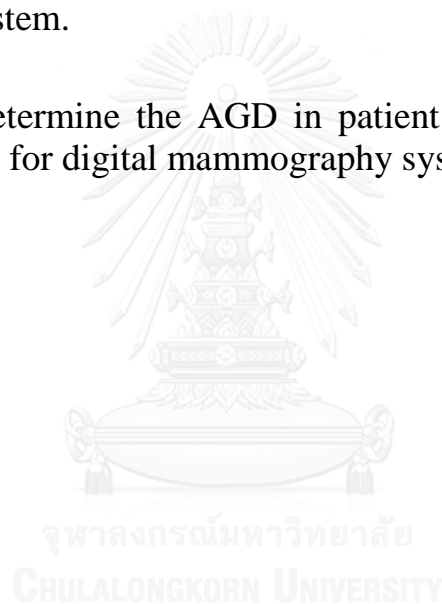
### 1.1.5 Image quality in digital mammography.

It aims to improve the early detection of cancer and other pathological lesions in the breasts. The image quality can be quantified by measuring the contrast noise ratio and the signal noise ratio. In order to assess the image quality, phantoms are needed to optimize the dose and image quality.

## 1.2 Research objectives

1.2.1 To determine the AGD and image quality (SNR, CNR) in phantom at different target filters (W/Rh and W/Ag) for digital mammography system.

1.2.2 To determine the AGD in patient at different target filters (W/Rh and W/Ag) for digital mammography system.



## CHAPTER 2

### LITERATURE REVIEW

#### 2. Literature review

Many researchers studied about the average of glandular dose and effect of reduced radiation dose in digital mammography.

In 2002, Hermann KP, et al. [4] Determined of average glandular dose with a full-field digital mammography system using a flat-panel X-ray detector based on amorphous silicon technology for a large group of patients. The number of women was 591 and only cranio-caudal projections were considered. Various quantities, including entrance surface air kerma, tube loading, and compressed breast thickness, were determined during actual mammography. The average glandular dose was average 1.51 mGy, compressed breast thickness was 55.7 mm, and the average age of patients was 55 years. The Rh anode with the Rh filter was the most common anode/filter combination selected by the automatic exposure control. The Mo anode was selected for 16.4 % of all exposures. The Mo filter was selected for 3.9 % and for 12.5 % with the Rh filter. The Rh filter has the highest relative frequency (%). The results demonstrate that full-field digital mammography with a flat-panel detector based on amorphous silicon needs about 25 % less dose in comparison with conventional screen-film mammography.

In 2011, Samei E, et al. [5] determined the relationship between radiation dose and observer accuracy in the detection and discrimination of simulated lesions for digital mammography. Three hundred normal cranio-caudal (CC) images were selected from digital mammograms. To simulate effects of reducing the radiation dose to one half and one quarter of the clinical dose. Images were read by five experienced breast-imaging radiologists. Determine effects of reduced dose from detection of micro calcifications and masses, discrimination between benign and malignant masses, and interpretation time. These findings suggest that dose reduction in digital mammography has a measurable but modest effect on diagnostic accuracy. The small magnitude of the effect in response to the drastic reduction of dose suggests potential for modest dose reductions in



digital mammography. Both studies demonstrate the methods to optimize the mammography dose. One simple method is the use of high atomic number target of tungsten and rhodium silver filter materials in an x-ray tube with the advantage of short exposure time, better contrast and dose reduction.

In 2010, Baldelli P, et al. [6] studied on 'Investigation of the effect of anode/filter materials on the dose and image quality of a digital mammography system based on an amorphous selenium flat panel detector'. A comparison, in terms of image quality and glandular breast dose, was carried out between two similar digital mammography systems using amorphous selenium flat panel detectors. The two digital mammography systems currently available from Lorad - Hologic were compared. The original system used Mo/Mo and Mo/Rh as target/filter combinations, while the new system uses W/Rh and W/Ag. Images of multiple mammography phantoms with simulated compressed breast thicknesses of 4 cm, 5 cm and 6 cm and various glandular tissue equivalence were acquired under different spectral conditions. Results show that the W/Rh combination is the best choice for all the detection tasks studied, but for thicknesses greater than 6 cm the W/Ag combination would probably be the best choice. In addition, the new system with W filter presents a better optimization of the automatic exposure control in comparison with the original system with Mo filter.

In 2011, Emanuelli S. [7] et al studied about the dosimetric and image quality comparison of two digital mammography units with different target/filter combinations: Mo/Mo, Mo/Rh, W/Rh, W/Ag. To allocate a digital mammography unit to the screening program on the basis of the ALARA radiation protection principle. Two Hologic Selenia mammography units were studied: one with a molybdenum anode (Mo/Mo, Mo/Rh) and the other with a tungsten anode (W/Rh, W/Ag). Exposed a polymethyl-methacrylate (PMMA) phantom to the two mammography units and recorded the exposure parameters used by them. Dosimetric assessments of exposure data were recorded from the mammographic examinations of approximately 400 women (1,600 exposures). Result show that the unit with the tungsten anode achieved a lower patient dose. As a result, the Selenia W device was allocated to the breast screening program.

In 1999, DR. Dance, et al [8] discussed the estimation of breast dose during a diagnostic mammogram. They suggested that dose measurements be quantified by using thermoluminescent dosimeters (TLD) placed on the breast or by correlating patient dose with machine exposure parameters. They described that a major pitfall could be the position of the ionization chamber, because the position could cause a variation in the estimate of mean glandular dose by 12%. They suggested that machine output be measured during the annual medical physics survey to give an indication of the stability of the mammography unit. In discussing TLD use, they suggested that placement would have to be such that it would not interfere with the clinical image. The other drawback to using a TLD on a patient is the obvious processing time and quality control needed to provide an accurate measurement. The authors also discussed the strong dependence of the TLD with the dosimeter thickness at low energies. At the end of the article, the authors reviewed the national protocols in Europe and the United States and concluded that, because of the variation in protocols, it was hard to compare them. They reported that the European protocols called for 1.0-1.5 background optical density (OD) in mammograms, whereas the United States and United Kingdom called for 1.4-1.8 OD. Dance et al. suggested that there was a need for an international consensus protocol.

In 2015, Biegala M, et al [3] studied about the effect of anode/filter combination on average glandular dose in mammography. A comparative analysis of the mean glandular doses was conducted in 100 female patients who underwent screening mammography in 2011 and 2013. Siemens Mammomat Novation with the application of the W/Rh anode/filter combination was used in 2011, whereas in 2013 anode/filter combination was Mo/Mo or Mo/Rh. The functioning of mammography was checked and the effectiveness of the automatic exposure control (AEC) system was verified by measuring compensation of changes in the phantom thickness and measuring tube voltage. On the base of exposure parameters, an average glandular dose for each of 100 female patients was estimated. The images obtained by using AEC system had the acceptable threshold contrast visibility irrespective of the applied anode/filter combination. Mean glandular doses in the females, examined with the application of the W/Rh anode/filter combination, were on average 23.6% lower than that of the Mo/Mo or Mo/Rh anode/filter combinations. It is recommended to use a combination of the W/Rh anode /filter which exhibited lower mean glandular doses.

In 2008, Tavakoli M.B, et al [9] studied about Evaluation of the relation between breast glandular absorbed dose and radiographic quality in mammography. It is the aim of this study to measure mean glandular dose and image contrast in terms of different mammographic parameters. In this study two mammography machines located at Said-al Shohada (Giotto) and Shahid Behesti (GE) hospitals were used. According to the recommendations of ACR and MQSA, breast phantoms were constructed and used for this study. For dose evaluation TLD dosimetry method was used. The TLD dosimeters were of LiF type and the reader was a Solaro TLD reader. To obtain a constant contrast when increasing kVp from 22 to 24, it was necessary to reduce mAs by 12 percent. The obtained relation between these two parameters is:  $\text{contrast} = 0.2829D - 0.2427$ . It was also found that there is a linear relationship between contrast and image quality. The relation between these two parameters is:  $\text{Image quality} = 28.117 \text{ Contrast} + 20.134$ . Increasing kVp and hence decreasing mAs results a reduction to the glandular dose, especially in patients with large breast. Increasing kVp from 28 to 30 results in reduction of dose from 6.8mGy to 5mGy. It was found that there has been a linear relationship between contrast and image quality. It was also found that increasing kVp necessitate to reduce mAs for a constant contrast and hence reduction of glandular dose.

In 2015, Izdihar K, et al [10] studied about the determination of tube output and exposure mode for breast phantom of various thickness/glandularity for digital mammography. This study aims to observe the effects of kVp, anode/filter material, and exposure mode on the dose and image quality of 2D mammography. This experimental study was conducted using full-field digital mammography. The entrance surface air kerma was determined using thermoluminescent dosimeter (TLD) 100H and ionization chamber (IC) on three types of Computerized Imaging Reference System (CIRS) phantom with 50/50, 30/70, and 20/80 breast glandularity, respectively, in the auto-time mode and auto-filter mode. The Euref protocol was used to calculate the AGD while the image quality was evaluated using contrast-to-noise ratio (CNR), figure of merit (FOM), and image quality figure (IQF). In the result, it is shown that AGD values in the auto-time mode did not decrease significantly with the increasing tube voltage of the silver filter ( $r = -0.187$ ,  $P > 0.05$ ) and rhodium filter ( $r = -0.131$ ,  $P > 0.05$ ) for all the phantoms. The general linear model showed that AGD for all phantoms had a significant effect between different exposure factors [ $F(6,12.3) = 4.48$  and mode of

exposure  $F(1,86) = 4.17$ ,  $P < 0.05$ , respectively] but there is no significant difference between the different anode/filter combination [ $F(1,4) = 0.571$ ]. In conclusion: In summary, the 28, 29, and 31 kVp are the optimum kVp for 50%, 30%, and 20% breast glandularity, respectively. Besides the auto-filter mode is suitable for 50%, 30%, and 20% breast glandularity because it is automatic, faster, and may avoid error done by the operator.

In 2009, D.F. Uhlenbrock et al [11] studied about the comparison of anode/filter combination in digital mammography with respect to average glandular dose. To investigate the average glandular dose (AGD) applied for clinical digital mammograms acquired with the anode/filter combinations molybdenum/molybdenum (Mo/Mo), molybdenum/rhodium (Mo/Rh), and tungsten/rhodium (W/Rh). Materials and Methods: Using the method of Dance, the AGD was evaluated from the exposure data of 4867 digital mammograms at two sites equipped with a full-field digital mammography (FFDM) system based on an amorphous selenium detector. 1793 images were acquired and analyzed with Mo/Mo, 643 with Mo/Rh, and 2431 with W/Rh. Results: In the Mo/Mo cases the mean compressed breast thickness was  $46 \pm 10$ mm with an average AGD of  $2.29 \pm 1.31$  mGy. For the Mo/Rh cases with a mean compressed thickness of  $64 \pm 9$ mm, we obtained  $2.76 \pm 1.31$  mGy. The W/Rh cases with a mean compressed thickness of  $52 \pm 13$ mm resulted in  $1.26 \pm 0.44$  mGy. The image quality was assessed as normal and adequate for diagnostic purposes in all cases. Conclusion: Applying a W/Rh beam quality permits the reduction of the patient dose by approximately 50% when using an FFDM system based on amorphous selenium. The dose reduction becomes larger as the breast thickness increases. The results are in agreement with simulations and phantom studies known from the literature.

In 2012, T.Olgar et al [12] studied about the average glandular dose in digital mammography and breast tomosynthesis. To determine the average glandular dose (AGD) in digital full-field mammography (2D imaging mode) and in breast tomosynthesis (3D imaging mode). Materials and Methods: Using the method described by Boone, the AGD was calculated from the exposure parameters of 2247 conventional 2D mammograms and 984 mammograms in 3D imaging mode of 641 patients examined with the digital mammographic system Hologic Selenia Dimensions. The breast glandular tissue content was estimated by the Hologic R2 Quantra automated volumetric breast density

measurement tool for each patient from right craniocaudal (RCC) and left craniocaudal (LCC) images in 2D imaging mode. Results: The mean compressed breast thickness (CBT) was 52.7mm for craniocaudal (CC) and 56.0mm for mediolateral oblique (MLO) views. The mean percentage of breast glandular tissue content was 18.0 % and 17.4 % for RCC and LCC projections, respectively. The mean AGD values in 2D imaging mode per exposure for the standard breast were 1.57 mGy and 1.66 mGy, while the mean AGD values after correction for real breast composition were 1.82 mGy and 1.94 mGy for CC and MLO views, respectively. The mean AGD values in 3D imaging mode per exposure for the standard breast were 2.19 mGy and 2.29 mGy, while the mean AGD values after correction for the real breast composition were 2.53 mGy and 2.63 mGy for CC and MLO views, respectively. No significant relationship was found between the AGD and CBT in 2D imaging mode and a good correlation coefficient of 0.98 in 3D imaging mode. Conclusion: In this study the mean calculated AGD per exposure in 3D imaging mode was on average 34 % higher than for 2D imaging mode for patients examined with the same CBT.

In 2010, Ranger N.T, et al [13] studied about a technique optimization protocol and the potential for the dose reduction in digital mammography. Digital mammography requires revisiting techniques that have been optimized for prior screen/film mammography systems. The objective of the study was to determine optimized radiographic technique for a digital mammography system and demonstrate the potential for dose reduction in comparison to the clinically established techniques based on screen- film. An objective figure of merit (FOM) was employed to evaluate a direct conversion amorphous selenium a-Se FFDM system Siemens Mammomat NovationDR, Siemens AG Medical Solutions, Erlangen, Germany and was derived from the quotient of the squared signal-difference-to-noise ratio to mean glandular dose, for various combinations of technique factors and breast phantom configurations including kilovoltage settings 23–35 kVp, target/filter combinations Mo/Mo and W/Rh, breast-equivalent plastic in various thicknesses 2-8 cm and densities 100% adipose, 50% adipose/50% glandular, and 100% glandular, and simulated mass and calcification lesions. When using a W/Rh spectrum, the optimized FOM results for the simulated mass and calcification lesions showed highly consistent trends with kVp for each combination of breast density and thickness. The optimized kVp ranged from 26 kVp for 2 cm 100% adipose breasts to 30 kVp for 8 cm 100% glandular breasts. The use of the optimized W–Rh technique compared to

standard Mo/Mo techniques provided dose savings ranging from 9% for 2 cm thick, 100% adipose breasts, to 63% for 6 cm thick, 100% glandular breasts, and for breasts with a 50% adipose/50% glandular composition, from 12% for 2 cm thick breasts up to 57% for 8 cm thick breasts.



## CHAPTER 3

### RESEARCH METHODOLOGY

#### 3.1 Research design

This study is an observational analytical research, retrospective and experimental study.

#### 3.2 Research question

3.2.1 What are the average glandular dose in phantom and in patients and the image quality (SNR, CNR) in phantom at different target-filters (tungsten-rhodium and tungsten-silver) in digital mammography system?

#### 3.3 Research Design Model.

The Model is displayed in **figure 3.1**

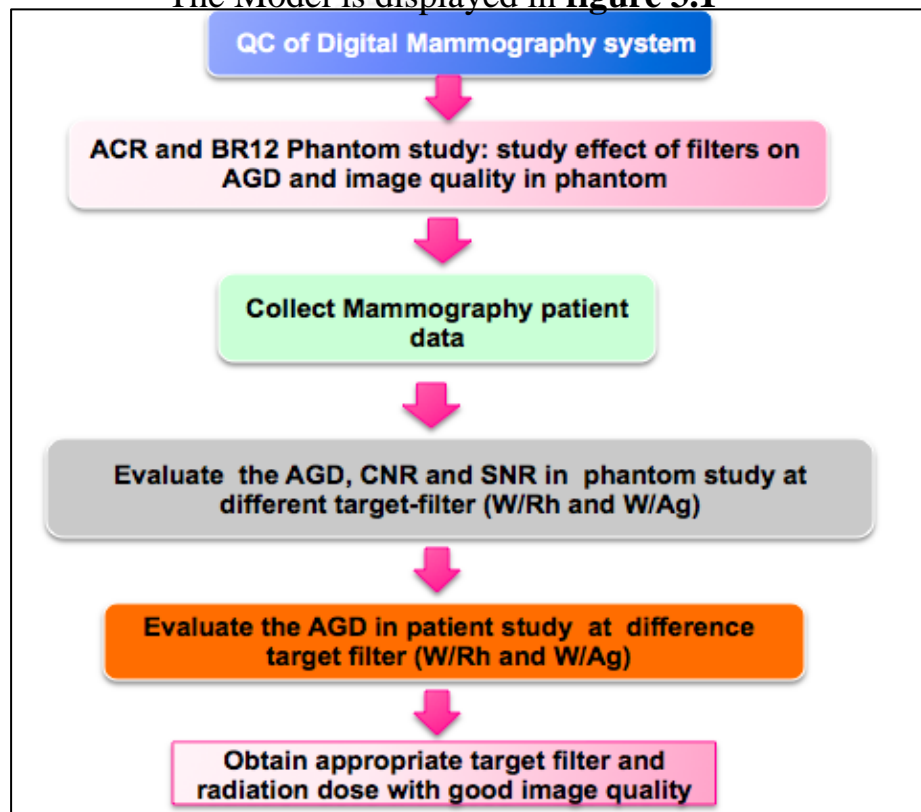


**Figure3. 1** The research design model.

### 3.4 Conceptual framework

The framework is displayed in figure 3.2 and 3.3

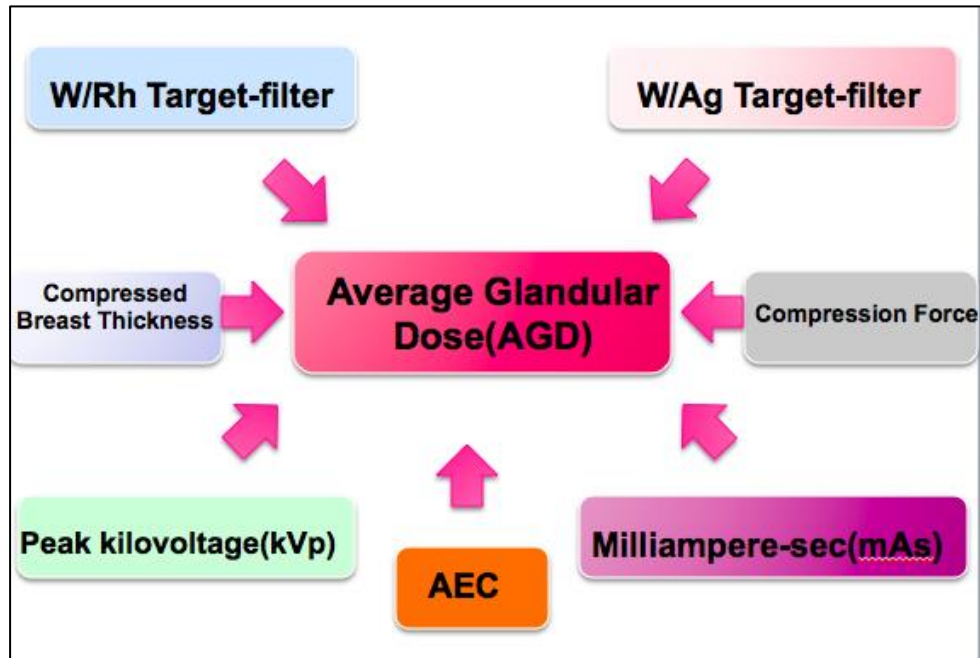


Figure3. 2 The framework.

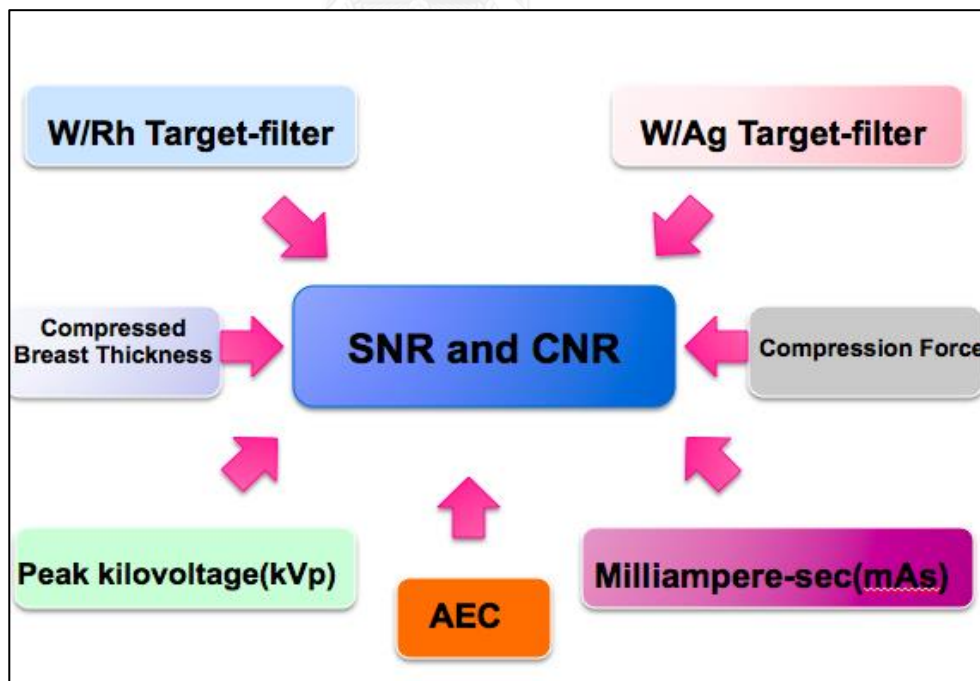


Figure3. 3 The framework.



### **3.5 The Sample**

#### **3.5.1 Target population**

Thai women aged range from 40-74 years old (BI-RADS 1 and 2) under screening mammogram at King Chulalongkorn Memorial Hospital.

##### **3.5.1.1 Inclusion criteria**

Thai women aged range from 40-74 years old (BI-RADS 1 and 2) under screening mammogram at King Chulalongkorn Memorial Hospital.

##### **3.5.1.2 Exclusion criteria**

- Breast conserving therapy (BCT) women
- Implant women
- Breast cancer women

#### **3.5.2 Sample population**

Thai women aged range from 40-74 years old (BI-RADS 1 and 2) under screening mammogram at King Chulalongkorn Memorial Hospital.

#### **3.5.3 Sample**

Thai women aged range from 40-74 years old (BI-RADS 1 and 2) under screening mammogram at King Chulalongkorn Memorial Hospital.

### 3.6 Materials

#### 3.6.1 Digital Mammography system: Hologic Selenia dimension



**Figure 3. 4** Digital Mammography system: Hologic Selenia dimension.

In this study, Digital Mammography system: Hologic Selenia Dimension at King Chulalongkorn Memorial Hospital has been used [14]. This system has a dual track X-ray tube with a filter combination Tungsten (W) anode with Rhodium (Rh) filter and Tungsten (W) anode with Silver (Ag) filter. Focal spot sizes are 0.3 mm for contact examinations and 0.1 mm for magnification examinations. The use of this digital detector offers the opportunity to directly acquire digital mammograms with a 14-bit resolution resulting in more than 16,000 gray levels. All images were acquired with a grid. The source to image distance (SID) is 66 cm. For AEC mode, one of three mode: auto kV, auto time, or auto filter could be selected. During AEC, the kVp is selected by set AEC table as a function of compression thickness. The pre-exposure (50 milliseconds) is used to calculate the mAs, the mA setting as a function of kV. During the pre-exposure, the resulting pixel values are determined. The CBT is estimated from the digital compression paddle height readout. The dose detection is measured of percentage of x-ray absorbed by the detector. To perform the mammography examination uses the technique table recommended by Hologic Selenia Dimension for large focal spot and small focal spot [Appendix A].

### 3.6.2 Phantom characteristics.

#### 3.6.2.1 Mammography phantom image Quality Evaluation:

##### ACR phantom

The GAMMEX/RMI mammographic accreditation phantom RMI 156 [15] is made of a wax block as shown in Figure 3.5. The technical data are 0.55 kg weight 4.5 cm height, 10.2 cm width, 10.8 cm length. This phantom was designed to attenuate the X-ray beam in the same way as a human breast of 50% adipose and 50% glandular tissue compressed to thickness of 4.2 cm. The test objects that represent malignancies or small breast structures are embedded as an insert in an acrylic base. It contains 6 fibrils, 5 speck groups of simulated microcalcifications and 6 masses. The phantom includes appropriate details that range from visible to invisible a standard mammographic film image. The fiber with diameter of 1.56, 1.12, 0.89, 0.75, 0.54 and 0.40 mm; specks with diameters of 0.54, 0.40, 0.32, 0.24 and 0.16 mm; and masses with decreasing diameters of 2.00, 1.00, 0.75, 0.50 and 0.25 cm are shown in Figure 3.5



**Figure3. 5** Mammography phantom image Quality Evaluation: ACR breast phantom model RMI 156.

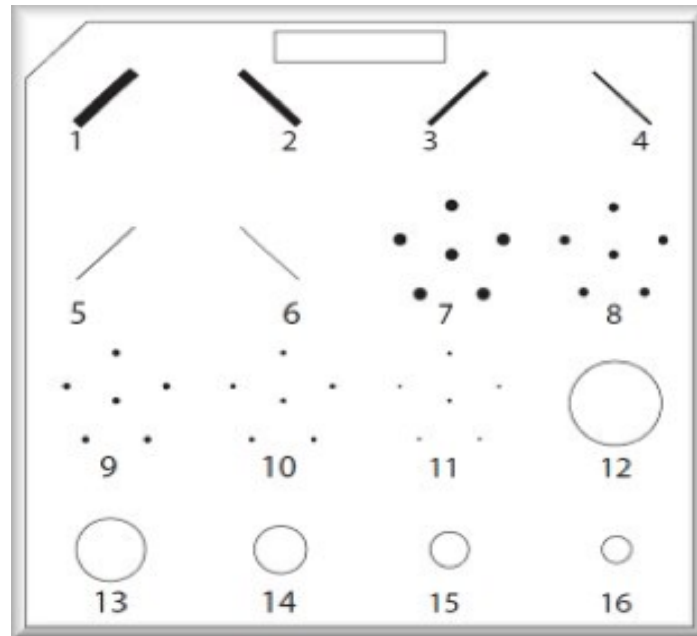


**Figure3. 6** Location of the test objects in the RMI 156 breast phantom

#### 3.6.2.2 Acrylic disc

4-mm thick, 1-cm diameter placed on the top of the phantom in a consistent location in the image area so it will not obscure details in the phantom and where it cannot cast a shadow on any portion of the AEC detector. With current equipment can result from placing the disc along the central anode-cathode axis, where a varying fraction of the AEC detector area might be covered by the disc's shadow, depending on the exact position of the phantom and the detector. A suitable location is between and slightly below the first and second largest fiber.

### 3.6.2.3 Phantom BR12, 1 and 2 cm thickness

BR12 slap phantom [16] was used for the assessment of image quality and the AGD. The standard breast model of a superficial layer of adipose tissue was used in this study. The percentage glandular content (PGC) of each breast, defined as the percentage by mass of glandular tissue in the central region of the standard breast model was used. The BR12 slaps and the standard breast phantom with PGC of 50% were exposed at various target/filter/kV combinations. Tissue equivalent material H: 8.68%, C: 69.95%, N: 2.36%, O: 17.91%, Cl: 0.14%, Ca: 0.95%, Density: 0.97g/cm<sup>3</sup>, Electron Density (m<sup>-3</sup>x10<sup>26</sup>): 3170. BR12 simulated a 50% adipose, 50% glandular breast [17].



**Figure3. 7** Phantom BR12, 1 and 2 cm thickness

### 3.7 Methods

#### 3.7.1 Phantom study

3.7.1.1 Quality Control of digital mammography system using guideline from IAEA human health series no 17. (Quality Assurance Program for digital mammography) [18]

- Mammographic Unit Assembly Evaluation
- Collimator assessment
- Artifact evaluation
- kVp Accuracy/Reproducibility
- Beam quality assessment (HVL measurement)
- Evaluation of system resolution
- Breast entrance exposure and AGD
- Phantom Image Quality Evaluation
- Monitor Quality Control

#### 3.7.1.2 Image quality study

3.7.1.2.1 Image quality study: Use the ACR phantom 4 cm thickness and add 1, 2 cm BR12 phantom above ACR phantom

- Position phantom in center close to the chest wall and put the acrylic disk above the phantom and compress the paddle by using the compression force 29.2 lbs. (from IAEA human health series no 17).
- Use the AEC technique.
- Use the manual technique, choose the filter and expose.

3.7.1.2.2 Calculate CNR and SNR for each filter at different thickness by drawing the ROIs in object (acrylic disk) and background (outside the acrylic disk)

3.7.1.2.3 Record exposure parameters and AGD.

3.7.1.2.4 Evaluate the AGD, CNR, and SNR for each phantom thickness at different target-filter.

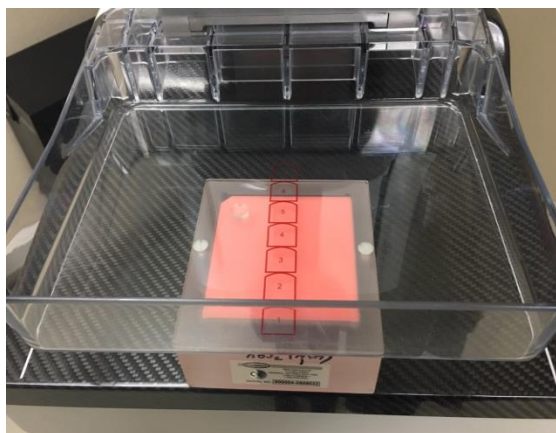


**Figure3. 8** ACR phantom 4 cm thickness in CC view.

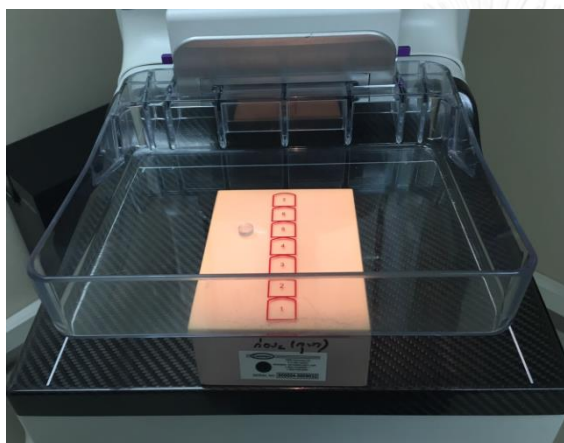


**Figure3. 9** ACR and BR12 phantom 5 cm thickness in CC view.

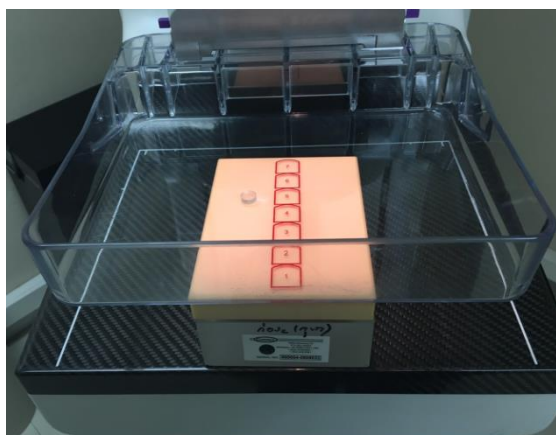


**Figure3. 10** ACR and BR12 phantom 6 cm thickness in CC view.



**Figure3. 11** ACR and BR12 phantom 7 cm thickness in CC view.

### 3.7.1.3 Evaluate the quantitative image quality

Evaluate the quantitative image quality by determining contrast to noise ratio (CNR) and signal to noise ratio (SNR). Calculate CNR and SNR for each filter at different thickness by drawing the ROIs in object (acrylic disk) and background (outside the acrylic disk)

#### 3.7.1.3.1 Contrast-to-noise ratio (CNR)

$$\text{CNR} = \frac{PV_B - PV_d}{\sqrt{\frac{\sigma_B^2 + \sigma_d^2}{2}}}$$

Where;

$PV_B$  = the pixel value measured in the background

$PV_d$  = the pixel value measured in the object

$\sigma_B$  = the standard deviation of the background

$\sigma_d$  = the standard deviation of the object

#### 3.7.1.3.2 Signal-to-noise ratio (SNR)

$$\text{SNR} = \frac{\text{Mean pixel value}}{\text{SD of pixel value}}$$

Where;

Mean pixel value = the mean pixel value measure in the object

SD of pixel value = the standard deviation of the object



### 3.7.2 Patients study.

Our study involved recruitment 200 Thai women aged range from 40-74 years old (BI-RADS 1 and 2) under screening mammogram at King Chulalongkorn Memorial Hospital. The data was collected 800 mammograms from 200 women and included contact, automatic exposure control (AEC) mammograms of cranio-caudal and medio-lateral projections from preventive examinations, screening and after care. The data was collected 100 women for W/Rh and 100 women for W/Ag. The data were delivered from PACS through the local data network and automatically sent to the workstation. The computer program reads the DICOM file and dose values from header.

The following information was recorded for each mammogram:

- tube voltage (kVp);
- post exposure tube loading (mAs),
- target and filter materials,
- compressed breast thickness (mm),
- compression force (lbs.),
- the patient dose: AGD (mGy),

The records were analyzed and compared between tungsten-rhodium target-filter and tungsten-silver target-filter.

### 3.8 Sample size

Thai women aged range from 40-74 years old (BI-RADS 1 and 2) under screening mammogram at King Chulalongkorn Memorial Hospital. The sample population is independent, retrospective data, determined by formula;

$$N = \frac{2(Z_{\alpha/2} + Z_{\beta})^2 \sigma^2}{(x_1 - x_2)^2}$$

$$\text{where; } \alpha = 0.05, Z_{\alpha/2} = 1.96$$

$$90\% \beta = 0.1, Z_{\beta} = 1.28$$

reference from literature review ;

$$X_1 = 2.15 \quad X_2 = 2.36$$

$$n_1 = n_2 = 200, SD_1 = 0.5, SD_2 = 0.4$$

N= 98 sample size per method

### 3.9 Measurement Variable

#### 3.9.1 Independence variable

- Compress breast thickness (mm)
- Compression force (lbs.)
- Target filter (W/Rh and W/Ag)
- kVp
- mAs

#### 3.9.2 Dependence variable

- Average glandular dose (mGy)
- CNR
- SNR

### 3.10 Statistical analysis

#### 3.10.1 Descriptive statistic

Calculated the average glandular dose in maximum, minimum, standard deviation

#### 3.10.2 Presentation format in bar graph, scatter plot, tables

3.10.3 Using Statistic software (SPSS v.17) and Microsoft excel for data analyzing.

### 3.11 Data Collection

In this study, the information of the mammographic examinations were delivered from PACS through the local data network and automatically sent to the workstation. The computer program reads the DICOM file, extracts patients data and dose values from header, and recorded in excel program. The study involved 200 Thai women aged range from 40-74 years old (BI-RADS 1 and 2) under screening mammogram at King Chulalongkorn Memorial Hospital. The data was collected 400 mammograms from 200 women and included contact, automatic exposure control (AEC) mammograms of cranio-caudal and medio-lateral projections from preventive examinations, screening and after care. The number of images per examination is 4. Inclusion criteria

for population were Thai women aged range from 40-74 years old (BI-RADS 1 and 2) under screening mammogram at King Chulalongkorn Memorial Hospital. Exclusion criteria were breast conserving therapy (BCT) women, implant women, breast cancer women.

### **3.12 Data analysis**

3.12.1 The image quality data was analyzed with excel program developed by the American Association of Physicist in Medicine (AAPM)

3.12.2 The qualitative image quality was analyzed by CNR and SNR for each target filter in the different breast thickness as presented in form of table and scatter plots.

3.12.3 Patient data such as, exposure factors, CBT, compression force and patient dose were analyzed to obtain, the mean, median, ranges and standard deviation (SD) by SPSS statistical program.

3.12.5 Compare and correlate of the data from dependent variables and independent variables. Multiple regression analysis was used determine the correlation of target filter with variables.

3.12.6 Data presentation, the table, charts and scatter plot were presented.

### **3.13 Outcome**

3.13.1 The distribution of technique factors for patient study in digital mammography system, such as mAs, kVp, CBT, compression force, target/filter combination.

3.13.2 The correlate AGD and influence factors.

### **3.14 Expected benefits and application**

3.14.1 The appropriate parameters: mAs, kVp, CF, CBT, AGD for the patient under screening mammography at King Chulalongkorn Memorial Hospital at different target-filter (W/Rh and W/Ag) for patient dose reduction and good image quality.

### 3.15 Ethic consideration

This research involves the determination of patient dose and image quality in digital mammography. The patient data collection during the period from Jan 2016 to Feb 2017 had been extracted from the image DICOM header. The research proposal will be submitted for approval by Ethical Committee of Faculty of Medicine, Chulalongkorn University.



## CHAPTER 4

### RESULTS

#### 4.1 Image quality evaluation: the phantom study

##### 4.1.1 Image quality evaluation for different thickness of mammography phantom.

The images of mammographic phantom were sent from PACS through the local data network and automatically to the workstation. The computer program reads the DICOM file and extracts dose values, the exposure parameter from the header. The CNR and SNR were calculated and recorded in excel program.

The CNR and SNR were shown in different phantom thickness and tube voltage with AEC and manual techniques in table 4.1 to 4.4. The CNR and SNR were plotted against the tube potential for each anode/filter combination at different thickness in AEC technique (Figure 4.1-4.8), respectively. The CNR and SNR were plotted against the tube current-time for each anode/filter combination in manual technique (Figure 4.9-4.12), respectively.

**Table 4. 1** The CNR, SNR and AGD using W/Rh target-filter in phantom of different thickness when varying kVp for AEC technique.

CBT (mm)	kVp	mAs	CF (lbs.)	AGD (mGy)	CNR	SNR
40	27	90	29.2	0.88	21.57	41.95
	28	78	29.2	0.88	21.48	42.58
	29	68	29.2	0.85	20.83	42.29
	30	58	29.2	0.82	20.43	42.5
50	27	129	29.2	1.15	21.90	42.78
	28	102	29.2	1.05	21.21	41.77
	29	96	29.2	1.09	21.26	42.43
	30	84	29.2	1.07	20.66	42.41
60	27	356	29.2	2.64	25.47	48.69
	28	294	29.2	2.48	24.86	47.81
	29	250	29.2	2.39	24.02	47.21
	30	207	29.2	2.21	23.13	47.33
70	32	250	29.2	3.03	26.61	53.94
	33	207	29.2	2.75	25.29	52.77
	34	173	29.2	2.5	24.18	52.68
	35	145	29.2	2.28	23.21	51.4

**Table 4. 2** The CNR, SNR and AGD using W/Rh target-filter in phantom of different thickness when increasing kVp, mAs for manual technique.

CBT(mm)	kVp	mAs	CF (lbs.)	AGD (mGy)	CNR	SNR
40	28	60	29.2	0.67	18.08	47.92
	28	80	29.2	0.89	22.89	53.75
	28	100	29.2	1.12	27.04	57.8
	28	120	29.2	1.34	31.57	63.16
50	29	80	29.2	0.93	19.83	52.58
	29	100	29.2	1.14	23.71	56.52
	29	120	29.2	1.4	27.02	59.34
	29	140	29.2	1.6	30.42	62.17
60	30	120	29.2	1.28	15.74	47.67
	30	140	29.2	1.49	17.75	49.83
	30	180	29.2	1.89	21.61	56.12
	30	220	29.2	2.35	25.23	58.69
70	31	140	29.2	1.54	15.57	47.43
	31	180	29.2	1.98	19.08	52.07
	31	220	29.2	2.42	22.34	56.84
	31	260	29.2	2.86	25.32	59.16

**Table 4. 3** The CNR, SNR and AGD using W/Ag target-filter in phantom of various thicknesses when varying kVp for AEC technique.

CBT (mm)	kVp	mAs	CF (lbs.)	AGD (mGy)	CNR	SNR
60	27	202	29.2	2.09	23.41	47.36
	28	189	29.2	2.24	25.67	51.5
	29	138	29.2	1.9	22.64	48.42
	30	118	29.2	1.82	22.41	47.36
70	30	206	29.2	2.97	28.44	56.45
	31	177	29.2	2.85	28.34	57.07
	32	151	29.2	2.69	27.24	55.19
	33	129	29.2	2.54	26.45	55.2
	34	113	29.2	2.41	26.18	55.22
	35	99	29.2	2.3	25.45	54.89

**Table 4. 4** The CNR, SNR and AGD using W/Ag target-filter in phantom of different thickness when varying kVp, mAs for manual technique.

CBT (mm)	kVp	mAs	CF (lbs.)	AGD (mGy)	CNR	SNR
60	30	60	29.2	0.92	14.24	45.28
	30	80	29.2	1.22	17.56	50.16
	30	100	29.2	1.54	20.84	53.13
	30	120	29.2	1.84	24.11	57.33
	30	140	29.2	2.15	27.37	61.01
	30	180	29.2	2.78	32.7	64.71
70	31	60	29.2	0.96	12.8	45.46
	31	80	29.2	1.28	15.82	48.95
	31	100	29.2	1.6	19.29	53.43
	31	120	29.2	1.93	21.85	57.23
	31	140	29.2	2.25	24.81	61.42
	31	180	29.2	2.89	29.8	66.19

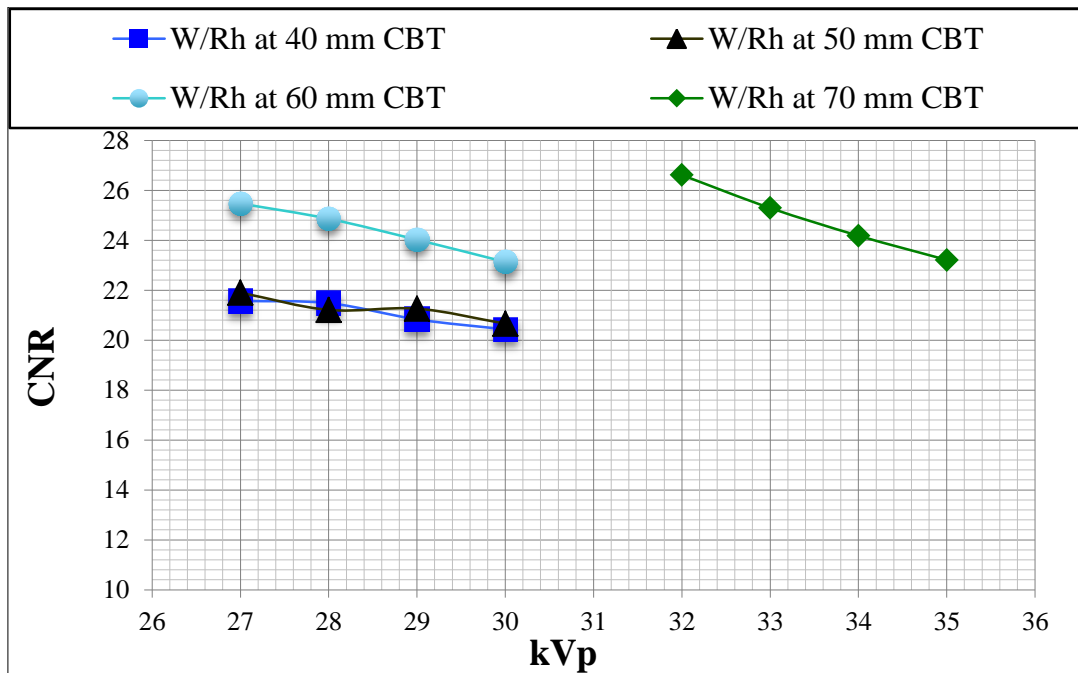


**Figure4. 1** The CNR in ACR and BR12 phantoms when varying kVp in W/Rh for AEC technique

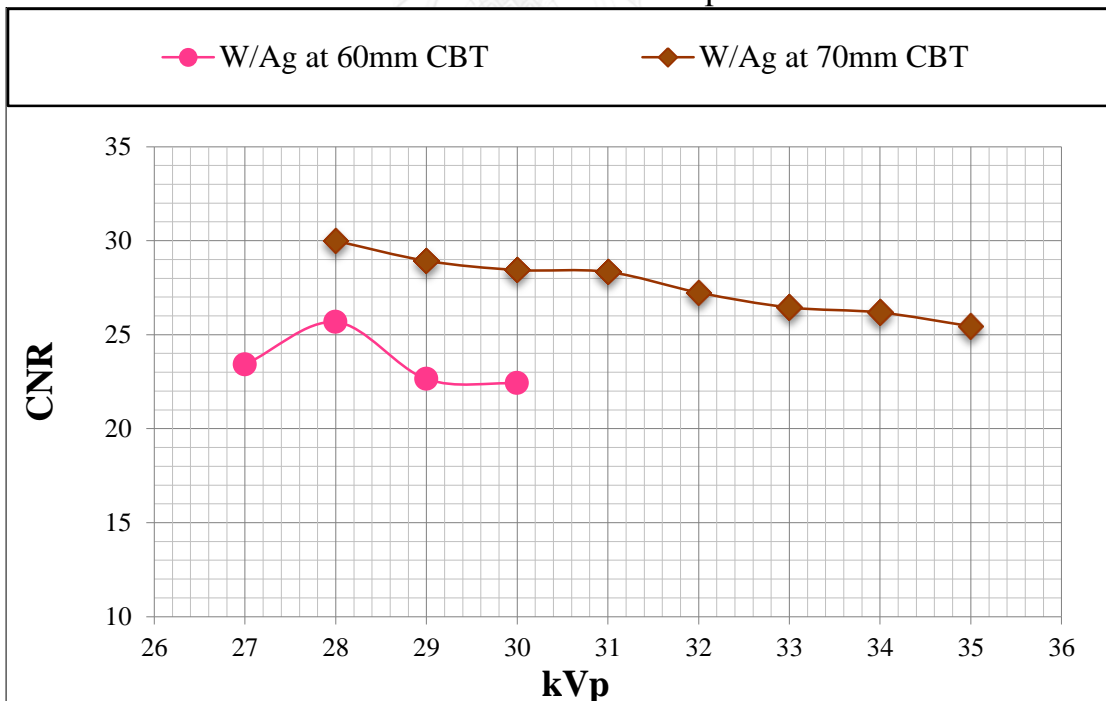


**Figure4. 2** The CNR in ACR and BR12 phantoms when varying kVp for W/Ag in AEC technique.



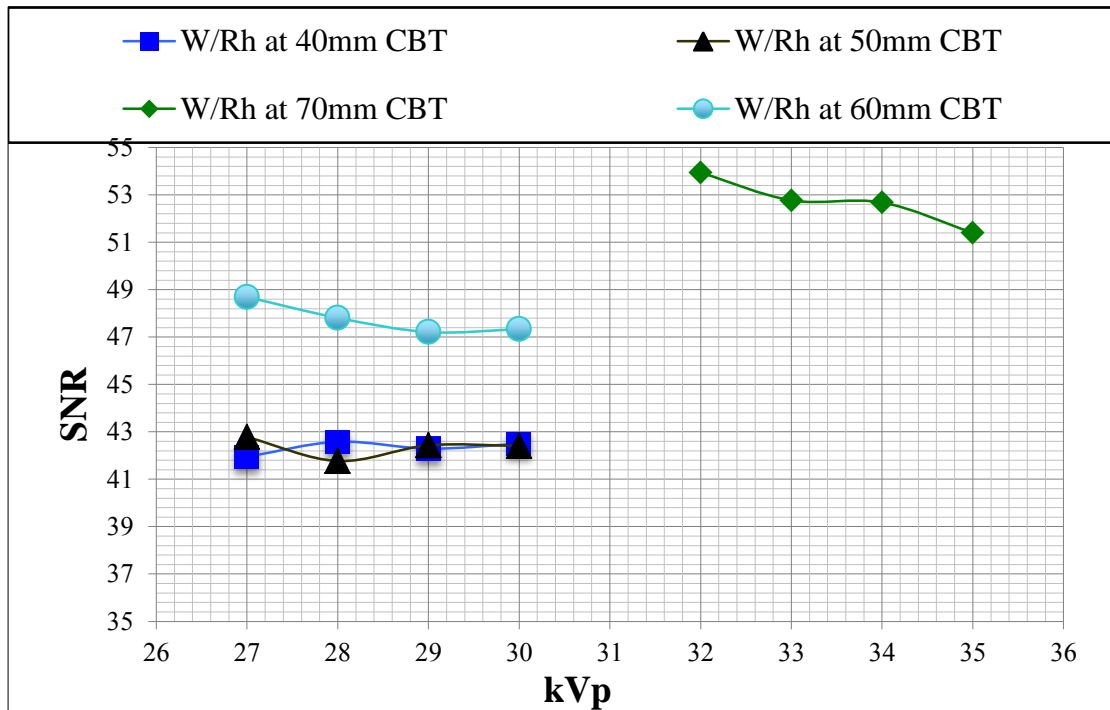


**Figure4. 3** The SNR in ACR and BR12 phantoms when varying kVp for W/Rh in AEC technique

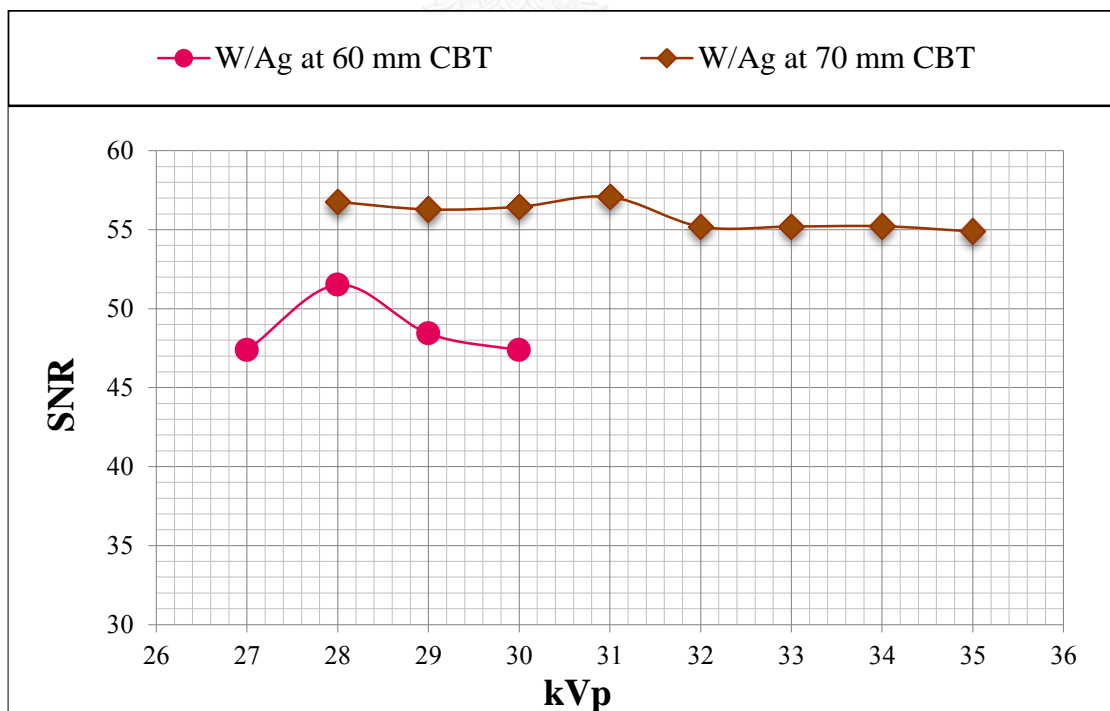


**Figure4. 4** The SNR in ACR and BR12 phantoms when varying kVp for W/Ag in AEC technique.

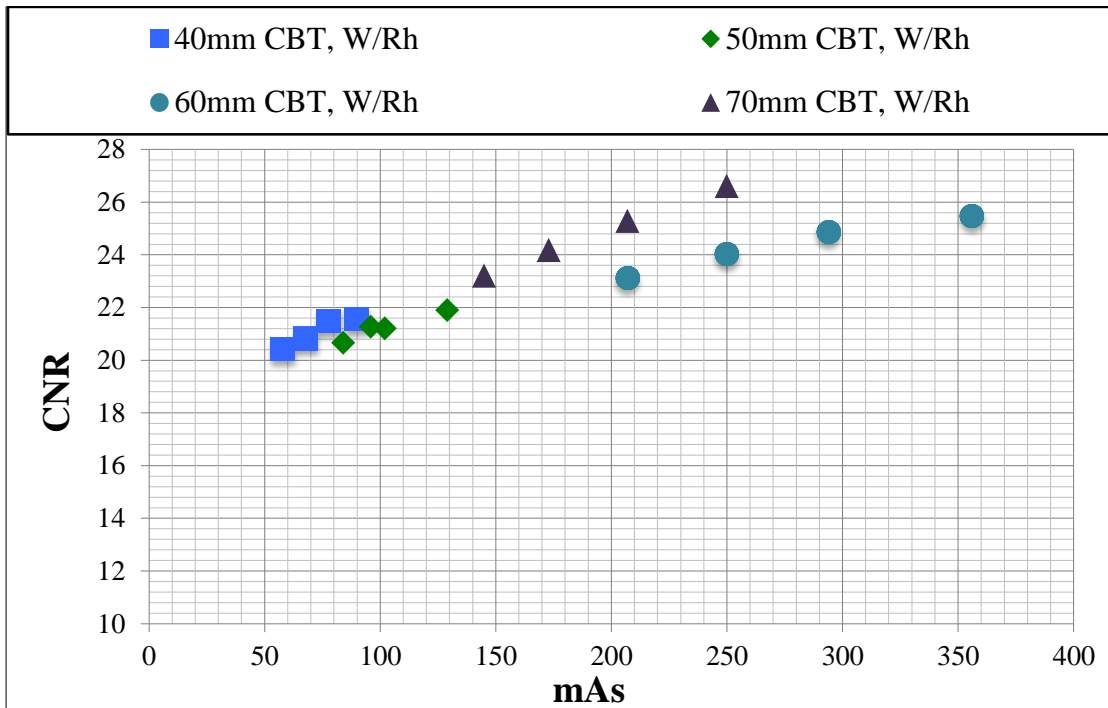


**Figure4. 5** The CNR vs mAs in ACR and BR12 phantoms for W/Rh in AEC technique

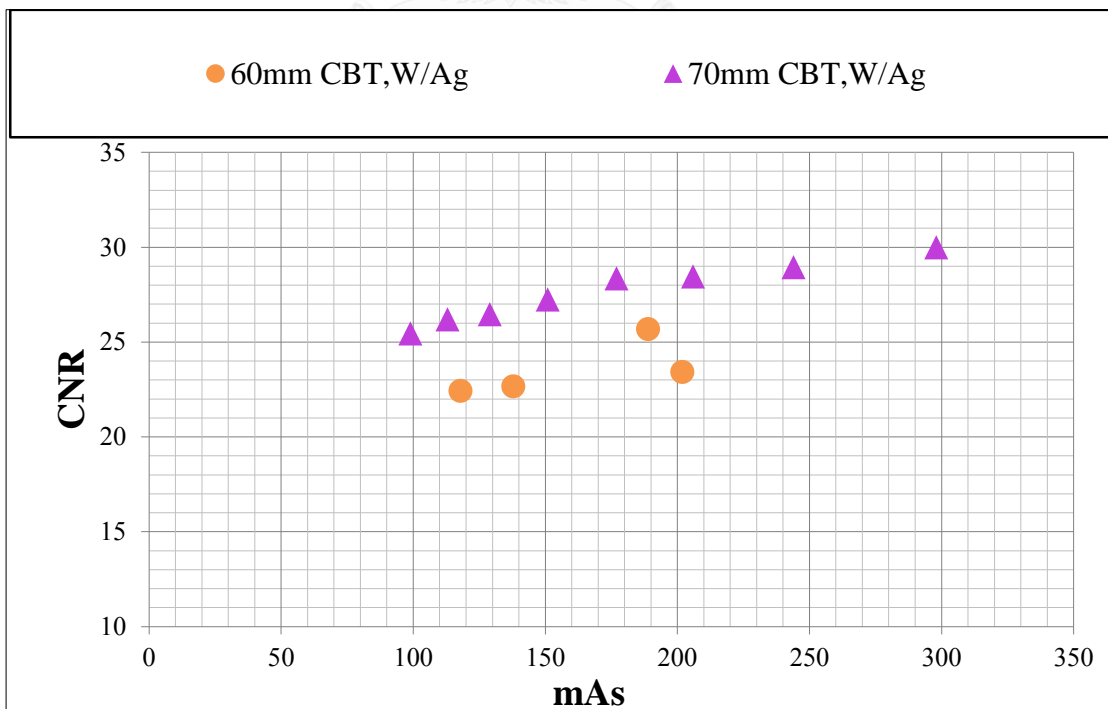


**Figure4. 6** The CNR vs mAs in ACR and BR12 phantoms when varying phantom thickness for W/Ag in AEC technique.

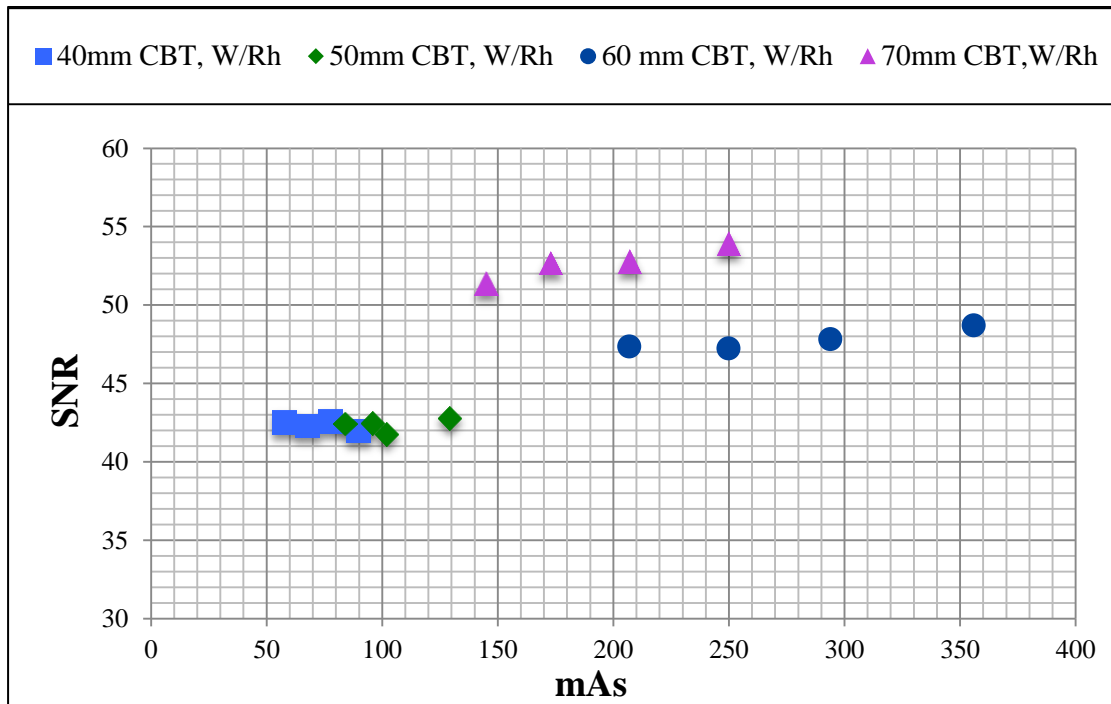


**Figure4. 7** The SNR vs mAs in ACR and BR12 phantoms when varying thickness for W/Rh in AEC technique.

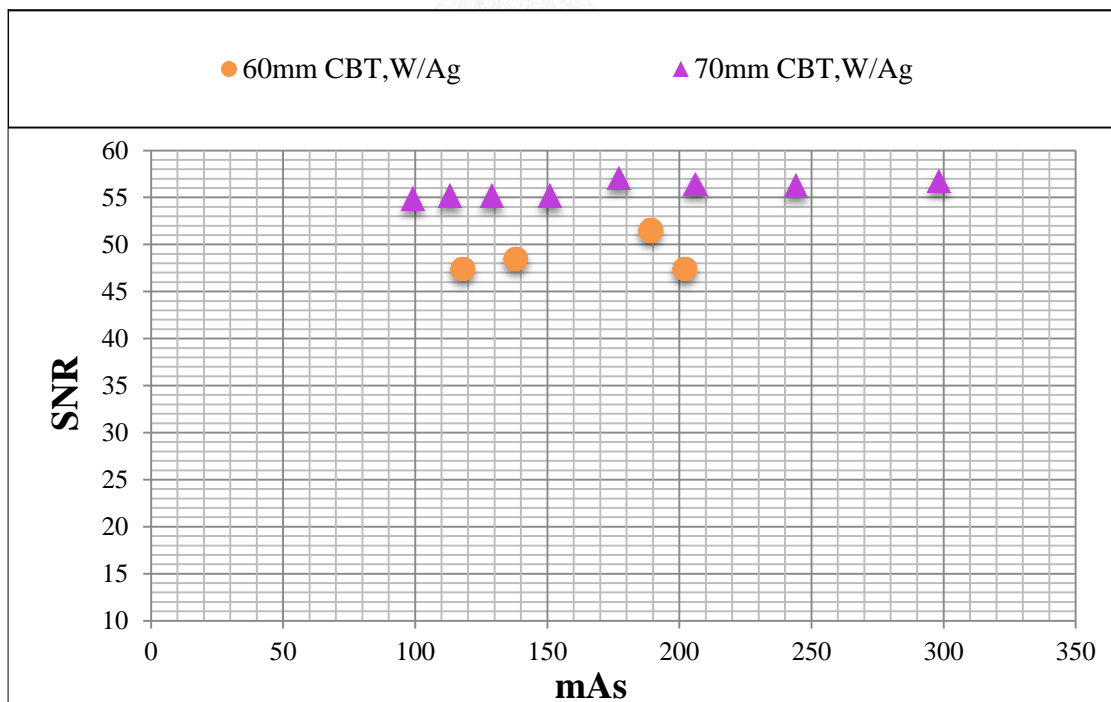


**Figure4. 8** The SNR vs mAs in ACR and BR12 phantoms when varying thickness for W/Ag in AEC technique.

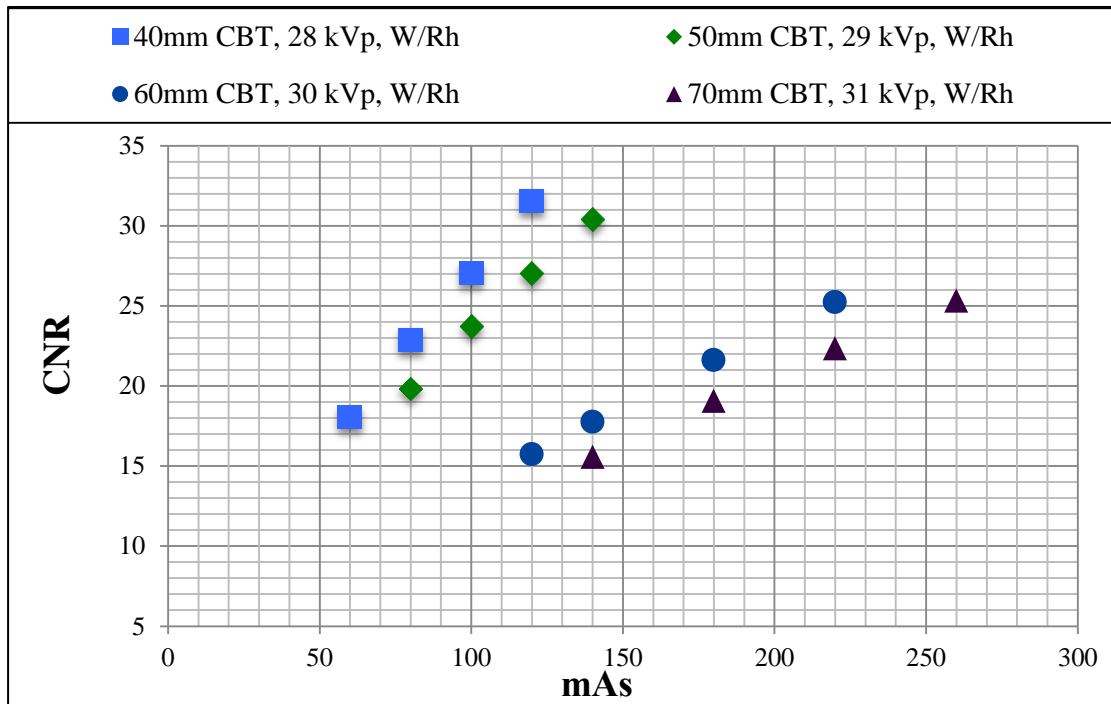


**Figure4. 9** The CNR in ACR and BR12 phantoms when varying mAs for W/Rh in manual technique

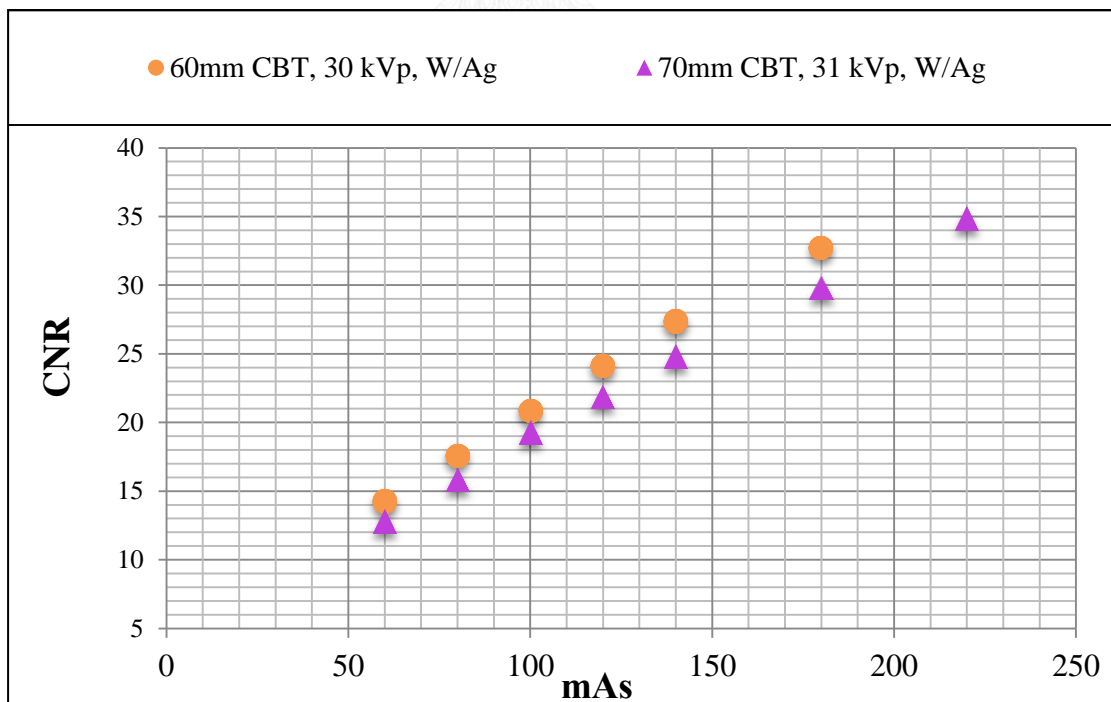


**Figure4. 10** The CNR in ACR and BR12 phantoms when varying mAs for W/Ag in manual technique

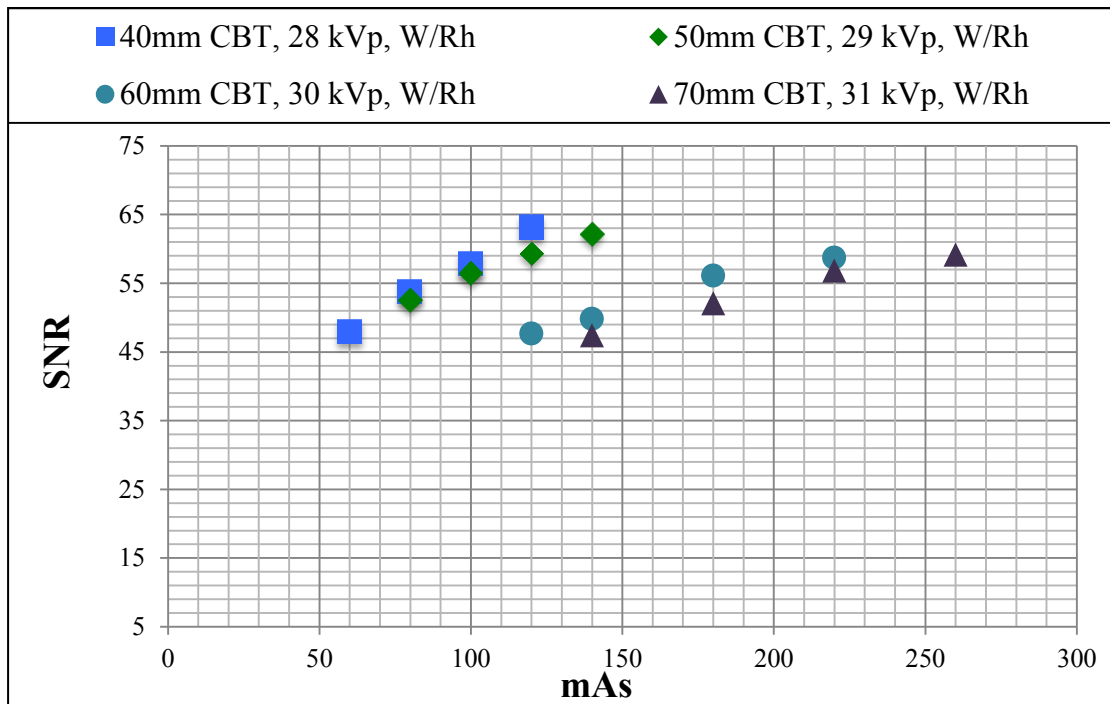


**Figure4. 11** The SNR in ACR and BR12 phantoms when varying mAs for W/Rh in manual technique

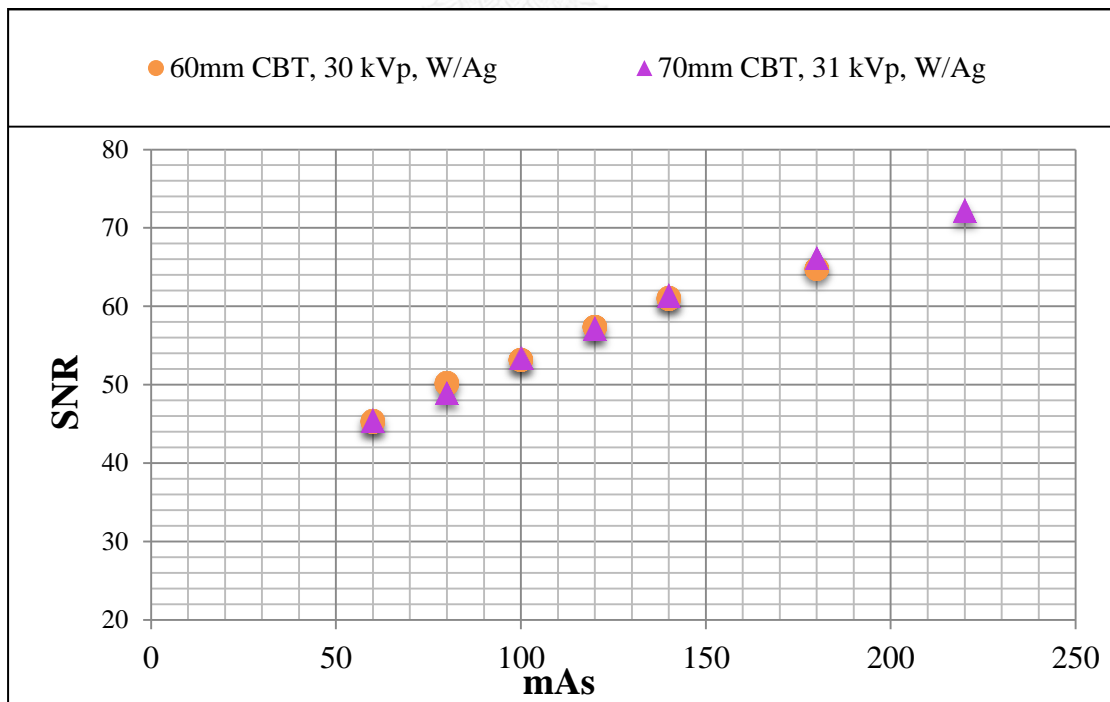


**Figure4. 12** The SNR in ACR and BR12 phantoms when varying mAs for W/Ag in manual technique.

#### 4.1.2 The average glandular dose in phantom study

In this study, the ACR and BR12 phantoms of various thickness were used to determine the average glandular dose, the AGD value obtained from the phantom study increased with thickness in AEC and manual technique (table 4.1 to 4.4). The AGD was plotted against and tube voltage and the tube current-time for each anode/filter in AEC and manual techniques, respectively (Figures 4.5 and 4.6).

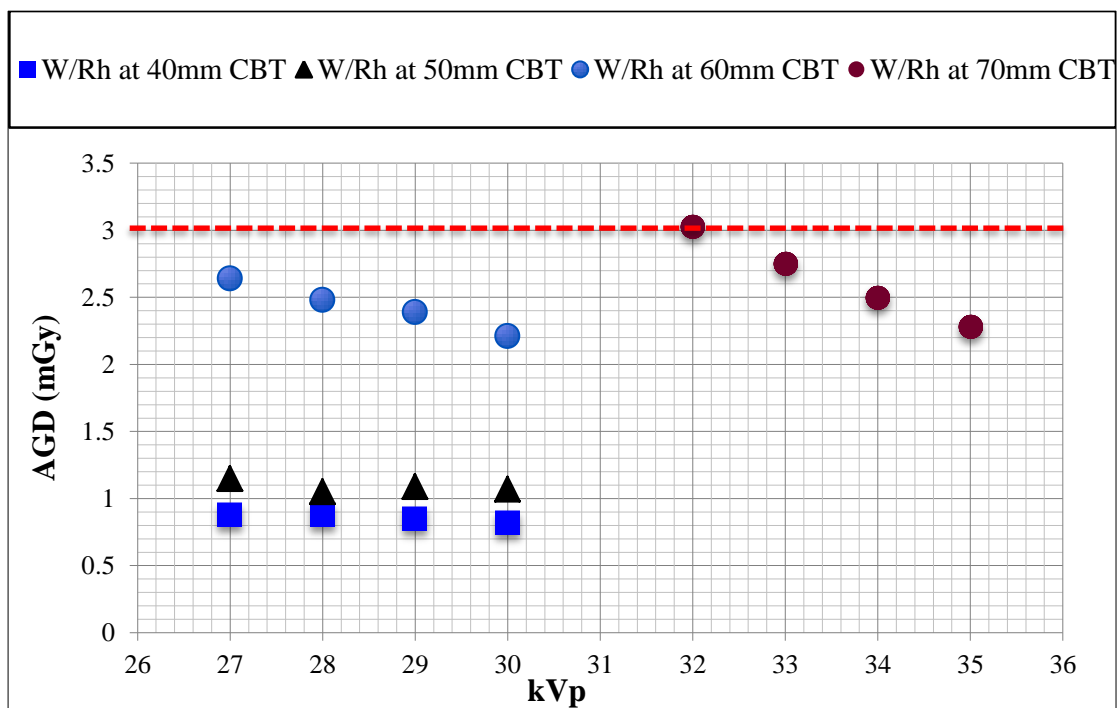


**Figure 4.13** The AGD in ACR and BR12 phantoms when varying kVp for W/Rh in AEC technique.

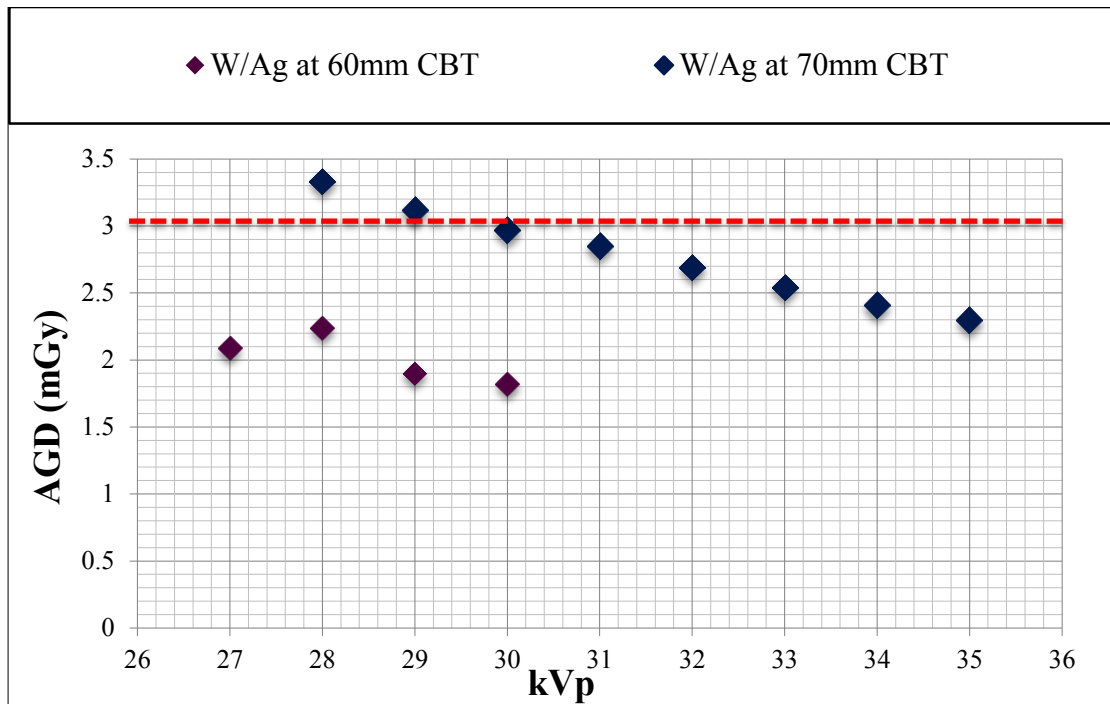


**Figure4. 14** The AGD in ACR and BR12 phantoms when varying kVp for W/Ag in AEC technique.

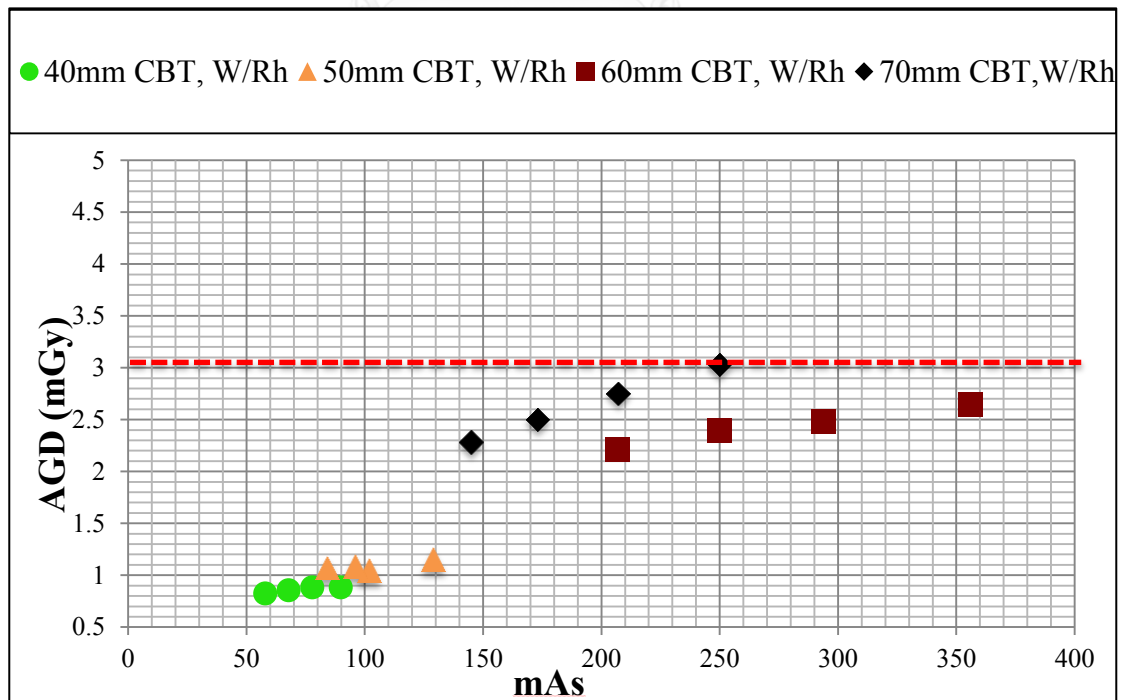


**Figure4. 15** The AGD vs mAs in ACR and BR12 phantoms when varying thickness for W/Rh in AEC technique.

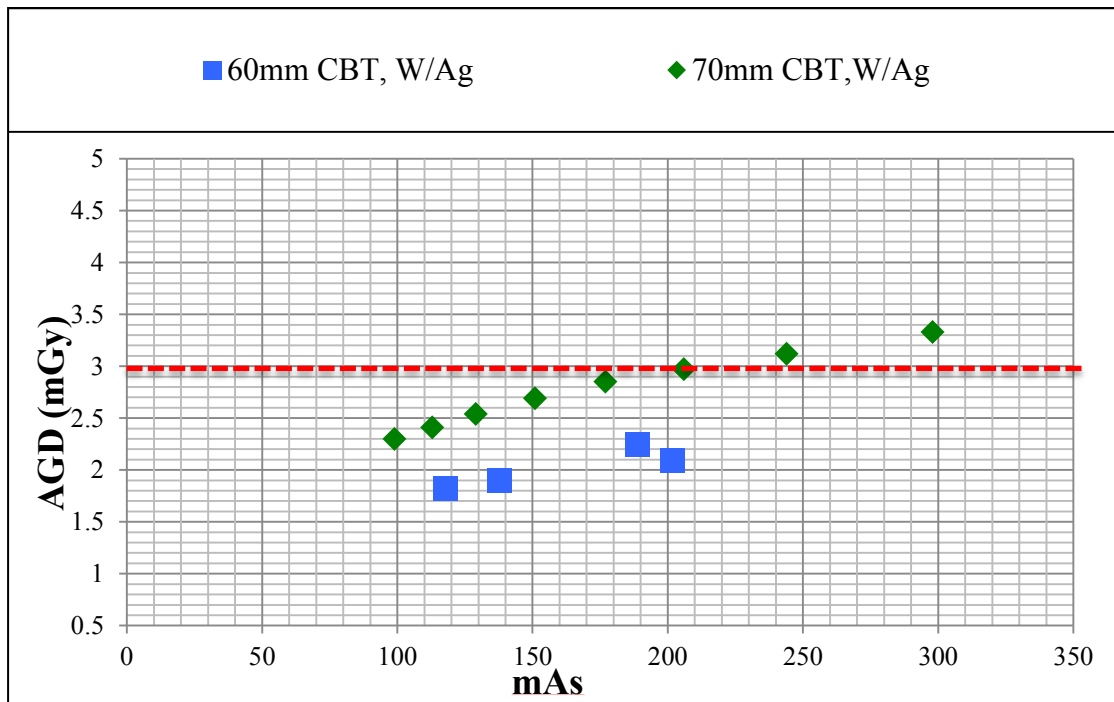


**Figure4. 16** The AGD vs mAs in ACR and BR12 phantoms when varying thickness for W/Ag in AEC technique.

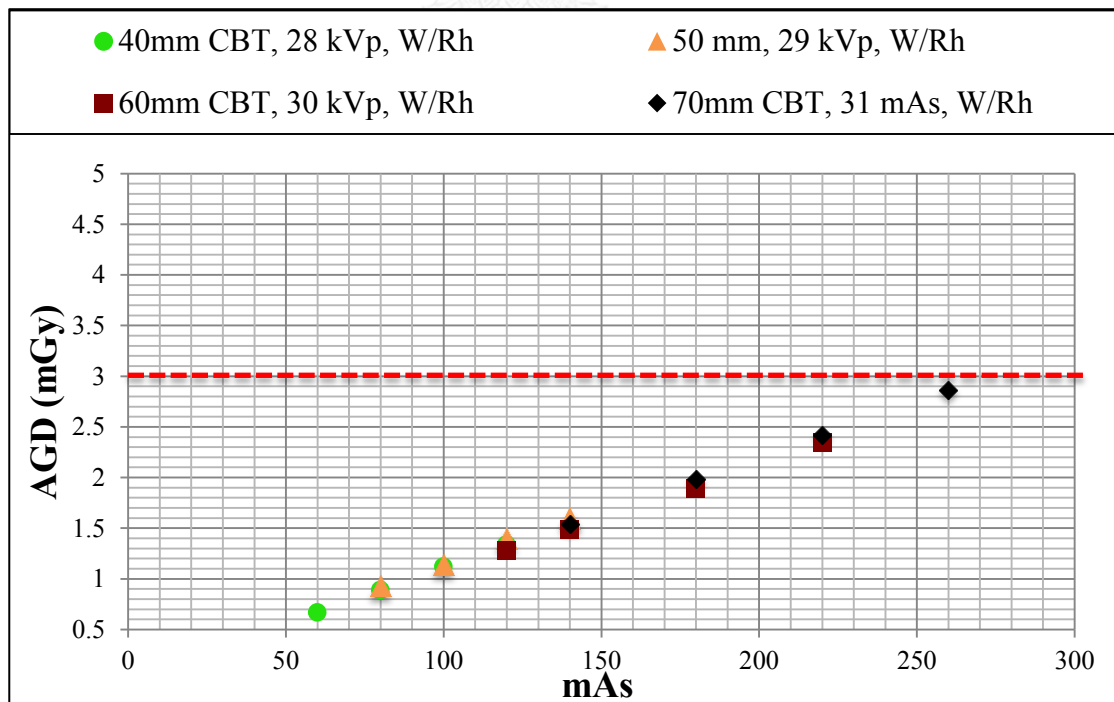


**Figure4. 17** The AGD in ACR and BR12 phantoms when varying mAs for W/Rh in manual technique



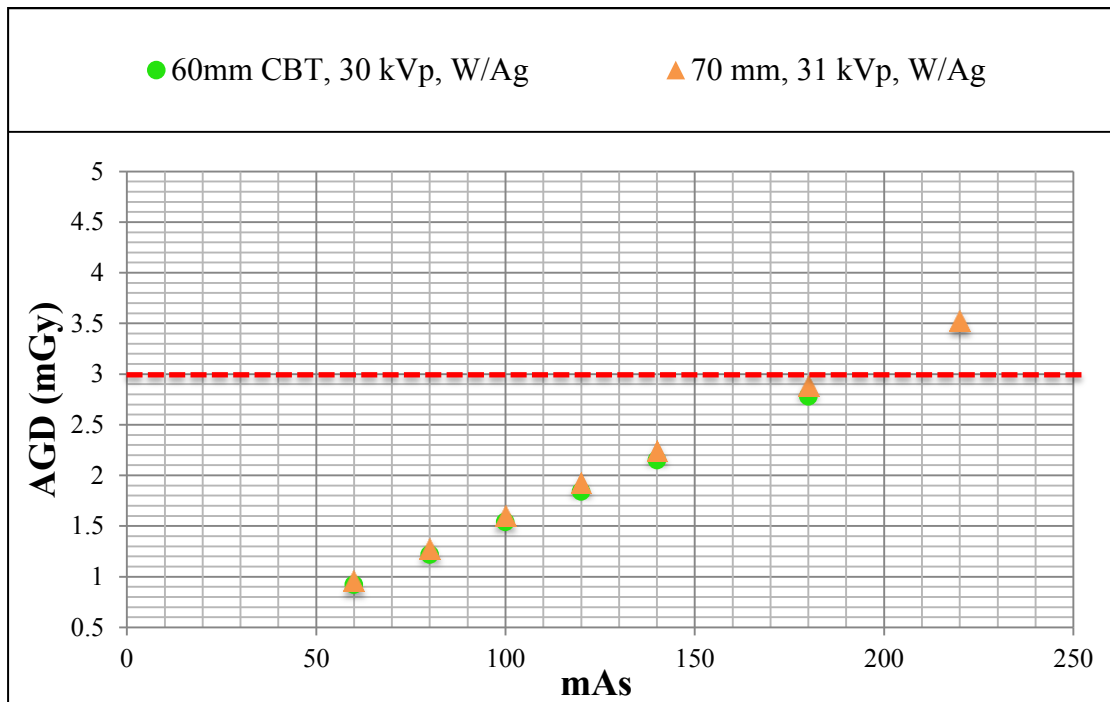


**Figure4. 18** The AGD in ACR and BR12 phantoms when varying mAs for W/Ag in manual technique

## 4.2 Patient information and technique factor.

The study involved recruitment 200 Thai women aged between 40-74 years old under screening mammogram at King Chulalongkorn Memorial Hospital. 800 mammogram views were collected from included contact, automatic exposure control (AEC) mammograms of cranio-caudal and medio-lateral projections from preventive examinations, screening and after care. The 100 women data was collected for W/Rh and 100 for W/Ag.

### 4.2.1 Breast thickness

For women who were examined with W anode X-ray spectra usually the anode/filter combination, W/Rh was used for thinner breasts. The average compressed breast thickness and range in W/Rh target-filter was  $54.18 \pm 10.4$  (21-69) mm was shown in Table 4.5. In the case of thicker breasts, the W/Ag anode/filter combination was used with average thickness of  $81 \pm 7.7$  mm (70-116 mm) as shown in table 4.6.

### 4.2.2 Average glandular dose

The average glandular dose (range) of W/Rh target-filter was  $1.26 \pm 0.6$  (0.37-3.84) mGy. The AGD and range of the W/Ag target-filter was  $1.79 \pm 0.6$  (0.97-4.23) mGy. The results for AGD and thickness are summarized in table 4.5 and 4.6.

### 4.2.3 Compression force

The average and range of compression force of W/Rh and W/Ag target-filters were  $13.24 \pm 5.4$  (3.2-31.6),  $14.15 \pm 4.7$  (4.7-29.4) lbs. The results for compression force are summarized in table 4.5 and 4.6.

**Table 4. 5** The scatter plot shows the correlation between the AGD and mAs ( $R^2 = 0.98$ ) of patient study in W/Rh.

View (image)	Target/ Filter	Compress Breast thickness (mm)	Compression Force (lbs.)	AGD (mGy)	kVp	mAs
		Mean (Range) ±SD	Mean (Range) ±SD	Mean (Range) ±SD	Mean (Range) ±SD	Mean (Range) ±SD
RCC (100)	W/Rh	54.18 (21-69) ±10.4	13.24 (3.2-31.6) ±5.4	1.26 (0.37-3.84) ±0.6	29.68 (25-32) ±1.7	106.75 (32-316) ±47.3
LCC (100)	W/Rh	53.56 (18-71) ±10.1	12.12 (4.1-26.1) ±5.1	1.08 (0.41-3.4) ±0.5	29.46 (25-32) ±1.6	104.05 (36-301) ±47.3
RMLO (100)	W/Rh	50.43 (19-68) ±11.2	18.49 (4.6-33.3) ±7	1.12 (0.38-2.88) ±0.5	29 (25-32) ±1.7	94.54 (35-301) ±41.4
LMLO (100)	W/Rh	51.77 (18-68) ±10.3	17.63 (6.2-38.6) ±6.1	1.21 (0.38-3.73) ±0.6	29.29 (25-32) ±1.7	95.77 (35-241) ±42.5

**Table 4. 6** The scatter plot shows the correlation between the AGD and mAs ( $R^2 = 0.89$ ) of patient study in W/Ag

View (image)	Target/ Filter	Compress Breast thickness (mm)	Compression Force (lbs.)	AGD (mGy)	kVp	mAs
		Mean (Range) $\pm$ SD	Mean (Range) $\pm$ SD	Mean (Range) $\pm$ SD	Mean (Range) $\pm$ SD	Mean (Range) $\pm$ SD
RCC (100)	W/Ag	81 (70-116) $\pm$ 7.7	14.15 (4.7-29.4) $\pm$ 4.7	1.79 (0.97-4.23) $\pm$ 0.6	31.79 (30-38) $\pm$ 1.5	113.34 (64-305) $\pm$ 38.4
LCC (100)	W/Ag	82.2 (68-110) $\pm$ 10.1	13.1 (5.6-25.8) $\pm$ 4.7	1.78 (1.09-4.85) $\pm$ 0.6	32.1 (30-37) $\pm$ 1.4	112.21 (70-337) $\pm$ 38.9
RMLO (100)	W/Ag	79.56 (69-110) $\pm$ 7.6	17.85 (7.7-31.3) $\pm$ 5.8	1.78 (1.09-4.85) $\pm$ 0.6	31.5 (30-37) $\pm$ 1.5	115 (18.8-322) $\pm$ 40.9
LMLO (100)	W/Ag	80.12 (66-104) $\pm$ 8.2	18.4 (7.5-33.2) $\pm$ 6.3	1.76 (1.04-4.8) $\pm$ 0.6	31.77 (30-36) $\pm$ 1.5	112.81 (71-297) $\pm$ 35.8

**Table 4. 7** The parameters of W/Rh in 100 patients in right cranio-caudal view (RCC).

	Patient no	Filter	kVp	mAs	AGD (mGy)	ESD (mGy)	EI	CF (lbs.)	CBT (mm)
1	1403441	Rh	31	88	1.09	4.28	393	9.9	60
2	5785539	Rh	31	59	0.7	2.93	396	4.1	64
3	10776655	Rh	31	188	2.26	9.25	393	6.3	63
4	8171650	Rh	31	137	1.64	6.73	394	11.6	63
5	2333147	Rh	31	140	1.73	6.78	389	8.6	60
6	8848355	Rh	27	80	0.91	2.5	304	22.9	36
7	8104959	Rh	32	160	2.01	8.57	442	13.6	67
8	10051859	Rh	30	162	1.94	7.17	352	11	55
9	8681731	Rh	28	48	0.51	1.91	317	11.2	54
10	2245748	Rh	32	80	1.03	4.26	453	6.6	65
11	1403441	Rh	31	88	1.09	4.28	393	9.9	60
12	5785539	Rh	31	59	0.7	2.93	396	4.1	64
13	10776655	Rh	31	188	2.26	9.25	393	6.3	63
14	8171650	Rh	31	137	1.64	6.73	394	11.6	63
15	2333147	Rh	31	140	1.73	6.78	389	8.6	60
16	8848355	Rh	27	80	0.91	2.5	304	22.9	36
17	8104959	Rh	32	160	2.01	8.57	442	13.6	67
18	8713059	Rh	31	103	1.25	5.05	394	6.8	62
19	10051859	Rh	30	162	1.94	7.17	352	11	55
20	3974447	Rh	31	139	1.72	6.67	390	9.5	60
21	5274246	Rh	31	86	1.04	4.21	396	10.6	61
22	6004541	Rh	29	147	1.67	5.86	316	10.3	50
23	6980646	Rh	32	128	1.59	6.88	440	5.9	68
24	12002846	Rh	29	98	1.08	3.95	314	7.7	53
25	8212749	Rh	30	88	1	3.93	353	11	58
26	3727559	Rh	32	125	1.55	6.71	448	9.3	68
27	14393442	Rh	28	48	0.49	1.74	304	12.7	49
28	8392249	Rh	29	57	0.63	2.26	315	10.6	51
29	9215859	Rh	27	112	1.2	3.54	296	14.9	39
30	1318344	Rh	30	86	0.98	3.86	356	11.9	59
31	10358742	Rh	31	76	0.93	3.71	403	9.7	61
32	9754852	Rh	32	143	1.79	7.65	441	16	67
33	9869359	Rh	31	152	1.82	7.46	395	13.9	63
34	3935055	Rh	28	103	1.15	3.68	301	15.7	44
35	2430856	Rh	30	135	1.54	6.03	354	12.6	58
36	1020146	Rh	29	43	0.49	1.73	317	12.5	51
37	379642	Rh	29	104	1.13	4.19	315	9.4	54
38	7025856	Rh	27	127	1.4	4.03	304	27.3	38
39	10866058	Rh	26	46	0.55	1.26	301	3.2	27

40	8753936	Rh	30	94	1.05	4.21	356	5	59
41	6465156	Rh	31	126	1.52	6.15	398	11.8	62
42	4630053	Rh	28	86	0.96	3.07	303	12.7	44
43	196857	Rh	28	62	0.7	2.23	305	18.5	44
44	6220158	Rh	31	127	1.57	6.19	397	9	60
45	8625846	Rh	29	92	1.04	3.67	316	12.9	50
46	9653151	Rh	27	61	0.65	1.95	306	12.6	39
47	7035058	Rh	31	206	2.47	10.11	390	6.9	63
48	7034753	Rh	31	142	1.75	6.88	390	12.2	60
49	953450	Rh	28	128	1.35	4.65	297	11.6	48
50	33696257	Rh	32	150	1.93	7.96	451	17.8	65
51	14713042	Rh	26	53	0.62	1.44	307	9.1	28
52	13337745	Rh	30	52	0.6	2.31	347	16.4	57
53	4572330	Rh	31	112	1.36	5.5	396	11.6	62
54	4935930	Rh	32	85	1.08	4.53	448	8.6	66
55	826749	Rh	30	46	0.54	2.04	353	11.7	56
56	3192246	Rh	28	64	0.73	2.28	298	13.2	43
57	3030749	Rh	29	91	0.99	3.68	317	16	53
58	5951833	Rh	29	104	1.19	4.15	322	9.1	50
59	1264171	Rh	27	70	0.76	2.23	305	13	38
60	5527959	Rh	28	98	1.05	3.5	302	10.1	46
61	10450358	Rh	30	205	2.45	9.07	355	12	55
62	8715256	Rh	29	116	1.3	4.67	313	15.1	52
63	1270854	Rh	28	96	1.13	3.4	321	20.2	41
64	1847140	Rh	30	101	1.2	4.46	354	13.3	55
65	10373959	Rh	29	118	1.32	4.73	320	7.5	51
66	930650	Rh	28	32	0.37	1.11	307	12.7	40
67	9429541	Rh	31	92	1.13	4.44	392	15.7	60
68	3301129	Rh	32	66	0.83	3.51	449	18.3	66
69	335549	Rh	30	74	0.86	3.27	355	15.2	57
70	13869740	Rh	31	74	0.87	3.6	394	15	63
71	52346728	Rh	28	84	0.91	3.01	304	21.4	46
72	7911458	Rh	31	108	1.31	5.3	396	15.3	62
73	9790532	Rh	29	55	0.62	2.21	315	17.6	51
74	14997540	Rh	32	104	1.27	5.59	447	16.9	69
75	10796238	Rh	28	110	1.19	3.95	306	11.8	46
76	7350958	Rh	32	215	2.74	11.46	446	11.2	66
77	167753	Rh	29	146	1.59	5.9	313	9.2	54
78	10066731	Rh	26	64	0.65	1.78	307	10.5	34
79	530932	Rh	29	100	1.15	4	316	8.2	50
80	13102943	Rh	29	79	0.89	3.16	317	11.5	50
81	8332651	Rh	30	196	2.21	8.78	348	13.4	59
82	11426049	Rh	29	74	0.82	2.99	317	26.1	53
83	52289030	Rh	31	66	0.81	3.2	397	26.6	60

84	589348	Rh	30	47	0.55	2.06	358	17	55
85	5811053	Rh	30	71	0.82	3.17	357	13	57
86	9796341	Rh	31	54	0.65	2.63	396	12.9	61
87	9087158	Rh	29	111	1.25	4.44	309	12.2	51
88	4239347	Rh	30	159	1.85	7.07	354	25.2	57
89	7149359	Rh	31	316	3.84	15.51	388	15.4	62
90	7907440	Rh	30	122	1.46	5.38	356	20.8	55
91	7761456	Rh	26	69	0.71	1.9	304	13.8	33
92	1378457	Rh	30	196	2.21	8.77	354	26.8	59
93	5906959	Rh	28	76	0.77	2.75	299	21.6	49
94	9481152	Rh	30	96	1.15	4.25	354	17.1	55
95	1492459	Rh	30	128	1.51	5.65	353	31.6	56
96	1229829	Rh	31	131	1.62	6.38	397	18.7	60
97	5702355	Rh	26	55	0.68	1.5	300	17.4	26
98	9717259	Rh	25	36	0.43	0.85	302	11.9	21
99	5692458	Rh	32	143	1.84	7.59	440	8.8	65
100	8497655	Rh	32	139	1.75	7.42	440	10	67

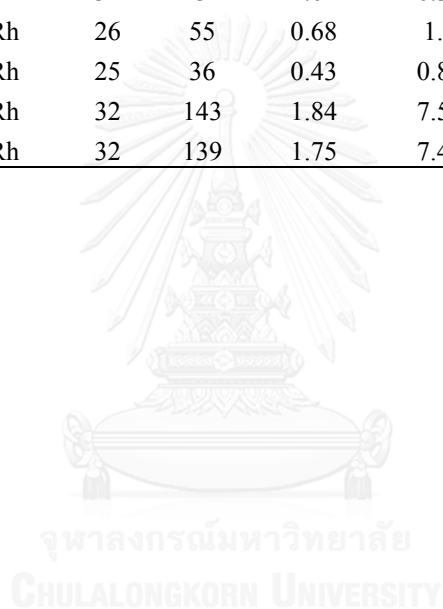


**Table 4. 8** The parameters of W/Rh in 100 patients in right medio-lateral view (RMLO).

	Patient no	Filter	kVp	mAs	AGD (mGy)	ESD (mGy)	EI	CF (lbs.)	CBT (mm)
1	1403441	Rh	30	82	0.93	3.69	355	7.7	59
2	5785539	Rh	31	62	0.76	3.03	396	11.8	61
3	10776655	Rh	30	165	1.89	7.38	356	4.6	58
4	8171650	Rh	30	117	1.31	5.23	356	11.6	59
5	2333147	Rh	29	106	1.2	4.25	316	9.5	51
6	8848355	Rh	27	80	0.87	2.54	307	8.8	38
7	8104959	Rh	28	96	0.99	3.5	303	19.5	49
8	10051859	Rh	28	139	1.43	5.05	310	10.5	49
9	8681731	Rh	30	49	0.57	2.15	358	15.1	55
10	2245748	Rh	32	85	1.09	4.5	457	8.3	65
11	1403441	Rh	30	82	0.93	3.69	355	7.7	59
12	5785539	Rh	31	62	0.76	3.03	396	11.8	61
13	10776655	Rh	30	165	1.89	7.38	356	4.6	58
14	8171650	Rh	30	117	1.31	5.23	356	11.6	59
15	2333147	Rh	29	106	1.2	4.25	316	9.5	51
16	8848355	Rh	27	80	0.87	2.54	307	8.8	38
17	8104959	Rh	28	96	0.99	3.5	303	19.5	49
18	8713059	Rh	30	110	1.24	4.92	359	8.9	59
19	10051859	Rh	28	139	1.43	5.05	310	10.5	49
20	3974447	Rh	30	145	1.64	6.5	354	16.8	59
21	5274246	Rh	31	92	1.1	4.5	398	10.3	62
22	6004541	Rh	28	100	1.15	3.53	306	10.9	42
23	6980646	Rh	32	124	1.53	6.73	448	11.1	68
24	12002846	Rh	32	81	1.04	4.28	455	11.7	65
25	8212749	Rh	29	80	0.86	3.22	318	16.5	54
26	3727559	Rh	29	86	0.93	3.47	319	22.2	54
27	14393442	Rh	28	44	0.48	1.57	310	18.5	45
28	8392249	Rh	28	45	0.49	1.61	311	19.3	44
29	9215859	Rh	28	58	0.65	2.06	308	21.6	44
30	1318344	Rh	31	79	0.98	3.84	397	14.5	60
31	10358742	Rh	28	58	0.6	2.09	310	23.1	49
32	9754852	Rh	32	141	1.78	7.48	449	30.4	66
33	9869359	Rh	32	200	2.56	10.6	453	33.3	65
34	3935055	Rh	28	92	1	3.3	303	14.1	45
35	2430856	Rh	29	105	1.19	4.21	315	22.5	51
36	1020146	Rh	26	53	0.62	1.46	306	20.4	28
37	379642	Rh	28	87	0.93	3.15	312	23.5	47
38	7025856	Rh	28	145	1.6	5.21	309	27.7	45



39	10866058	Rh	26	59	0.71	1.6	303	19.1	26
40	8753936	Rh	28	58	0.65	2.04	308	20.5	43
41	6465156	Rh	29	97	1.05	3.94	322	24	54
42	4630053	Rh	28	86	1	3.03	312	26.2	41
43	196857	Rh	28	79	0.87	2.82	309	26.3	45
44	6220158	Rh	30	114	1.31	5.09	363	13.8	58
45	8625846	Rh	28	66	0.77	2.33	314	13	41
46	9653151	Rh	28	63	0.73	2.25	308	29.4	42
47	7035058	Rh	30	182	2.09	8.14	360	8.3	58
48	7034753	Rh	29	129	1.42	5.21	323	19.6	53
49	953450	Rh	27	94	1.05	2.98	310	26.3	37
50	33696257	Rh	31	161	1.93	7.92	401	28	63
51	14713042	Rh	25	41	0.48	0.97	301	22.5	21
52	13337745	Rh	29	55	0.59	2.21	323	17.2	54
53	4572330	Rh	30	96	1.09	4.28	360	11.8	58
54	4935930	Rh	31	72	0.87	3.51	401	11.4	61
55	826749	Rh	31	62	0.76	3.02	398	17.2	60
56	3192246	Rh	28	66	0.77	2.34	309	21.5	41
57	3030749	Rh	29	83	0.93	3.33	320	23.6	51
58	5951833	Rh	28	72	0.82	2.55	310	16.7	42
59	12641741	Rh	27	76	0.82	2.43	308	20.2	39
60	5527959	Rh	27	84	0.97	2.66	319	21.9	36
61	10450358	Rh	28	175	1.81	6.36	306	11	49
62	8715256	Rh	28	101	1.1	3.6	306	27.6	45
63	1270854	Rh	27	77	0.88	2.44	310	21.7	36
64	1847140	Rh	28	70	0.8	2.5	308	28.8	43
65	10373959	Rh	27	94	1	2.98	313	15.7	39
66	930650	Rh	28	35	0.41	1.23	306	13.3	41
67	9429541	Rh	30	92	1.08	4.07	357	23	56
68	3301129	Rh	32	77	0.98	4.11	450	26.6	66
69	335549	Rh	30	101	1.15	4.53	362	10.7	59
70	13869740	Rh	31	65	0.8	3.15	401	16.1	60
71	52346728	Rh	31	78	0.92	3.81	400	16.9	64
72	7911458	Rh	30	90	1.04	4.03	359	16.1	58
73	9790532	Rh	29	53	0.57	2.14	320	14.8	54
74	14997540	Rh	32	86	1.08	4.59	456	15.1	67
75	10796238	Rh	26	81	0.83	2.26	307	27	34
76	7350958	Rh	29	148	1.63	5.96	318	27.9	53
77	167753	Rh	28	101	1.15	3.58	308	19.9	43
78	10066731	Rh	26	50	0.62	1.6	303	22.2	32
79	530932	Rh	28	69	0.82	2.42	309	16.5	40
80	13102943	Rh	27	60	0.68	1.88	306	21.5	36
81	8332651	Rh	29	136	1.53	5.48	316	11.9	52
82	11426049	Rh	30	74	0.87	3.26	362	19.5	56

83	52289030	Rh	32	68	0.87	3.63	457	17.1	66
84	589348	Rh	30	48	0.57	2.13	358	18.9	55
85	5811053	Rh	30	74	0.87	3.31	361	16.6	57
86	9796341	Rh	31	71	0.87	3.44	399	23.3	60
87	9087158	Rh	27	85	0.92	2.72	317	23.6	39
88	4239347	Rh	30	172	1.95	7.71	363	30.5	59
89	7149359	Rh	30	301	3.4	13.48	365	21.2	59
90	7907440	Rh	29	100	1.13	4	322	28.4	51
91	7761456	Rh	26	52	0.63	1.4	305	27.9	26
92	1378457	Rh	29	168	1.83	6.8	319	22.8	54
93	5906959	Rh	29	89	0.98	3.59	313	32.8	53
94	9481152	Rh	28	92	0.94	3.32	308	27.9	49
95	1492459	Rh	29	113	1.22	4.57	319	32.4	54
96	1229829	Rh	32	159	1.97	8.52	456	26.4	68
97	5702355	Rh	26	56	0.71	1.52	310	23.7	25
98	9717259	Rh	25	35	0.41	0.81	303	16.8	19
99	5692458	Rh	31	113	1.36	5.55	396	15	63
100	8497655	Rh	30	97	1.09	4.36	353	12.5	59

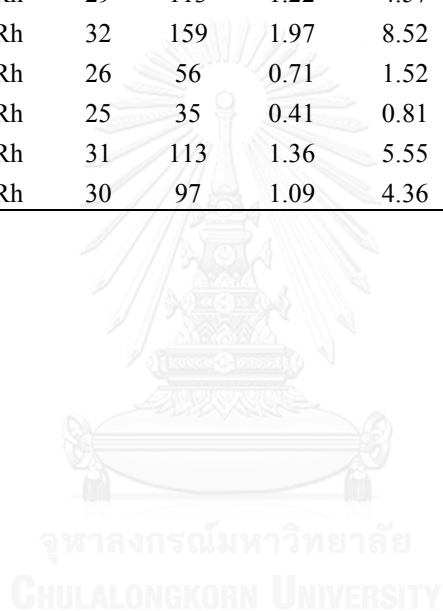


**Table 4. 9** The parameters of W/Rh in 100 patients in left cranio-caudal view (LCC).

	Patient no	Filter	kVp	mAs	AGD (mGy)	ESD (mGy)	EI	CF (lbs.)	CBT (mm)
1	1403441	Rh	30	74	0.86	3.27	356	5.4	57
2	5785539	Rh	32	65	0.83	3.45	451	5	65
3	10776655	Rh	31	179	2.19	8.73	394	5.5	61
4	8171650	Rh	31	127	1.53	6.23	395	10.5	62
5	2333147	Rh	30	124	1.46	5.48	356	6.5	56
6	8848355	Rh	28	97	1.08	3.46	303	7.6	44
7	8104959	Rh	30	124	1.42	5.53	359	8.2	58
8	10051859	Rh	30	198	2.28	8.84	366	9.1	58
9	8681731	Rh	29	45	0.49	1.79	317	7.3	52
10	2245748	Rh	32	79	1	4.21	452	5.6	66
11	1403441	Rh	30	74	0.86	3.27	356	5.4	57
12	5785539	Rh	32	65	0.83	3.45	451	5	65
13	10776655	Rh	31	179	2.19	8.73	394	5.5	61
14	8171650	Rh	31	127	1.53	6.23	395	10.5	62
15	2333147	Rh	30	124	1.46	5.48	356	6.5	56
16	8848355	Rh	28	97	1.08	3.46	303	7.6	44
17	8104959	Rh	30	124	1.42	5.53	359	8.2	58
18	8713059	Rh	30	93	1.1	4.11	358	9.2	55
19	10051859	Rh	30	198	2.28	8.84	366	9.1	58
20	3974447	Rh	32	152	1.94	8.11	451	6	66
21	5274246	Rh	31	91	1.07	4.48	396	5.7	64
22	6004541	Rh	29	188	2.05	7.63	311	11.2	54
23	6980646	Rh	32	110	1.38	5.82	445	11.3	66
24	12002846	Rh	31	87	1.03	4.26	399	11.3	64
25	8212749	Rh	30	80	0.92	3.59	356	15	58
26	3727559	Rh	31	119	1.42	5.86	403	9.4	63
27	14393442	Rh	28	52	0.55	1.87	310	11.8	46
28	8392249	Rh	28	43	0.46	1.53	317	13.4	46
29	9215859	Rh	26	114	1.18	3.18	330	18.9	34
30	1318344	Rh	30	77	0.88	3.45	357	14.5	58
31	10358742	Rh	30	62	0.71	2.78	359	15	58
32	9754852	Rh	29	96	1.05	3.89	320	25.6	53
33	9869359	Rh	32	154	1.97	8.17	458	10.9	65
34	3935055	Rh	28	116	1.26	4.15	321	16.6	45
35	2430856	Rh	31	161	1.93	7.92	408	9.1	63
36	1020146	Rh	28	40	0.43	1.42	314	15.9	44
37	379642	Rh	29	110	1.2	4.46	324	8.4	54
38	7025856	Rh	28	141	1.57	5.03	317	19.4	44
39	10866058	Rh	27	81	0.88	2.57	308	4.1	38

40	8753936	Rh	28	70	0.74	2.53	318	9	48
41	6465156	Rh	30	128	1.44	5.75	369	7.9	59
42	4630053	Rh	28	88	1.02	3.11	313	17.1	42
43	196857	Rh	27	59	0.63	1.86	306	21.2	39
44	6220158	Rh	30	122	1.43	5.4	366	7.8	56
45	8625846	Rh	27	62	0.66	1.98	312	11.5	39
46	9653151	Rh	27	64	0.7	2.02	313	18.6	38
47	7035058	Rh	29	142	1.6	5.67	327	5.4	51
48	7034753	Rh	31	180	2.15	8.81	407	9.2	63
49	953450	Rh	28	119	1.26	4.28	315	8.1	47
50	33696257	Rh	29	88	0.98	3.53	313	17.2	52
51	14713042	Rh	26	53	0.57	1.45	308	10.8	30
52	13337745	Rh	30	60	0.68	2.65	357	7.6	57
53	4572330	Rh	31	110	1.32	5.38	396	10.8	62
54	4935930	Rh	31	86	1.02	4.23	393	7.7	64
55	826749	Rh	31	63	0.76	3.1	394	5.3	63
56	3192246	Rh	28	79	0.86	2.84	315	9.5	46
57	3030749	Rh	30	98	1.18	4.34	362	15.3	55
58	5951833	Rh	28	73	0.87	2.57	317	10	40
59	12641741	Rh	28	78	0.89	2.75	318	11.1	42
60	5527959	Rh	28	84	0.97	2.99	319	9.6	42
61	10450358	Rh	29	164	1.87	6.55	325	8.5	50
62	8715256	Rh	29	118	1.31	4.75	326	9.9	52
63	1270854	Rh	28	104	1.16	3.73	316	7.5	44
64	1847140	Rh	29	97	1.08	3.91	326	17.1	52
65	10373959	Rh	28	110	1.2	3.95	323	12.9	45
66	930650	Rh	27	36	0.38	1.14	306	10.3	39
67	9429541	Rh	31	118	1.4	5.82	391	14.3	64
68	3301129	Rh	31	61	0.73	2.97	403	18.3	62
69	335549	Rh	30	78	0.92	3.45	358	16.7	56
70	13869740	Rh	31	68	0.82	3.3	404	15	62
71	52346728	Rh	31	73	0.87	3.56	402	19.5	63
72	7911458	Rh	31	110	1.35	5.38	399	16.3	61
73	9790532	Rh	29	54	0.57	2.18	319	16.4	54
74	14997540	Rh	32	91	1.15	4.84	450	10.4	66
75	10796238	Rh	28	120	1.24	4.36	310	13.8	49
76	7350958	Rh	30	222	3.15	14.17	512	17	71
77	167753	Rh	29	120	1.37	4.78	313	16.3	50
78	10066731	Rh	26	55	0.6	1.52	303	8.4	31
79	530932	Rh	28	103	1.05	3.73	309	11.4	49
80	13102943	Rh	28	73	0.8	2.61	307	15.5	45
81	8332651	Rh	31	200	2.4	9.84	402	12.6	63
82	11426049	Rh	29	63	0.7	2.53	323	20.5	52
83	52289030	Rh	30	64	0.73	2.89	357	26.1	59

84	589348	Rh	30	52	0.59	2.33	359	9.2	59
85	5811053	Rh	31	87	1.04	4.28	397	13.5	63
86	9796341	Rh	31	62	0.73	3.04	399	10.9	64
87	9087158	Rh	29	126	1.38	5.09	321	10.9	53
88	4239347	Rh	30	151	1.71	6.76	354	13.7	59
89	7149359	Rh	31	301	3.73	14.64	400	14.4	60
90	7907440	Rh	30	117	1.37	5.19	362	19.1	56
91	7761456	Rh	27	65	0.76	2.04	304	13.6	35
92	1378457	Rh	30	160	1.86	7.13	363	23.2	57
93	5906959	Rh	28	84	0.87	3.05	309	19.3	49
94	9481152	Rh	30	108	1.26	4.76	359	22.3	56
95	1492459	Rh	30	114	1.32	5.07	362	23.7	57
96	1229829	Rh	31	154	1.82	7.57	399	14.7	64
97	5702355	Rh	26	65	0.74	1.78	308	7.4	29
98	9717259	Rh	25	36	0.41	0.82	306	19.7	18
99	5692458	Rh	31	120	1.48	5.88	399	9.5	61
100	8497655	Rh	31	128	1.51	6.3	393	10.4	64

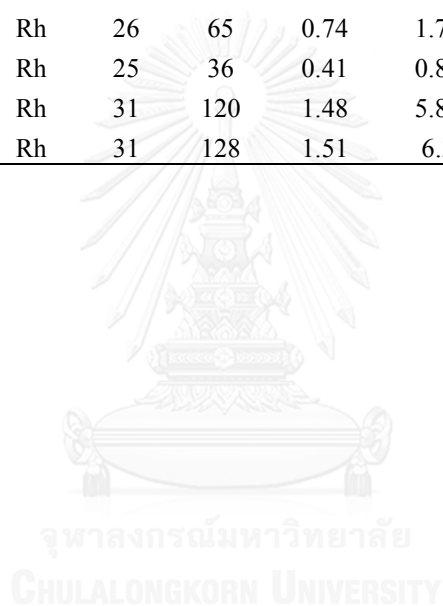


**Table 4. 10** The parameters of W/Rh in 100 patients in left medio-lateral view (LMLO).

	Patient no	Filter	kVp	mAs	AGD (mGy)	ESD (mGy)	EI	CF (lbs.)	CBT (mm)
1	1403441	Rh	30	68	0.82	3.01	356	9.6	55
2	5785539	Rh	32	62	0.8	3.28	450	12.6	65
3	10776655	Rh	31	189	2.27	9.28	391	6.2	63
4	8171650	Rh	32	143	1.84	7.57	452	13.2	65
5	2333147	Rh	30	119	1.41	5.28	356	14.3	56
6	8848355	Rh	27	82	0.89	2.6	304	18.6	38
7	8104959	Rh	29	111	1.2	4.5	318	28.1	54
8	10051859	Rh	29	135	1.54	5.4	315	14.1	50
9	8681731	Rh	30	49	0.57	2.16	356	12.6	56
10	2245748	Rh	32	72	0.93	3.81	451	10.5	65
11	1403441	Rh	30	68	0.82	3.01	356	9.6	55
12	5785539	Rh	32	62	0.8	3.28	450	12.6	65
13	10776655	Rh	31	189	2.27	9.28	391	6.2	63
14	8171650	Rh	32	143	1.84	7.57	452	13.2	65
15	2333147	Rh	30	119	1.41	5.28	356	14.3	56
16	8848355	Rh	27	82	0.89	2.6	304	18.6	38
17	8104959	Rh	29	111	1.2	4.5	318	28.1	54
18	8713059	Rh	31	116	1.38	5.69	400	15.5	63
19	10051859	Rh	29	135	1.54	5.4	315	14.1	50
20	3974447	Rh	31	160	1.94	7.82	397	17.9	62
21	5274246	Rh	30	66	0.76	2.93	355	11.6	57
22	6004541	Rh	27	99	1.07	3.16	307	13	39
23	6980646	Rh	31	86	1.02	4.25	391	14.3	64
24	12002846	Rh	31	75	0.89	3.66	394	12.3	62
25	8212749	Rh	30	85	1	3.78	353	9.6	56
26	3727559	Rh	30	88	1.04	3.86	356	19.8	55
27	14393442	Rh	28	46	0.46	1.63	309	12.4	48
28	8392249	Rh	28	46	0.49	1.64	307	11.7	47
29	9215859	Rh	28	74	0.78	2.68	307	24.5	47
30	1318344	Rh	29	64	0.7	2.59	315	10.9	54
31	10358742	Rh	29	55	0.62	2.2	320	23.7	51
32	9754852	Rh	31	127	1.53	6.19	395	38.6	62
33	9869359	Rh	32	196	2.5	10.44	460	22.9	66
34	3935055	Rh	28	99	1.07	3.55	303	19.4	46
35	2430856	Rh	29	113	1.25	4.55	318	13.3	53
36	1020146	Rh	28	44	0.44	1.57	309	15.3	48
37	379642	Rh	28	89	0.94	3.22	310	19.7	47
38	7025856	Rh	28	185	1.92	6.73	314	26.8	49
39	10866058	Rh	27	76	0.88	2.4	299	10.2	35

40	8753936	Rh	28	59	0.65	2.11	311	18.1	44
41	6465156	Rh	30	118	1.37	5.26	368	18.6	57
42	4630053	Rh	28	109	1.15	3.94	310	17.8	47
43	196857	Rh	28	69	0.74	2.46	311	25.4	45
44	6220158	Rh	29	101	1.14	4.03	323	21.4	51
45	8625846	Rh	27	55	0.62	1.74	304	11	37
46	9653151	Rh	28	58	0.68	2.06	311	25.1	41
47	7035058	Rh	28	118	1.35	4.21	324	12	43
48	7034753	Rh	30	148	1.75	6.57	358	11.1	56
49	953450	Rh	28	87	1.04	3.06	322	17.5	40
50	33696257	Rh	29	98	1.08	3.96	323	27.6	53
51	14713042	Rh	26	45	0.54	1.23	305	15.5	27
52	13337745	Rh	30	58	0.68	2.54	362	16.5	56
53	4572330	Rh	31	88	1.09	4.3	394	15.2	60
54	4935930	Rh	31	71	0.86	3.44	397	12.8	61
55	826749	Rh	31	63	1.76	3.05	395	15.2	62
56	3192246	Rh	28	64	0.74	2.26	310	16.6	41
57	3030749	Rh	29	85	0.97	3.39	323	19.8	50
58	5951833	Rh	28	64	0.76	2.25	312	11.2	40
59	12641741	Rh	27	80	0.86	2.54	310	20.1	39
60	5527959	Rh	27	83	0.91	2.63	320	15	38
61	10450358	Rh	28	176	1.85	6.38	322	10.6	48
62	8715256	Rh	28	88	0.98	3.16	316	19.3	44
63	1270854	Rh	28	86	1.02	3.01	308	17.6	40
64	1847140	Rh	28	97	0.99	3.51	315	25.1	49
65	10373959	Rh	27	89	0.98	2.82	313	16.9	38
66	930650	Rh	28	35	0.38	1.24	301	15	44
67	9429541	Rh	31	116	1.42	5.65	389	18.8	61
68	3301129	Rh	31	60	0.71	2.92	395	20.4	62
69	335549	Rh	30	90	1.02	4.03	357	13.3	59
70	13869740	Rh	31	71	0.85	3.48	397	12.5	63
71	52346728	Rh	30	75	0.85	3.35	357	29	59
72	7911458	Rh	31	93	1.11	4.53	397	13.1	62
73	9790532	Rh	30	60	0.71	2.63	357	12.2	55
74	14997540	Rh	31	69	0.85	3.33	398	17.7	60
75	10796238	Rh	28	82	0.92	2.94	305	15.4	44
76	7350958	Rh	31	176	2.16	8.61	393	12.8	61
77	167753	Rh	28	94	1.09	3.32	303	21.3	42
78	10066731	Rh	27	63	0.68	2	301	18.1	38
79	530932	Rh	28	75	0.83	2.68	304	21.1	44
80	13102943	Rh	28	69	0.81	2.45	305	16.6	41
81	8332651	Rh	31	222	2.63	10.96	393	14.9	64
82	11426049	Rh	29	61	0.68	2.44	316	25.2	51
83	52289030	Rh	32	76	0.93	4.05	447	20.2	68

84	589348	Rh	31	53	0.65	2.58	396	16	61
85	5811053	Rh	31	83	1.02	4.05	393	11.6	61
86	9796341	Rh	31	82	0.98	4.03	394	28.1	63
87	9087158	Rh	28	86	0.98	3.07	307	19.8	43
88	4239347	Rh	31	190	2.25	9.35	388	21.9	64
89	7149359	Rh	30	241	2.88	10.67	352	19.2	55
90	7907440	Rh	29	108	1.22	4.34	313	20.9	51
91	7761456	Rh	26	59	0.66	1.61	304	25.7	29
92	1378457	Rh	30	158	1.89	7.01	354	26.9	55
93	5906959	Rh	30	103	1.2	4.55	353	34	56
94	9481152	Rh	28	84	0.88	3.02	308	29.9	47
95	1492459	Rh	29	105	1.14	4.26	313	25.6	54
96	1229829	Rh	32	180	2.27	9.63	447	22.3	67
97	5702355	Rh	26	64	0.76	1.74	304	15	27
98	9717259	Rh	25	35	0.41	0.81	304	25.8	18
99	5692458	Rh	31	93	1.15	4.5	389	15.8	60
100	8497655	Rh	30	81	0.93	3.59	354	14	57

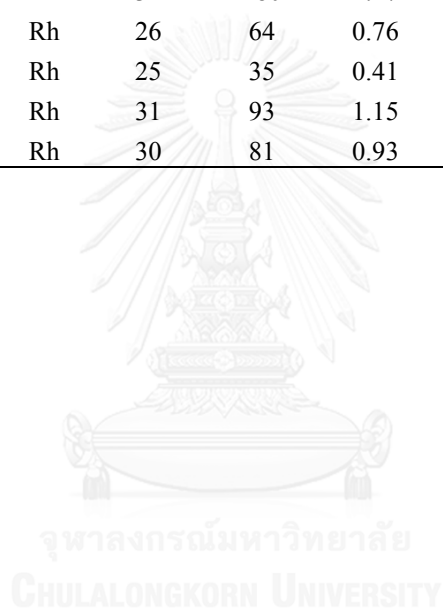




**Table 4. 11** The parameters of W/Ag in 100 patients in right cranio-caudal view (RCC).

	Patient no	Filter	kVp	mAs	AGD (mGy)	ESD (mGy)	EI	CF (lbs.)	CBT (mm)
1	8291640	Ag	31	112	1.64	7.96	519	8	79
2	9858046	Ag	30	188	2.65	12.05	511	9.9	72
3	10219259	Ag	31	177	2.66	12.52	511	11.3	77
4	5164536	Ag	30	136	1.92	8.72	508	13.5	72
5	1658958	Ag	34	182	3.26	16.64	509	16.5	90
6	2832339	Ag	31	98	1.49	6.88	512	6.4	75
7	6413154	Ag	30	80	1.15	5.09	506	15.8	70
8	5786641	Ag	34	112	2.03	10.34	519	11.1	94
9	6445153	Ag	32	131	2.1	10.06	530	7.6	80
10	8122659	Ag	32	113	1.83	8.69	516	7.4	80
11	3827731	Ag	32	96	1.51	7.44	523	11.6	83
12	6619959	Ag	31	94	1.42	6.59	515	5.3	76
13	1372958	Ag	31	134	2.04	9.47	513	6.3	76
14	6225451	Ag	32	105	1.7	8.09	528	7.5	80
15	1915656	Ag	33	129	2.16	10.97	515	6.5	88
16	4471158	Ag	32	121	1.95	9.36	513	8.7	81
17	5826430	Ag	30	96	1.37	6.09	510	6.9	70
18	12118551	Ag	30	79	1.09	5.11	510	8.6	74
19	10219259	Ag	31	177	2.66	12.52	511	11.3	77
20	4185652	Ag	30	144	1.99	9.32	512	12.8	74
21	4851353	Ag	32	134	2.12	10.36	516	11.8	82
22	14386841	Ag	34	83	1.48	7.57	516	10.4	90
23	5668856	Ag	32	92	1.46	7.09	515	13.3	82
24	10110459	Ag	31	78	1.16	5.46	506	13.5	76
25	7034952	Ag	32	80	1.29	6.15	505	12.9	80
26	7800948	Ag	34	134	2.42	12.35	516	8.8	93
27	1604155	Ag	33	146	2.44	12.32	508	17.8	87
28	6949953	Ag	32	110	1.75	8.52	518	16.9	82
29	5768849	Ag	32	115	1.82	8.96	508	20.6	83
30	4339738	Ag	35	87	1.74	8.64	523	11.9	96
31	7077150	Ag	33	84	1.42	7.05	522	13.6	86
32	3643334	Ag	31	100	1.48	7.13	516	13.7	79
33	5729554	Ag	32	93	1.44	7.25	509	7.7	84
34	395439	Ag	33	96	1.59	8.18	519	13.1	89
35	70151338	Ag	33	110	1.83	9.3	520	15.8	88
36	12321941	Ag	31	108	1.63	7.67	515	11.2	77
37	7008836	Ag	30	97	1.35	6.21	514	18.6	73
38	142855	Ag	31	158	2.34	11.18	507	17.3	78

39	10436558	Ag	35	208	4.19	20.82	514	9.4	99
40	4841642	Ag	33	75	1.26	6.36	518	15.6	87
41	9068058	Ag	33	97	1.64	8.18	519	14.9	86
42	7888156	Ag	31	83	1.25	5.82	512	12.6	76
43	10742958	Ag	30	71	1	4.57	513	14.7	72
44	6986545	Ag	30	172	2.41	11.09	510	21	73
45	6168840	Ag	34	97	1.75	8.97	514	14	94
46	9200158	Ag	33	126	2.1	10.63	522	16.2	87
47	149745	Ag	35	119	2.36	11.75	514	14.8	96
48	2961150	Ag	32	110	1.74	8.59	511	12.9	83
49	6018159	Ag	30	115	1.63	7.4	520	9.8	72
50	2172157	Ag	31	88	1.31	6.25	512	16.5	78
51	4660950	Ag	32	132	2.1	10.18	514	19.8	81
52	2454454	Ag	30	108	1.51	6.94	516	18.2	73
53	5441758	Ag	30	81	1.15	5.15	515	11.6	71
54	9171358	Ag	32	116	1.86	8.92	509	19.8	80
55	13749546	Ag	30	94	1.35	5.98	520	29.4	70
56	5847055	Ag	33	76	1.26	6.48	502	18.4	88
57	7789154	Ag	31	195	2.86	13.86	514	11.3	79
58	12196647	Ag	31	64	0.97	4.55	516	13.2	77
59	6692745	Ag	38	67	1.78	8.38	379	15.1	116
60	2292229	Ag	32	119	1.87	9.25	519	14.3	83
61	226960	Ag	30	305	4.23	19.71	503	23.9	74
62	33777255	Ag	33	151	2.53	12.78	499	19.4	87
63	2508235	Ag	32	71	1.09	5.51	513	18.8	84
64	7167752	Ag	32	117	1.84	9.15	512	12.8	84
65	33436457	Ag	32	97	1.54	7.48	516	9.8	81
66	70426441	Ag	31	105	1.61	7.36	510	4.7	75
67	851445	Ag	31	75	1.15	5.16	512	23.9	75
68	9685658	Ag	31	106	1.63	7.48	514	12.5	75
69	4851353	Ag	32	134	2.12	10.36	516	11.8	82
70	14386841	Ag	34	83	1.48	7.57	516	10.4	90
71	5668856	Ag	32	92	1.46	7.09	515	13.3	82
72	10110459	Ag	31	78	1.16	5.46	506	13.5	76
73	7034952	Ag	32	80	1.29	6.15	505	12.9	80
74	7800948	Ag	34	134	2.42	12.35	516	8.8	93
75	1604155	Ag	33	146	2.44	12.32	508	17.8	87
76	6949953	Ag	32	110	1.75	8.52	518	16.9	82
77	5768849	Ag	32	115	1.82	8.96	508	20.6	83
78	4339738	Ag	35	87	1.74	8.64	523	11.9	96
79	7077150	Ag	33	84	1.42	7.05	522	13.6	86
80	3643334	Ag	31	100	1.48	7.13	516	13.7	79
81	5729554	Ag	32	93	1.44	7.25	509	7.7	84
82	7751454	Ag	31	129	1.97	9.09	525	12.8	75

83	32696657	Ag	31	128	1.97	9.02	511	19.9	75
84	7219355	Ag	31	102	1.52	7.23	504	16.8	78
85	8874354	Ag	34	81	1.44	7.36	514	10.8	90
86	10218447	Ag	33	75	1.26	6.38	516	11.9	87
87	12485434	Ag	31	157	2.31	11.18	511	20.1	79
88	9431743	Ag	30	106	1.48	6.76	508	21.4	72
89	11879848	Ag	31	92	1.36	6.55	510	19	79
90	471149	Ag	30	87	1.2	5.59	518	17.5	73
91	11879848	Ag	31	92	1.36	6.55	510	19	79
92	471149	Ag	30	87	1.2	5.59	518	17.5	73
93	572750	Ag	31	83	1.22	5.88	519	14.1	78
94	318756	Ag	32	220	3.51	17.09	505	17.9	82
95	7318658	Ag	30	200	2.8	12.85	515	13.4	73
96	2264445	Ag	30	96	1.35	6.13	516	21.8	72
97	9049556	Ag	31	102	1.53	7.15	518	19.5	76
98	7842356	Ag	30	122	1.75	7.82	511	15.2	71
99	269154	Ag	31	80	1.19	5.69	503	25.2	78
100	13818146	Ag	32	110	1.75	8.47	520	17.3	81

**Table 4. 12** The parameters of W/Ag in 100 patients in right medio-lateral view (RMLO).

	Patient no	Filter	kVp	mAs	AGD (mGy)	ESD (mGy)	EI	CF (lbs.)	CBT (mm)
1	8291640	Ag	30	92	1.31	5.88	519	9.5	71
2	9858046	Ag	30	152	2.18	9.65	522	8.5	70
3	10219259	Ag	30	187	2.64	12.02	509	27	72
4	5164536	Ag	32	96	1.54	7.44	514	19.5	81
5	1658958	Ag	34	203	3.64	18.54	515	17.4	91
6	2832339	Ag	31	99	1.52	6.96	517	10	75
7	6413154	Ag	30	84	1.19	5.4	513	14.9	72
8	5786641	Ag	33	92	1.56	7.73	515	15	85
9	6445153	Ag	30	132	1.9	8.43	508	8.3	70
10	8122659	Ag	30	108	1.53	6.9	527	10.7	71
11	3827731	Ag	32	87	1.4	6.75	521	12.2	81
12	6619959	Ag	30	107	1.49	6.88	526	9.9	73
13	1372958	Ag	30	126	1.81	8.02	525	7.8	70
14	6225451	Ag	30	96	1.37	6.13	525	12.7	71
15	1915656	Ag	30	128	1.77	8.27	524	12.2	74
16	4471158	Ag	31	105	1.61	7.36	521	16	75
17	5826430	Ag	30	109	1.51	7.05	513	8.3	74
18	12118551	Ag	30	82	1.15	5.28	525	15	73
19	10219259	Ag	30	187	2.64	12.02	509	27	72
20	4185652	Ag	32	141	1.73	7.57	451	12.2	69
21	4851353	Ag	31	121	1.86	8.5	522	7.7	75
22	14386841	Ag	34	100	1.81	9.22	516	24.1	93
23	5668856	Ag	32	95	1.53	7.32	514	13	80
24	10110459	Ag	31	88	1.31	6.19	510	17	77
25	7034952	Ag	32	90	1.42	7.03	509	22.6	83
26	7800948	Ag	32	122	1.92	9.47	519	17.4	83
27	1604155	Ag	31	162	2.41	11.52	519	21.2	78
28	6949953	Ag	31	107	1.57	7.61	519	19.3	79
29	5768849	Ag	32	89	1.42	6.88	510	14	81
30	4339738	Ag	35	99	1.97	9.77	519	15.5	96
31	7077150	Ag	30	82	1.15	5.28	519	16.2	73
32	3643334	Ag	31	105	1.55	7.44	520	24.2	78
33	5729554	Ag	30	88	1.21	5.69	515	17.4	74
34	395439	Ag	33	93	1.54	7.9	516	14.2	88
35	70151338	Ag	33	109	1.81	9.22	518	15.3	88
36	12321941	Ag	31	107	1.63	7.53	525	13	76
37	7008836	Ag	30	90	1.26	5.8	528	11.2	73
38	142855	Ag	31	143	2.19	10.02	512	27.9	75
39	10436558	Ag	31	202	3.07	14.21	523	19.9	76

40	4841642	Ag	32	100	1.55	7.76	519	27.2	84
41	9068058	Ag	32	109	1.75	8.43	523	23.5	81
42	7888156	Ag	30	89	1.25	5.67	523	17.5	72
43	10742958	Ag	30	79	1.09	5.05	516	16.6	73
44	6986545	Ag	32	119	1.86	9.26	519	22.8	84
45	6168840	Ag	32	89	1.4	6.9	517	18.2	83
46	9200158	Ag	31	131	2.01	9.22	525	24.2	75
47	149745	Ag	32	122	1.9	9.51	518	15.8	84
48	2961150	Ag	33	113	1.93	9.48	518	17.1	85
49	6018159	Ag	30	128	1.76	8.25	521	10.8	74
50	2172157	Ag	30	101	1.42	6.48	518	24.5	72
51	4660950	Ag	32	116	1.86	8.96	517	14	81
52	2454454	Ag	30	102	1.43	6.51	522	20.9	72
53	5441758	Ag	30	102	1.44	6.57	517	23.6	72
54	9171358	Ag	31	156	2.3	11.11	517	21	79
55	13749546	Ag	31	95	1.42	6.69	518	24.8	77
56	5847055	Ag	35	85	1.71	8.52	515	15.7	99
57	7789154	Ag	30	164	2.31	10.52	524	14.6	72
58	12196647	Ag	33	82	1.36	6.94	514	18.2	88
59	6692745	Ag	37	68	1.66	7.96	406	14.5	110
60	2292229	Ag	31	131	1.95	9.31	520	19.8	78
61	226960	Ag	31	322	4.85	22.79	523	30.9	77
62	33777255	Ag	35	140	2.82	14.02	509	21.5	99
63	2508235	Ag	32	89	1.4	6.96	518	25.4	84
64	7167752	Ag	31	125	1.84	8.86	521	11	79
65	33436457	Ag	31	116	1.72	8.21	513	10	78
66	70426441	Ag	31	122	1.79	8.68	514	12.6	79
67	851445	Ag	32	80	1.4	6.19	516	14.3	84
68	9685658	Ag	31	99	1.52	6.96	519	12.7	75
69	4851353	Ag	31	121	1.86	8.5	522	7.7	75
70	14386841	Ag	34	100	1.81	9.22	516	24.1	93
71	5668856	Ag	32	95	1.53	7.32	514	13	80
72	10110459	Ag	31	88	1.31	6.19	510	17	77
73	7034952	Ag	32	90	1.42	7.03	509	22.6	83
74	7800948	Ag	32	122	1.92	9.47	519	17.4	83
75	1604155	Ag	31	162	2.41	11.52	519	21.2	78
76	6949953	Ag	31	107	1.57	7.61	519	19.3	79
77	5768849	Ag	32	89	1.42	6.88	510	14	81
78	4339738	Ag	35	99	1.97	9.77	519	15.5	96
79	7077150	Ag	30	82	1.15	5.28	519	16.2	73
80	3643334	Ag	31	105	1.55	7.44	520	24.2	78
81	5729554	Ag	30	88	1.21	5.69	515	17.4	74
82	7751454	Ag	31	200	2.97	14.19	514	22.8	78
83	32696657	Ag	33	98	1.67	8.22	521	31.3	85

84	7219355	Ag	31	134	1.98	9.47	508	26.7	78
85	8874354	Ag	32	96	1.51	7.44	520	16.9	83
86	10218447	Ag	30	89	1.26	5.71	515	22.8	89
87	12485434	Ag	30	165	2.32	10.56	508	29.6	72
88	9431743	Ag	32	105	1.68	8.07	518	17.7	80
89	11879848	Ag	32	83	1.31	6.42	517	14.4	82
90	4711149	Ag	32	80	1.29	6.15	520	20.1	80
91	11879848	Ag	32	83	1.31	6.42	517	14.4	82
92	4711149	Ag	32	80	1.29	6.15	520	20.1	80
93	572750	Ag	33	86	1.44	7.28	518	14.3	87
94	318756	Ag	32	243	3.84	18.93	522	26.9	83
95	7318658	Ag	31	214	3.15	15.22	521	12.3	79
96	2264445	Ag	32	104	1.66	7.98	525	22.3	80
97	9049556	Ag	31	18.8	1.59	7.46	523	18.8	77
98	7842356	Ag	30	170	2.36	11	517	25.5	74
99	269154	Ag	36	83	1.81	8.8	476	24.2	100
100	13818146	Ag	30	142	2.03	9.06	522	25.1	71

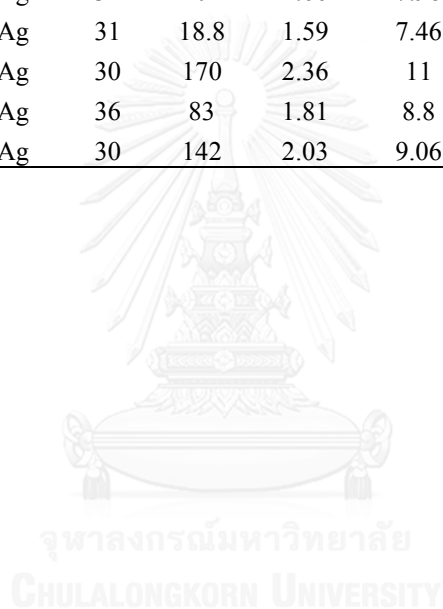


**Table 4. 13** The parameters of W/Ag in 100 patients in left cranio-caudal view (LCC).

	Patient no	Filter	kVp	mAs	AGD (mGy)	ESD (mGy)	EI	CF (lbs.)	CBT (mm)
1	8291640	Ag	30	106	1.48	6.84	518	8.2	73
2	9858046	Ag	31	175	2.65	12.31	516	8.9	76
3	10219259	Ag	30	150	2.14	9.6	505	9.8	71
4	5164536	Ag	33	94	1.54	7.98	511	11.9	89
5	1658958	Ag	34	168	3.03	15.4	510	14	91
6	2832339	Ag	31	101	1.53	7.05	514	5.7	75
7	6413154	Ag	31	87	1.32	6.09	511	13	75
8	5786641	Ag	34	114	2.07	10.53	519	11	94
9	6445153	Ag	31	137	2.09	9.63	512	7.9	75
10	8122659	Ag	32	112	1.81	8.61	521	7.6	80
11	3827731	Ag	32	97	1.51	7.53	522	8.9	84
12	6619959	Ag	31	101	1.51	7.11	522	5.6	77
13	1372958	Ag	30	127	1.83	8.09	531	10.1	70
14	6225451	Ag	32	107	1.73	8.25	524	11.2	80
15	1915656	Ag	33	117	1.99	9.8	523	9.6	85
16	4471158	Ag	33	113	1.9	9.59	527	11.4	87
17	5826430	Ag	32	119	1.47	6.36	451	7.3	68
18	12118551	Ag	31	77	1.18	5.4	524	9.3	75
19	10219259	Ag	30	150	2.14	9.6	505	9.8	71
20	4185652	Ag	30	149	2.07	9.61	516	8.6	74
21	4851353	Ag	32	124	1.98	9.6	514	8.8	81
22	14386841	Ag	34	86	1.54	7.9	517	8.8	94
23	5668856	Ag	32	103	1.62	7.98	512	6.6	83
24	10110459	Ag	31	90	1.32	6.42	505	9.4	79
25	7034952	Ag	32	70	1.11	5.4	507	13.7	81
26	7800948	Ag	33	119	1.99	10.06	515	10.2	87
27	1604155	Ag	31	185	2.74	13.09	527	25.4	78
28	6949953	Ag	33	92	1.55	7.75	520	13.3	86
29	5768849	Ag	32	110	1.75	8.55	510	11.8	82
30	4339738	Ag	34	92	1.66	8.52	530	11.8	94
31	7077150	Ag	32	77	1.2	5.96	512	12.1	83
32	3643334	Ag	32	82	1.31	6.34	522	10.6	81
33	5729554	Ag	32	79	1.26	6.09	526	11.6	81
34	395439	Ag	32	91	1.46	7.03	519	10.4	81
35	70151338	Ag	33	107	1.81	9.01	511	11.2	86
36	12321941	Ag	31	101	1.53	7.11	512	12.6	76
37	7008836	Ag	30	84	1.2	5.34	518	8.7	70
38	142855	Ag	30	164	2.27	10.59	528	12.9	74
39	10436558	Ag	35	212	4.21	20.9	536	13.5	95

40	4841642	Ag	32	79	1.26	6.07	510	25.8	80
41	9068058	Ag	30	115	1.62	7.34	525	22.5	72
42	7888156	Ag	31	92	1.38	6.51	530	13.5	77
43	10742958	Ag	32	99	1.55	7.69	512	8.9	83
44	6986545	Ag	35	105	2.08	10.36	525	13.2	95
45	6168840	Ag	34	94	1.7	8.64	521	14.3	93
46	9200158	Ag	30	119	1.64	7.67	528	20.9	74
47	149745	Ag	33	145	2.4	12.38	525	14.5	89
48	2961150	Ag	33	106	1.77	8.94	525	12.4	87
49	6018159	Ag	31	94	1.44	6.63	521	13.6	75
50	2172157	Ag	33	114	1.89	9.65	530	6	88
51	4660950	Ag	32	127	2.04	9.84	529	17	81
52	2454454	Ag	30	101	1.44	6.42	522	23.6	70
53	5441758	Ag	32	104	1.64	8.1	524	15.6	83
54	9171358	Ag	33	97	1.64	8.11	524	13.6	85
55	13749546	Ag	32	86	1.38	6.63	520	17.3	80
56	5847055	Ag	33	84	1.42	7.15	505	21.4	87
57	7789154	Ag	32	159	2.58	12.27	514	13	80
58	12196647	Ag	33	78	1.3	6.61	520	14.7	88
59	6692745	Ag	37	79	1.94	9.25	407	19.9	110
60	2292229	Ag	32	125	2	9.67	519	17.4	81
61	226960	Ag	30	337	4.76	21.62	533	18.8	72
62	33777255	Ag	33	128	2.15	10.82	497	20.5	87
63	2508235	Ag	33	72	1.22	6.03	520	20.4	85
64	7167752	Ag	31	110	1.67	7.69	523	9.8	75
65	33436457	Ag	33	122	2.08	10.31	520	10.5	86
66	70426441	Ag	31	120	1.83	8.47	518	8	76
67	851445	Ag	32	71	1.13	5.48	512	18.4	81
68	9685658	Ag	32	118	1.86	9.13	516	12.1	82
69	4851353	Ag	32	124	1.98	9.6	514	8.8	81
70	14386841	Ag	34	86	1.54	7.9	517	8.8	94
71	5668856	Ag	32	103	1.62	7.89	512	6.6	83
72	10110459	Ag	31	90	1.32	6.42	505	9.4	79
73	7034952	Ag	32	70	1.11	5.4	507	13.7	81
74	7800948	Ag	33	119	1.99	10.06	515	10.2	87
75	1604155	Ag	31	185	2.74	13.09	527	25.4	78
76	6949953	Ag	33	92	1.55	7.75	520	13.3	86
77	5768849	Ag	32	110	1.75	8.55	510	11.8	82
78	4339738	Ag	34	92	1.66	8.52	530	11.8	94
79	7077150	Ag	32	77	1.2	5.96	512	12.1	83
80	3643334	Ag	32	82	1.31	6.34	522	10.6	81
81	5729554	Ag	32	79	1.26	6.09	526	11.6	81
82	7751454	Ag	31	145	2.15	10.26	520	10.5	78
83	32696657	Ag	30	160	2.21	10.34	519	21.4	74



84	7219355	Ag	32	97	1.53	7.5	517	16.3	82
85	8874354	Ag	35	96	1.89	9.47	523	12.5	95
86	10218447	Ag	32	78	1.26	6.03	513	16.7	80
87	12485434	Ag	33	159	2.62	13.51	508	16.8	89
88	9431743	Ag	30	94	1.3	6.03	517	13.9	74
89	11879848	Ag	33	84	1.4	7.07	515	13.5	87
90	471149	Ag	32	76	1.18	5.88	514	11.8	84
91	11879848	Ag	33	84	1.4	7.07	515	13.5	87
92	471149	Ag	32	76	1.18	5.88	514	11.8	84
93	572750	Ag	34	121	2.18	11.09	520	18.8	91
94	318756	Ag	31	238	3.53	16.86	527	23.3	78
95	7318658	Ag	31	92	1.4	6.51	517	14.1	76
96	2264445	Ag	31	98	1.43	6.96	520	9.2	79
97	9049556	Ag	34	128	2.31	11.81	526	12.1	93
98	7842356	Ag	30	142	1.99	9.17	521	9.7	73
99	269154	Ag	32	76	1.19	5.86	513	23.7	83
100	13818146	Ag	33	119	1.97	10.13	526	10.8	89

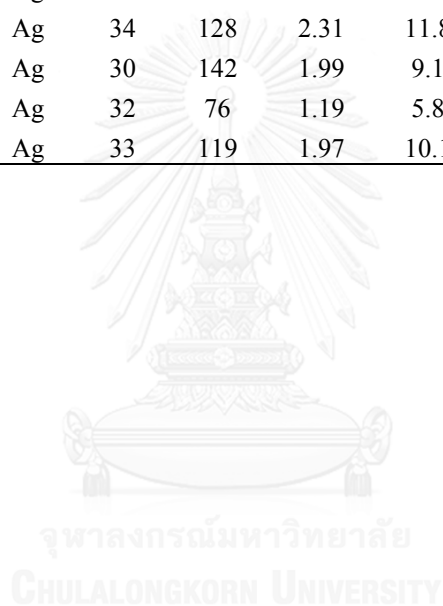
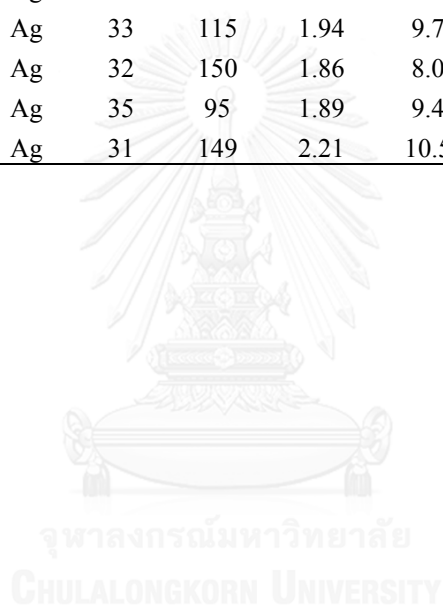


**Table 4. 14** The parameters of W/Ag in 100 patients in left medio-lateral view (LMLO).

	Patient no	Filter	kVp	mAs	AGD (mGy)	ESD (mGy)	EI	CF (lbs.)	CBT (mm)
1	8291640	Ag	32	93	1.14	5.01	446	12.7	69
2	9858046	Ag	32	136	1.73	7.23	447	13.8	66
3	10219259	Ag	30	181	2.55	11.59	505	33.2	72
4	5164536	Ag	34	80	1.43	7.34	510	13.5	91
5	1658958	Ag	34	193	3.51	17.86	506	18.7	94
6	2832339	Ag	30	96	1.33	6.15	514	10.9	73
7	6413154	Ag	30	80	1.14	5.13	507	16.4	71
8	5786641	Ag	32	105	1.64	8.14	513	16.4	83
9	6445153	Ag	30	129	1.84	8.22	511	7.5	71
10	8122659	Ag	31	101	1.53	7.09	517	11.3	76
11	3827731	Ag	33	88	1.49	7.38	521	10.3	85
12	6619959	Ag	31	95	1.41	6.73	518	11.4	78
13	1372958	Ag	32	146	1.78	7.84	448	9.4	69
14	6225451	Ag	30	96	1.33	6.17	521	12.7	73
15	1915656	Ag	31	111	1.64	7.92	524	12.3	79
16	4471158	Ag	31	120	1.81	8.51	523	8.9	77
17	5826430	Ag	30	124	1.72	8	508	8.8	74
18	12118551	Ag	31	88	1.31	6.23	521	11.1	77
19	10219259	Ag	30	181	2.55	11.59	505	33.2	72
20	4185652	Ag	30	131	1.88	8.35	518	19.3	70
21	4851353	Ag	30	125	1.74	8.09	518	11.9	74
22	14386841	Ag	35	98	1.97	9.85	513	26.4	99
23	5668856	Ag	31	103	1.54	7.28	509	11.7	77
24	10110459	Ag	31	81	1.22	5.65	511	20.7	75
25	7034952	Ag	31	94	1.38	6.63	514	27.3	78
26	7800948	Ag	32	128	2	10	513	19.3	84
27	1604155	Ag	30	167	2.36	10.69	521	26.7	72
28	6949953	Ag	32	96	1.53	7.38	511	15.9	81
29	5768849	Ag	31	101	1.53	7.11	510	21.8	76
30	4339738	Ag	34	86	1.53	7.84	522	13.1	90
31	7077150	Ag	31	82	1.22	5.78	515	17.9	77
32	3643334	Ag	30	100	1.42	6.42	521	22	72
33	5729554	Ag	31	81	1.19	5.76	527	12.3	79
34	395439	Ag	32	101	1.57	7.88	507	21.2	84
35	70151338	Ag	32	108	1.74	8.36	519	19.8	81
36	12321941	Ag	31	95	1.46	6.67	512	14.5	75
37	7008836	Ag	32	83	1.04	4.4	451	12.4	67
38	142855	Ag	30	175	2.41	11.27	515	26	74
39	10436558	Ag	31	221	3.29	15.68	528	22.6	78

40	4841642	Ag	35	83	1.64	8.22	517	19	96
41	9068058	Ag	31	101	1.49	7.15	513	17.7	78
42	7888156	Ag	31	89	1.33	6.32	523	13.6	77
43	10742958	Ag	34	133	2.41	12.28	514	14.6	93
44	6986545	Ag	34	102	1.84	9.35	514	15	91
45	6168840	Ag	32	85	1.37	6.51	518	20	80
46	9200158	Ag	31	105	1.61	7.36	520	21.4	75
47	149745	Ag	33	119	2	10.1	516	16.7	87
48	2961150	Ag	33	103	1.75	8.72	517	15.6	86
49	6018159	Ag	31	103	1.56	7.26	516	14	76
50	2172157	Ag	31	106	1.63	7.44	527	25.1	75
51	4660950	Ag	30	132	1.86	8.5	518	21.5	72
52	2454454	Ag	30	100	1.38	6.4	516	18.7	73
53	5441758	Ag	35	92	1.83	9.11	514	13.4	96
54	9171358	Ag	33	118	1.99	9.94	514	15.5	86
55	13749546	Ag	31	86	1.31	6.03	513	22	75
56	5847055	Ag	34	91	1.64	8.32	507	23.3	90
57	7789154	Ag	31	158	2.41	11.14	518	13	76
58	12196647	Ag	33	81	1.35	6.82	516	18	87
59	6692745	Ag	36	87	1.93	9.36	483	18.1	104
60	2292229	Ag	32	117	1.84	9.09	509	14.9	83
61	226960	Ag	32	297	4.8	22.9	525	19	80
62	33777255	Ag	35	133	2.66	13.27	501	20.6	99
63	2508235	Ag	33	85	1.42	7.17	519	29.8	87
64	7167752	Ag	31	101	1.52	7.15	508	13.7	77
65	33436457	Ag	32	130	2.04	10.14	513	10.3	84
66	70426441	Ag	31	111	1.65	7.82	513	13.5	77
67	851445	Ag	32	84	1.31	6.57	512	21.4	84
68	9685658	Ag	31	114	1.68	8.14	511	15.5	79
69	4851353	Ag	30	125	1.74	8.09	518	11.9	74
70	14386841	Ag	35	98	1.97	9.85	513	26.4	99
71	5668856	Ag	31	103	1.54	7.28	509	11.7	77
72	10110459	Ag	31	81	1.22	5.65	511	20.7	75
73	7034952	Ag	31	94	1.38	6.69	514	27.3	78
74	7800948	Ag	32	128	2	10	513	19.3	84
75	1604155	Ag	30	167	2.36	10.69	521	26.7	72
76	6949953	Ag	32	96	1.53	7.38	511	15.9	81
77	5768849	Ag	31	101	1.53	7.11	510	21.8	76
78	4339738	Ag	34	86	1.53	7.84	522	13.1	90
79	7077150	Ag	31	82	1.22	5.78	515	17.9	77
80	3643334	Ag	30	100	1.42	6.42	521	22	72
81	5729554	Ag	31	81	1.19	5.76	527	12.3	79
82	7751454	Ag	31	152	2.32	10.65	503	16.6	75
83	32696657	Ag	35	93	1.84	9.17	530	19.7	95

84	7219355	Ag	32	114	1.77	8.86	514	26.7	84
85	8874354	Ag	33	110	1.85	9.31	515	17.5	87
86	10218447	Ag	32	90	1.41	6.98	514	14.7	83
87	12485434	Ag	32	149	2.33	11.64	510	17.4	84
88	9431743	Ag	30	97	1.37	6.23	514	18.5	72
89	11879848	Ag	30	99	1.42	6.28	512	30	70
90	471149	Ag	31	91	1.4	6.42	508	33	75
91	11879848	Ag	30	99	1.42	6.28	512	30	70
92	471149	Ag	31	91	1.4	6.42	508	33	75
93	572750	Ag	34	71	1.26	6.46	525	10.1	90
94	318756	Ag	33	232	3.95	19.6	509	27.4	86
95	7318658	Ag	32	93	1.47	7.19	519	12.2	82
96	2264445	Ag	32	104	1.64	8.06	514	19.7	83
97	9049556	Ag	33	115	1.94	9.73	520	13.9	87
98	7842356	Ag	32	150	1.86	8.02	449	27.5	68
99	269154	Ag	35	95	1.89	9.44	509	28.2	98
100	13818146	Ag	31	149	2.21	10.55	522	24.9	78



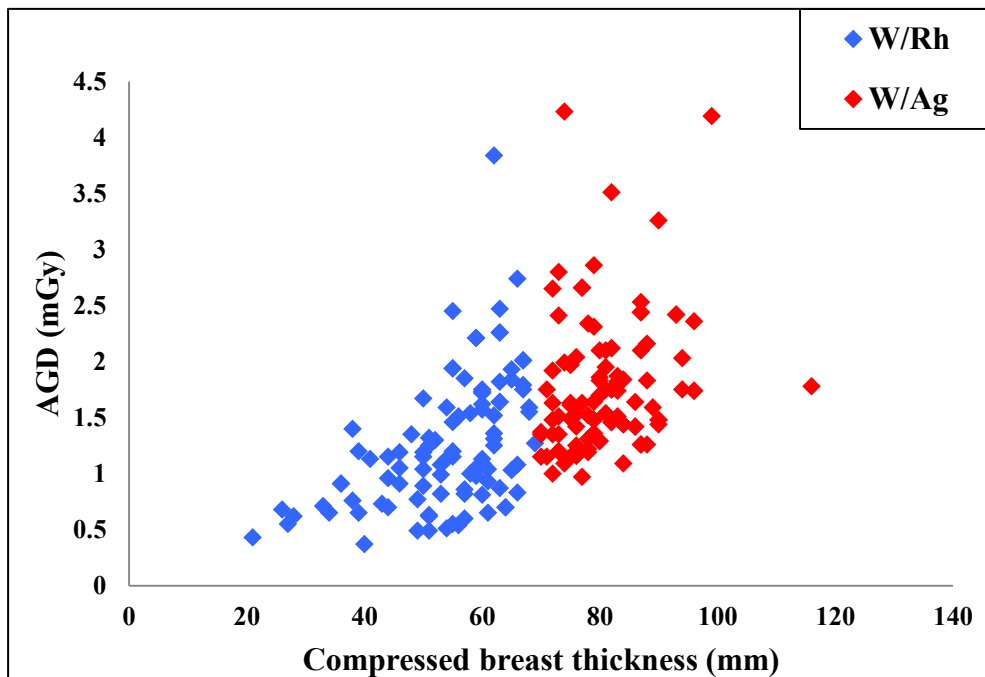


**Figure 4.19** AGD per exposure as a function of breast thickness in RCC view with W/Rh and W/Ag in patient study.

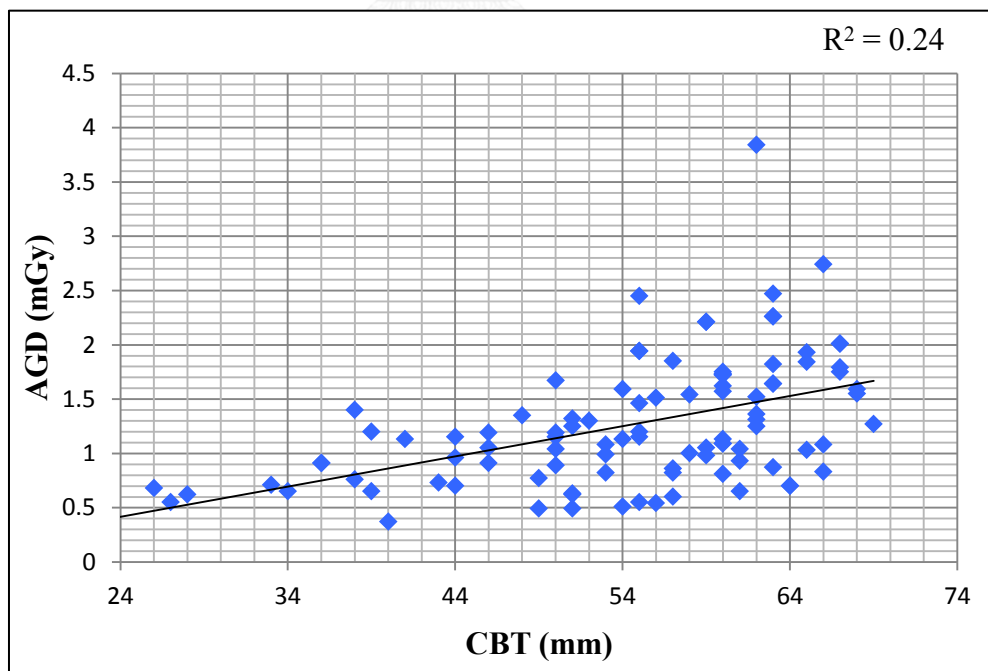


**Figure 4.20** The scatter plot shows the correlation between the AGD and CBT ( $R^2 = 0.24$ ) of patient study in W/Rh target-filter.

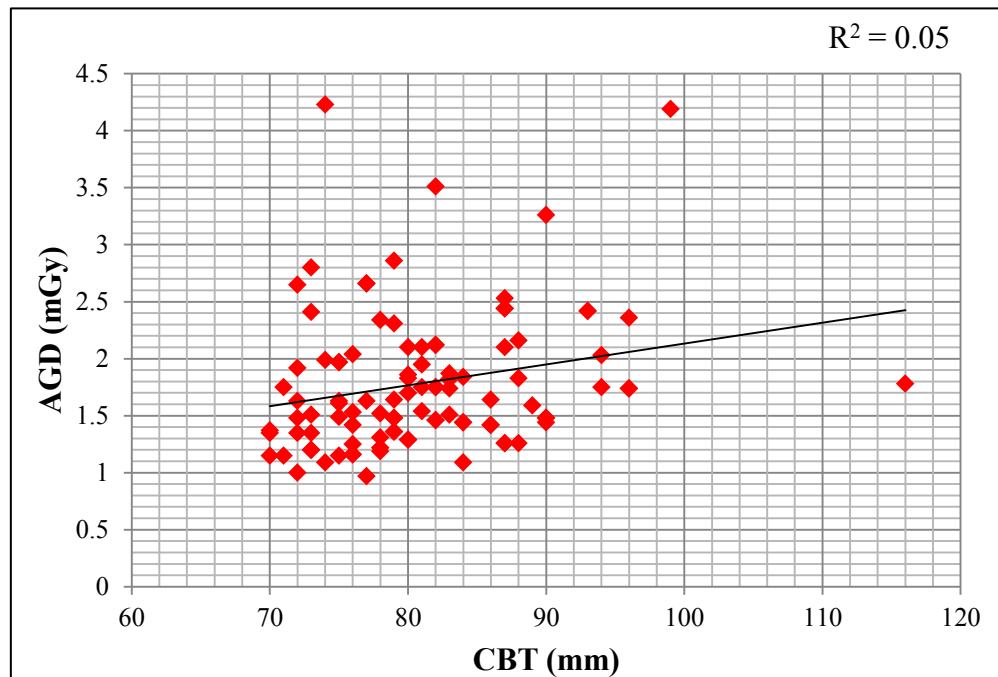


**Figure 4.21** The scatter plot shows the correlation between the AGD and CBT ( $R^2 = 0.05$ ) of patient study in W/Ag target-filter.

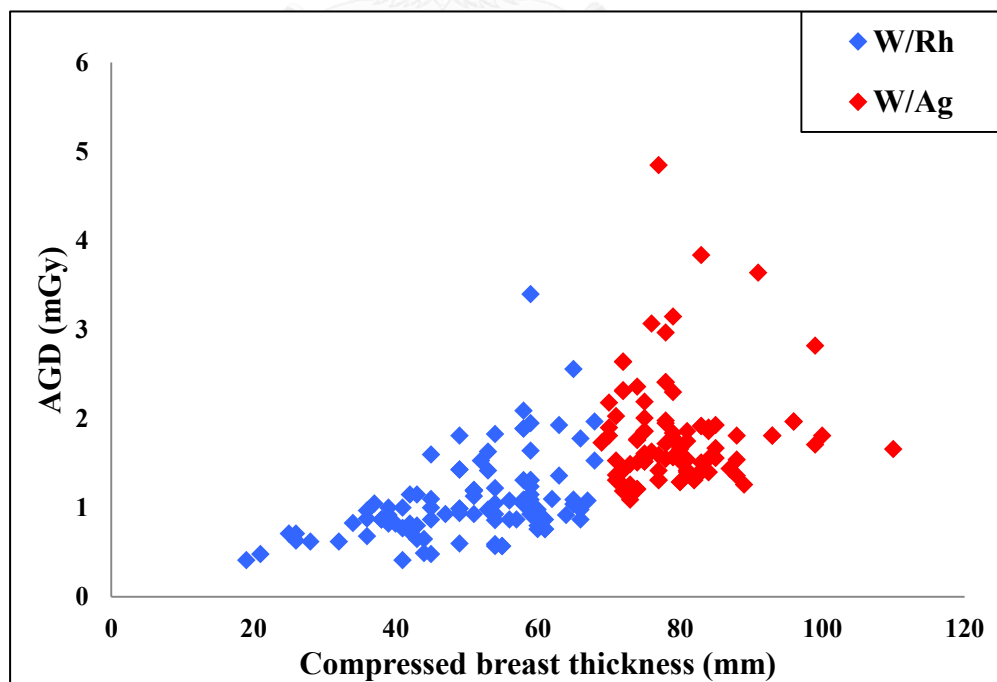


**Figure 4.22** AGD per exposure as a function of breast thickness in RMLO view with W/Rh and W/Ag in patient study.

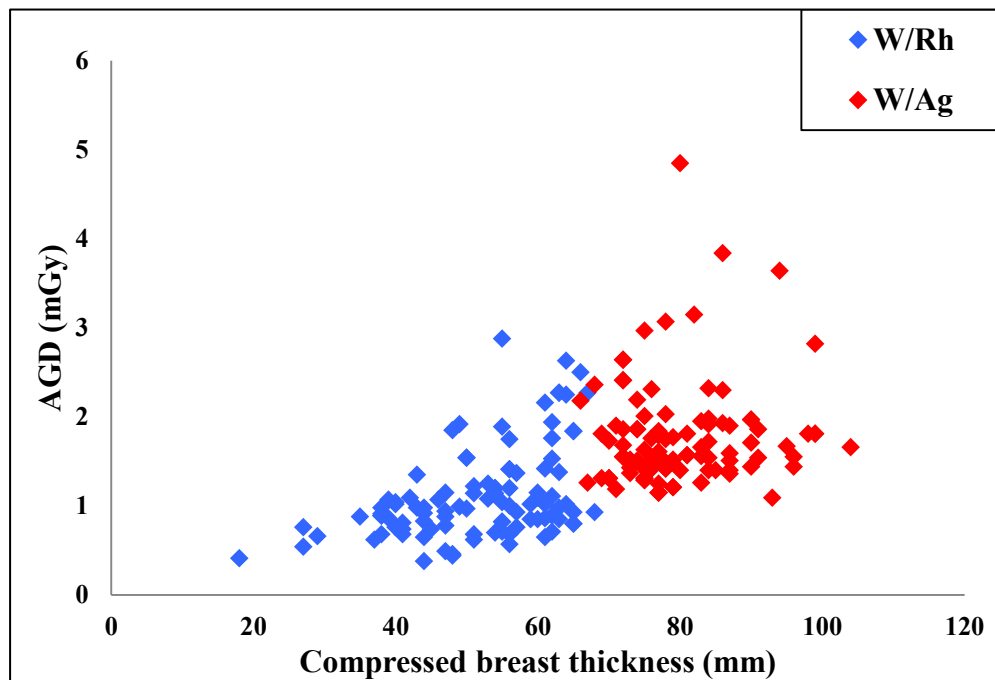


**Figure 4.23** AGD per exposure as a function of breast thickness in LMLO view with W/Rh and W/Ag in patient study.

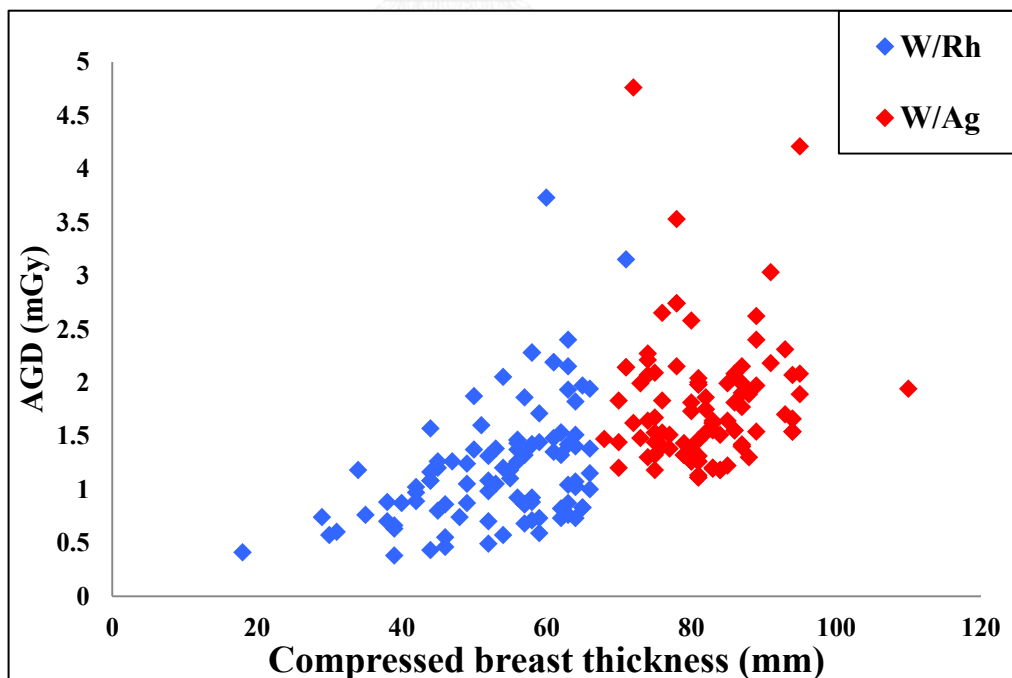


**Figure 4.24** AGD per exposure as a function of breast thickness in LCC view with W/Rh and W/Ag in patient study.

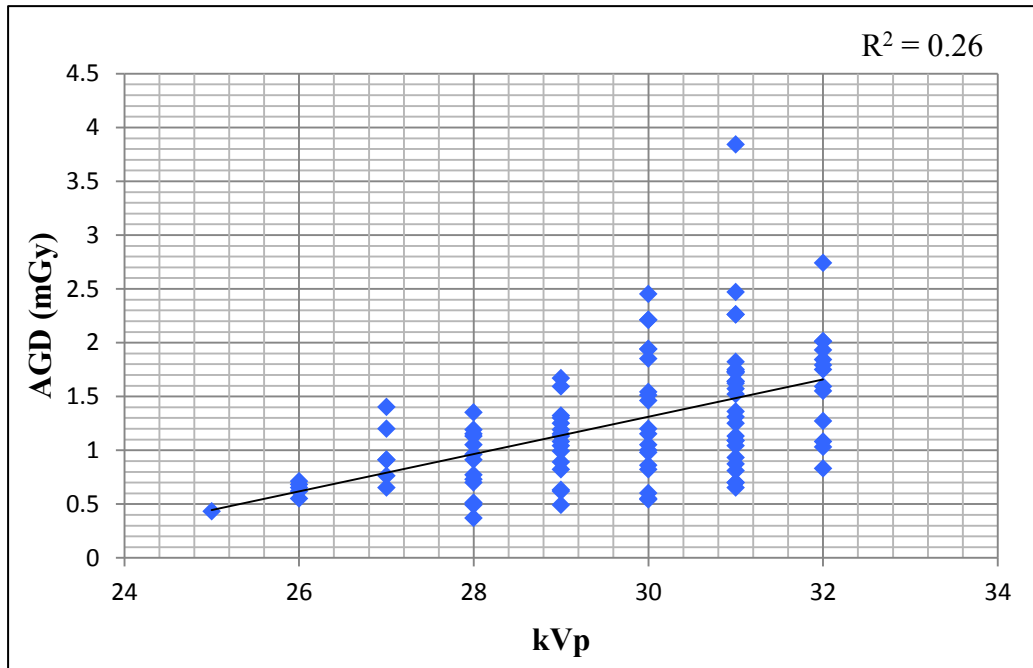


**Figure 4.25** The scatter plot shows the correlation between the AGD and kVp ( $R^2 = 0.26$ ) of patient study in W/Rh target-filter.

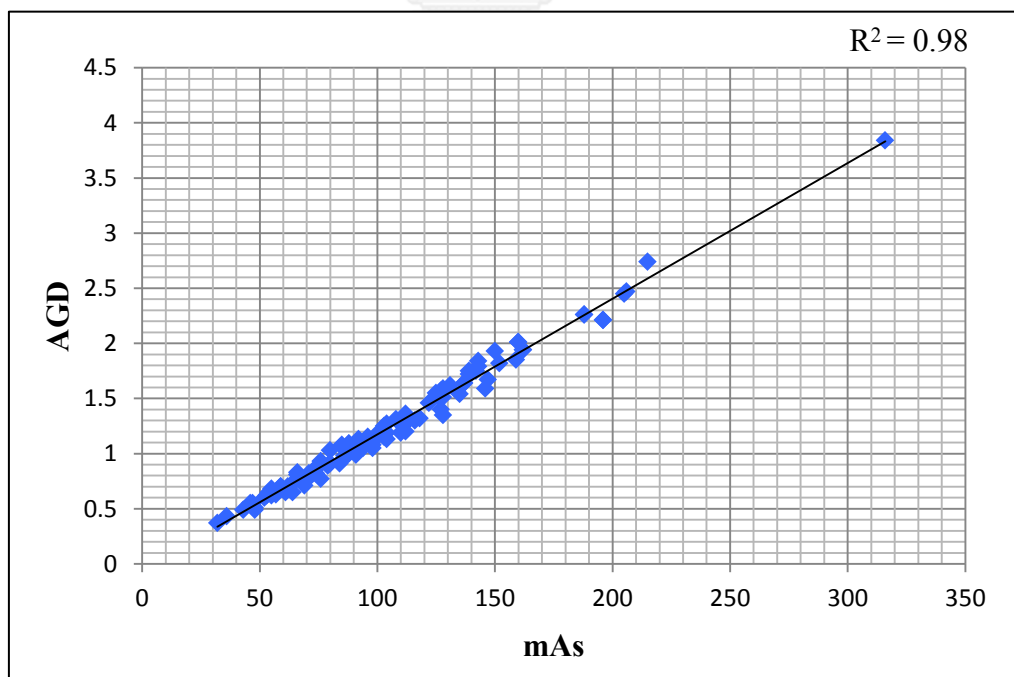


**Figure 4.26** The scatter plot shows the correlation between the AGD and mAs ( $R^2 = 0.98$ ) of patient study in W/Rh target-filter.



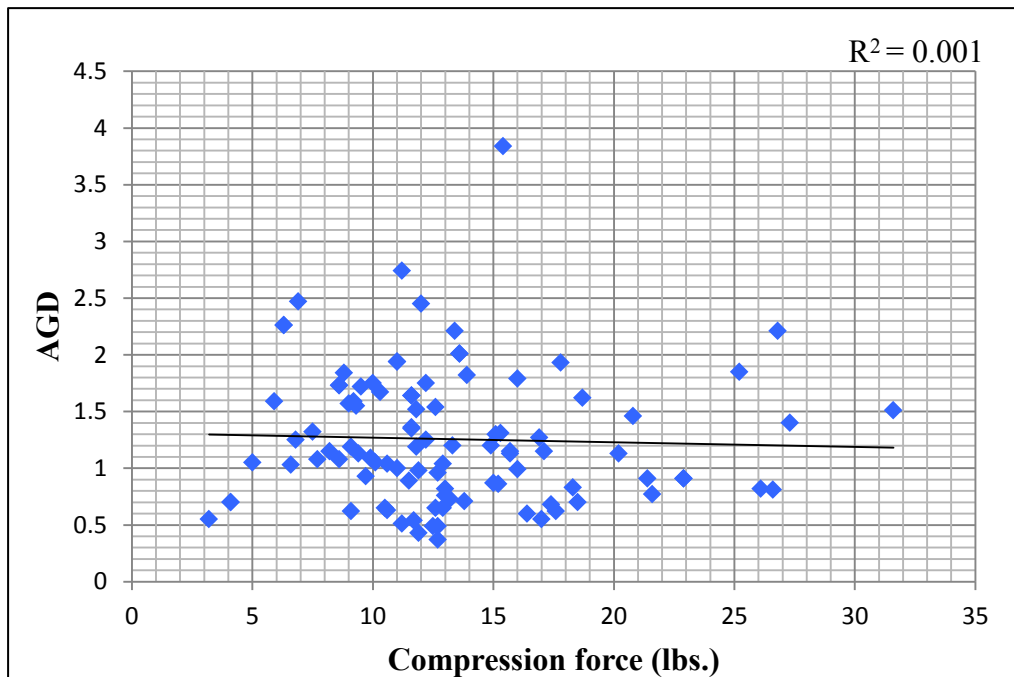


**Figure 4.27** The scatter plot shows the correlation between the AGD and compression force ( $R^2 = 0.001$ ) of patient study in W/Rh target-filter.

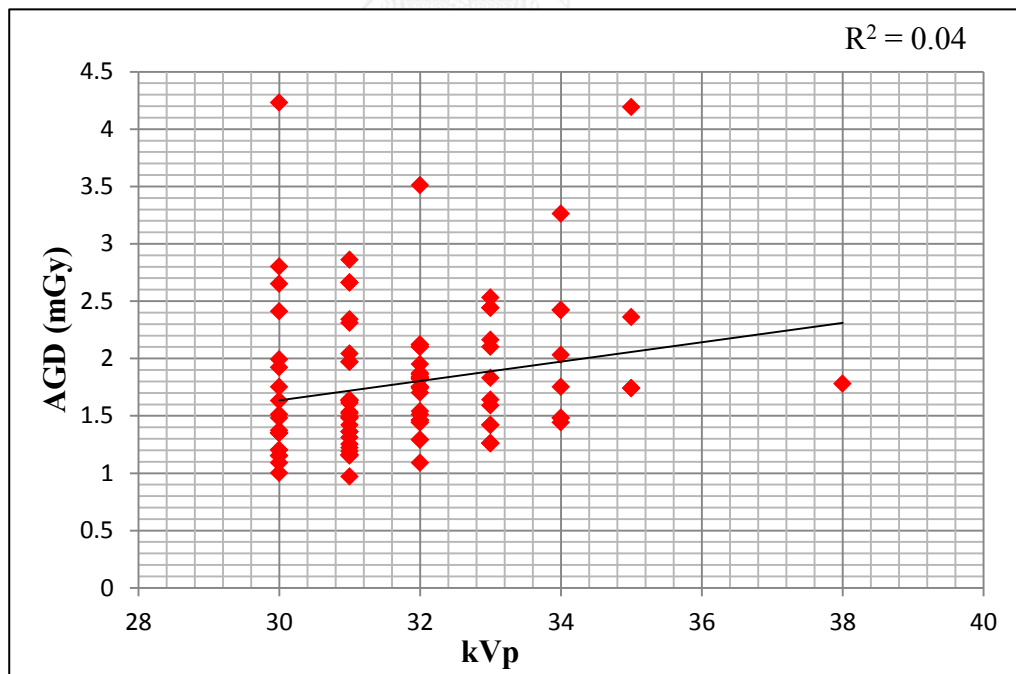


**Figure 4.28** The scatter plot shows the correlation between the AGD and kVp ( $R^2 = 0.04$ ) of patient study in W/Ag target-filter.

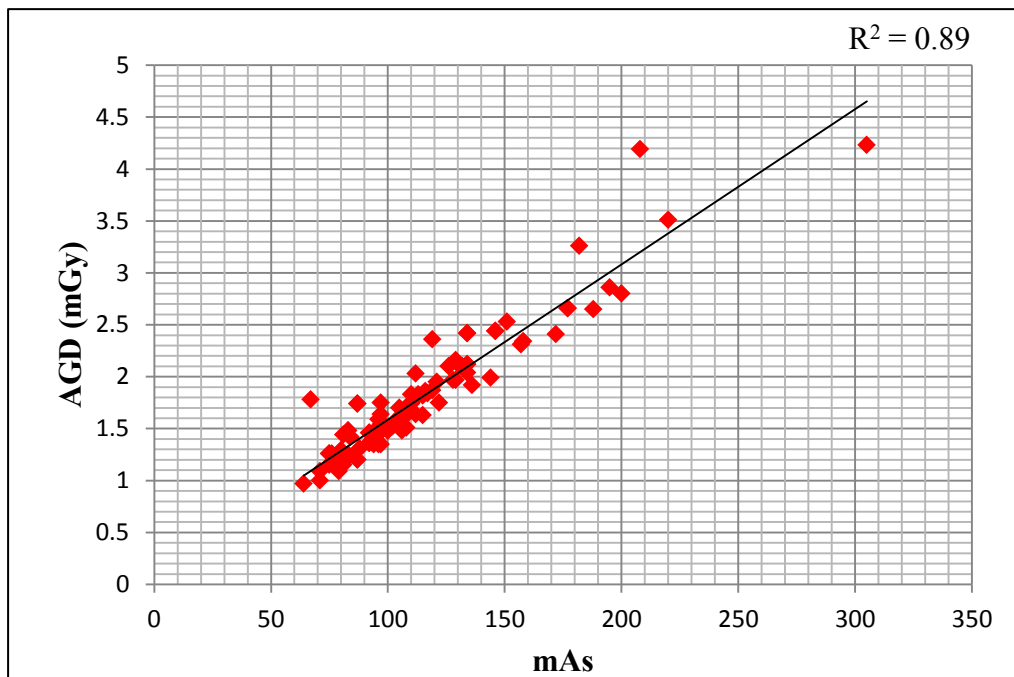


**Figure 4.29** The scatter plot shows the correlation between the AGD and mAs ( $R^2 = 0.89$ ) of patient study in W/Ag target-filter.

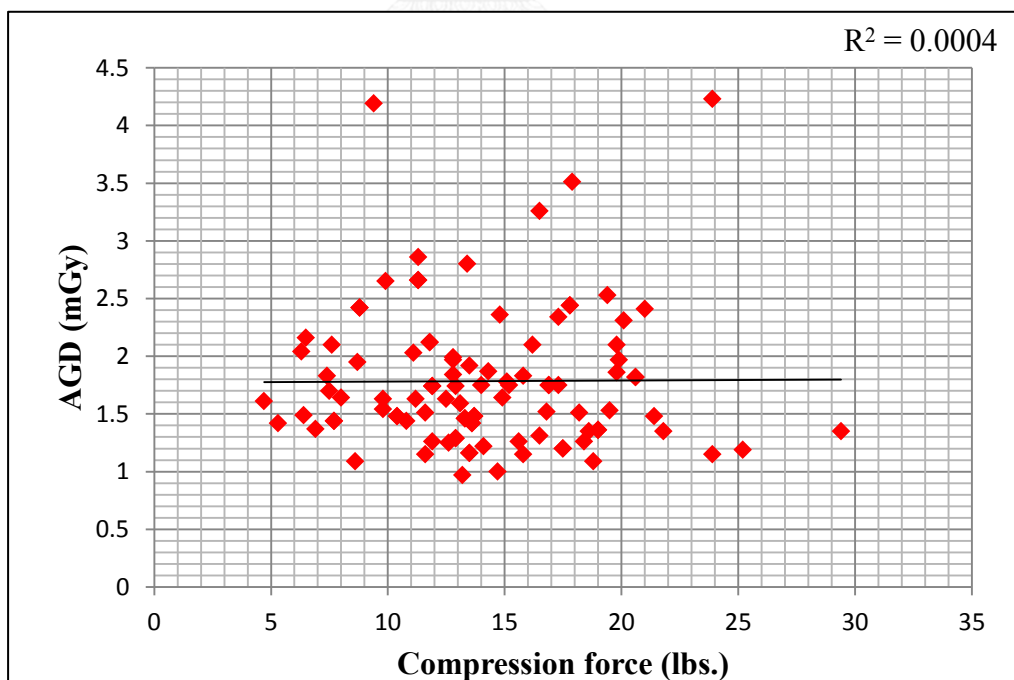


**Figure 4.30** The scatter plot shows the correlation between the AGD and compression force ( $R^2 = 0.0004$ ) of patient study in W/Ag target-filter.

## CHAPTER 5

### DISCUSSION AND CONCLUSION

#### 5.1 Discussion

##### 5.1.1 Image quality evaluation: the phantom study

5.1.1.1 Image quality evaluation for different thickness of mammography phantom.

Table 4.1 and 4.2 show that at CBT 40 mm and 50mm, the compression force is constant, the CNR decreased when the kVp increased at AEC technique. The SNR increased insignificantly with 40 and 50 mm phantom thickness. At 60 mm, the SNR decreased when the kVp increased and the mAs decreased. Table 4.3 shows that at 70 mm compressed breast thickness, the CNR and SNR decrease when the kVp increased and the mAs decreased. Table 4.4 shows that at 60 mm and 70 mm with 30 and 31 mAs, the SNR increases when the mAs decreased. When the kVp increased and the mAs decreased, CNR and SNR decreased because high kVp produces more penetrating x-ray beam and increases the scatter radiation; the image quality (CNR and SNR) decreases.

At 40 to 70 mm CBT of W/Rh in AEC, when the kVp increased, the CNR and SNR decreased because high kVp produces more penetrating x-ray beam and increased the scatter radiation; the image quality (CNR and SNR) was decreased. Low kVp is suitable in mammography. The low kVp for W/Rh at 40 to 60 mm CBT ranged from 27 to 30, CNR ranges from 20.43 to 25.47, SNR range from 42.5 to 48.69. Low kVp for W/Ag at 70 mm CBT ranged from 30 to 35, CNR ranges from 25.35 to 28.44, and SNR ranges from 54.45 to 56.45. At the same kVp and mAs of the W/Ag target filter, CNR and SNR in 70 mm CBT were higher than 60 mm CBT. According to the recommendation by Hologic Selenia Dimension suggest that W/Rh changed to W/Ag at 70 mm CBT.

In all CBT, the increasing mAs results in increasing CNR and SNR. The mAs is significantly affected the image quality, CNR and SNR.

#### 5.1.1.2 The average glandular dose in phantom study

The AGD increased when increasing the CBT (Table 4.1 to 4.4). The W/Rh target-filter should be used at the compressed breast range from 40 to 60 mm by using the low kVp range from 27 to 30 and mAs range from 58 to 356, the AGD range from 0.82 to 2.64 mGy. The W/Ag target-filter should be used at 70 mm CBT and over with the tube voltage ranged from 30 to 35 with using the mAs ranged from 99 to 206, the AGD ranges from 2.3 to 2.97 mGy.

The American College of Radiology (ACR) has established the diagnostic reference level of 3 mGy with grid as a mean glandular dose for breasts phantom with a thickness of 4.2 cm with a 50 % glandular composition [19]. In our study, the optimal mAs ranged from 58 to 356 for W/Rh and 99 to 206 for W/Ag in order to optimize the average glandular dose at less than 3 mGy [19]

#### 5.1.2 The patient study:

##### 5.1.2.1 The compressed breast thickness

The mean CBT of W/Rh target-filter in CC view was 54.2 mm and for the W/Ag was 81 mm, which were higher than those reported by T. Olgar et al [12] of 52.9 mm for W/Rh and 71 mm for W/Ag. The compression force reported by IAEA [18] was between 15.6 and 30 lbs., while our study was between 3.2 lbs. (lower than IAEA recommendation) and 38 lbs. (higher than IAEA recommendation).

##### 5.1.2.2 The average glandular dose

The result in table 4.5 and 4.6 shows the mean AGD of W/Rh was 1.26 mGy and CBT was 54.2 mm for CC view. The mean AGD of W/Ag was 1.79 mGy and the CBT was 81 mm for CC view. Those values are closely as reported by T. Olgar et al [12] of AGD was 1.76 mGy and CBT was 52.9 mm for W/Rh. For W/Ag, the AGD was 2.59 mGy and CBT was 71mm for W/Ag. The American College of Radiology (ACR) has established the DRL of 3 mGy with grid as a mean glandular dose for

breasts phantom with a thickness of 4.2 cm with a 50 % glandular composition [19]. In our study, there are 2.5% of the patients received the dose over the DRL [19]. DRL of 2.5 mGy per exposure for a standard breast with a breast thickness of 53 mm is recommended in the European protocol [20].

### 5.1.2.3 The technique factors

In our study, the kVp setting ranged from 25 to 32 for W/Rh target-filter and 30 to 38 for W/Ag target-filter. Those values are closely as reported by T. Olgar et al [12] of kVp setting ranged from 25 to 32 for W/Rh and 30 to 34 for W/Ag. The tube voltage increases with increasing compressed breast thickness and with increasing glandular content [14]. The higher kVp setting from 30 to 38 of W/Ag target-filter with the lower kVp from 25 to 32 with AEC technique for W/Rh target-filter indicates that a dose reduction due to the kVp setting.

From figure 4.13 and 4.26, there is a strong correlation between the AGD and mAs with  $R^2 = 0.98$  and  $R^2 = 0.89$  in W/Rh and W/Ag target-filter. The mAs is significant affect the AGD. The digital mammography system with auto filter and AEC the radiation dose would be adjusted, based on the patient breast thickness and compression force.

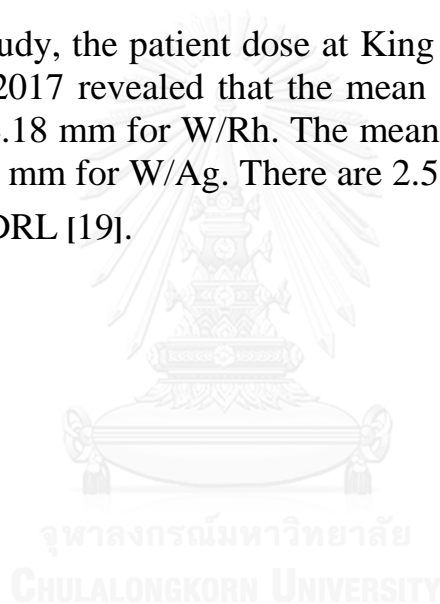
### 5.1.3 The optimization of the dose and image quality;

The objective of the optimization is to establish standardized imaging protocols by determining the optimal trade-off between image quality and dose, which is especially important for screening mammography given the lifetime risk to women who undergo annual mammography examinations. In this study, the radiation dose to the breast does not only depend on kVp but also on mAs and the anode/ filter combination. Therefore, the optimal kVp specific for each breast thickness should be identified in order to minimize the dose. The optimal kVp and mAs for W/Rh range from 27 to 30 and mAs ranges from 58 to 356, the AGD range from 0.82 to 2.64 mGy, the CNR ranges from 20.43 to 25.47 and SNR range from 42.5 to 48.69. The optimal kVp and mAs for W/Ag range from 30 to 35 and mAs ranges from 99 to 206, the AGD ranges from 2.3 to 2.97 mGy, the CNR ranges from 25.45 to 28.44 and SNR ranges from 54.45 to 56.45. When the AGD increased, CNR increases; therefore, the kVp, target-filter, and compression force should be optimized with the low dose as possible obtained with compromising the image quality.

## 5.2 Conclusion

In phantom study, the optimal kVp and mAs for W/Rh range from 27 to 30 and 58 to 356, the AGD range from 0.82 to 2.64 mGy, the CNR range from 20.43 to 25.47 and SNR ranges from 42.5 to 48.69. The optimal kVp for W/Ag ranges from 30 to 35 and mAs ranges from 99 to 206, the AGD ranges from 2.3 to 2.97 mGy, the CNR ranges from 25.45 to 28.44 and SNR ranges from 54.45 to 56.45. For compress breast thickness range from 40 to 60 mm, the W/Rh target-filter should be chosen and the compressed breast thickness greater than 70 mm, the W/Ag target-filter is appropriate in order to optimize image quality and dose.

In patient study, the patient dose at King Chulalongkorn Memorial Hospital in 2016-2017 revealed that the mean AGD was 1.26 mGy, the mean CBT was 54.18 mm for W/Rh. The mean AGD was 1.79 mGy, the mean CBT was 81 mm for W/Ag. There are 2.5% of the patients received the dose over the DRL [19].



### 5.3 Limitations.

The ACR phantom is composed of 50% adipose and 50% glandular tissue compressed to thickness of 4.2 cm. It consists of 6 fibrils, 5 speck groups of simulated micro-calcifications and 6 masses. The BR12 phantom is composed of 50% adipose and 50% glandular tissue compressed to thickness of 1 and 2 cm. The tissue equivalents of both phantoms are not the same. This is incompatible to the patients with different breast composition and the AGD per woman is associated with the glandular content.



**APPENDICES**





## APPENDIX A

### THE TECHNIQUE TABLE RECOMMENDED BY HOLOGIC SELINIA DIMENSION

In auto filter mode, the system automatically selects all the technique factors. The system automatically sets the kVp using the technique table based on the compressed breast thickness. The clinical range of breast thickness was shown in table I for large focal spot size. The clinical range of breast thickness was shown in table II for small focal spot size.

**Table 1A** The parameter of Hologic selenia dimension recommended technique table for large focal spot (LFS) [14]

CBT (cm)	Fatty breast			Normal breast			Dense breast		
	kVp	mAs	Filter	kVp	mAs	Filter	kVp	mAs	Filter
1	25	25	Rh	25	30	Rh	25	35	Rh
2	25	50	Rh	25	58	Rh	25	65	Rh
3	26	72	Rh	26	84	Rh	26	95	Rh
4	28	92	Rh	28	106	Rh	28	120	Rh
5	29	128	Rh	29	152	Rh	29	176	Rh
6	31	171	Rh	31	194	Rh	31	216	Rh
7	30	131	Ag	30	147	Ag	30	163	Ag
8	32	143	Ag	32	163	Ag	32	182	Ag
9	34	156	Ag	34	176	Ag	34	195	Ag
10	36	156	Ag	36	174	Ag	36	192	Ag
11	37	190	Ag	37	205	Ag	37	220	Ag
12	39	170	Ag	39	185	Ag	39	200	Ag
13	39	235	Ag	39	253	Ag	39	270	Ag
14	39	310	Ag	39	335	Ag	39	360	Ag
15	39	360	Ag	39	360	Ag	39	360	Ag

**Table 2A** The parameter of Hologic selenia dimension recommended technique table for small focal spot (SFS) [14]

CBT (cm)	Fatty breast			Normal breast			Dense breast		
	kVp	mAs	Filter	kVp	mAs	Filter	kVp	mAs	Filter
1	25	32	Rh	25	36	Rh	25	40	Rh
2	25	54	Rh	25	63	Rh	25	72	Rh
3	27	66	Rh	27	77	Rh	27	88	Rh
4	29	86	Rh	29	100	Rh	29	113	Rh
5	31	103	Rh	31	118	Rh	31	133	Rh
6	31	86	Ag	31	99	Ag	31	111	Ag
7	33	94	Ag	33	106	Ag	33	117	Ag
8	35	104	Ag	35	117	Ag	35	130	Ag
9	37	105	Ag	37	118	Ag	37	131	Ag
10	39	100	Ag	39	113	Ag	39	126	Ag
11	39	150	Ag	39	150	Ag	39	150	Ag
12	39	150	Ag	39	150	Ag	39	150	Ag
13	39	150	Ag	39	150	Ag	39	150	Ag
14	39	150	Ag	39	150	Ag	39	150	Ag
15	39	150	Ag	39	150	Ag	39	150	Ag

**Table 3A** g-factors (mGy/mGy) for breast thicknesses of 2-11 cm and the HVL range 0.30- 0.60 mm Al. The g-factors for breast thicknesses of 2-8 cm [1]

Breast thickness (cm)	g-factor(mGy/mGy)						
	HVL (mmAl)						
	0.30	0.35	0.4	0.45	0.50	0.55	0.60
2	0.390	0.433	0.473	0.509	0.543	0.573	0.587
3	0.274	0.309	0.342	0.374	0.406	0.437	0.466
4	0.207	0.235	0.261	0.289	0.318	0.346	0.374
4.5	0.183	0.208	0.232	0.258	0.285	0.311	0.339
5	0.164	0.187	0.209	0.232	0.258	0.287	0.31
6	0.135	0.154	0.172	0.192	0.214	0.236	0.261
7	0.114	0.130	0.145	0.163	0.177	0.202	0.224
8	0.098	0.112	0.126	0.14	0.154	0.175	0.195
9	0.0859	0.0981	0.1106	0.1233	0.1357	0.1543	0.1723
10	0.0763	0.0873	0.0986	0.1096	0.1207	0.1375	0.1540
11	0.0687	0.0786	0.0887	0.0988	0.1088	0.124	0.1385

**Table 4A** c-factors for average breasts for women in age group 50 to 64 [1]

Breast thickness (cm)	g-factor(mGy/mGy)						
	HVL (mmAl)						
	0.30	0.35	0.4	0.45	0.50	0.55	0.60
2	0.885	0.891	0.900	0.905	0.910	0.914	0.919
3	0.925	0.929	0.931	0.933	0.937	0.94	0.941
4	1.00	1.00	1.00	1.00	1.00	1.00	1.00
5	1.086	1.082	1.081	1.078	1.075	1.071	1.069
6	1.164	1.160	1.151	1.150	1.144	1.139	1.134
7	1.232	1.225	1.214	1.208	1.204	1.196	1.188
8	1.275	1.265	1.257	1.254	1.247	1.237	1.227
9	1.299	1.292	1.282	1.275	1.27	1.260	1.249
10	1.307	1.298	1.290	1.286	1.283	1.272	1.261
11	1.306	1.301	1.294	1.291	1.283	1.274	1.266

**Table 5A** c-factors for average breasts for women in age group 40 to 49  
[1]

Breast thickness (cm)	g-factor(mGy/mGy) HVL (mmAl)						
	0.30	0.35	0.4	0.45	0.50	0.55	0.60
2	0.885	0.891	0.900	0.905	0.910	0.914	0.919
3	0.894	0.898	0.903	0.906	0.911	0.915	0.918
4	0.940	0.943	0.945	0.947	0.948	0.952	0.955
5	1.05	1.005	1.005	1.004	1.004	1.004	1.004
6	1.08	1.078	1.074	1.074	1.071	1.068	1.006
7	1.152	1.147	1.141	1.138	1.135	1.130	1.127
8	1.220	1.213	1.206	1.205	1.199	1.190	1.183
9	1.270	1.264	1.254	1.248	1.244	1.235	1.225
10	1.295	1.287	1.279	1.275	1.272	1.262	1.251
11	1.294	1.290	1.283	1.281	1.273	1.264	1.256



**APPENDIX B  
CASE RECORD FORM**

<b>Tungsten-Rhodium filter</b>								
Centre/room					Equipment			
Procedure								
Data Record								
Patient no	View	AGD	kVp	mAs	ESAK	AGD	CBT	CF
	RCC							
	LCC							
	RMLO							
	LMLO							

<b>Tungsten-Silver filter</b>								
Centre/room					Equipment			
Procedure								
Data Record								
Patient no	View	AGD	kVp	mAs	ESAK	AGD	CBT	CF
	RCC							
	LCC							
	RMLO							
	LMLO							

## APPENDIX C

### QUALITY CONTROL OF MAMMOGRAPHY SYSTEM

#### 1. Mammographic Unit Assembly Evaluation

##### Objective

To ensure good and safe working conditions of all interlocks, mechanical detents and safety switches, and to ensure mechanical integrity of the x-ray tube and digital image receptor assembly.

##### Frequency

Annually

##### Test Procedure

- Perform this test in the same manner as described in the 1999 ACR Mammography Quality Control Manual, “Mammographic Unit Assembly Evaluation” section.
- Select Admin > QC > Physicist tab > Mammography Unit Assembly Evaluation procedure on the Acquisition Workstation.
- Select the Mark Completed button to label the status of this procedure as finished. Select the Yes button to mark the Quality Control procedure as completed.

**Mammography Unit Assembly Evaluation**  
**Table I** The mammographic unit assembly evaluated

	Pass/Fail/NA
1. Free-standing unit is mechanically stable	Pass
2. All moving parts move smoothly, without obstruction to motion	Pass
3. All locks and detents work properly	Pass
4. Image receptor holder assembly is free from vibrations	Pass
5. Image receptor slides smoothly into holder assembly	Pass
6. Image receptor is held securely by assembly in any orientation	Pass
7. Compressed breast thickness scale accurate to $\pm 0.5$ cm, reproducible $\pm 2$ mm	Pass
8. Patient or operator is not exposed to sharp or rough edges, or other hazards	Pass
9. Operator technique control charts are posted	Pass
10. Operator protected during exposure by adequate radiation shielding	Pass
11. All indicator lights working properly	Pass
12. Auto decompression can be overridden to maintain compression (status displayed)	Pass
13. Manual emergency compression release can be activated in the event of power failure	Pass

### Conclusion

All results of mammographic unit assembly evaluation are within recommended performance criteria. The result of the compressed breast thickness scale and compression force is within the control limits.

## 2. Collimator assessment

**Objective** To assure that:

- The x-ray field coincides with the light field
- The x-ray field is aligned with the image receptor
- The chest wall edge of the screening compression paddles is aligned with the chest wall edge of the digital image receptor

**Frequency** Annually

### Suggested Equipment

- X-ray recording media
- 24 × 29 cm compression paddle
- 8 × 24 cm compression paddle
- Small Breast compression paddle
- Four small attenuators, i.e., coins of one size

### Test Procedure

- Select Admin > Quality Control > Physicist tab > Collimation Assessment on the Acquisition Workstation. Select the Start button.
- Install the 24 × 29 cm compression paddle in the compression device to activate the x-ray tube collimation system.
- Raise the compression paddle to about 15 cm as indicated by the thickness display on the compression device.
- Turn the collimator light on and place the x-ray recording media on top of the image receptor to cross the four sides of the light field. Make sure that the x-ray recording media extend beyond the digital image receptor enclosure at the chest wall.

## Results

Deviation between X-ray field and light field:		
Anode material	W/Rh	W/Rh
Collimator size (cm)	18x24	24x30
Left edge deviation	0.64	0.03
Right edge deviation	0	-0.47
Sum of right and left edge deviations	0.55	-0.44
Sum as % of SID	0.83	-0.67
Anterior edge deviation	0.5	0
Chest edge deviation	0	0.14
Sum of anterior & chest edge deviations	1.15	0.14
Sum as % of SID		

Action limit: If the sum of the left plus right edge deviations or anterior plus chest edge deviation exceeds 2% of SID, seek service adjustment

### Deviation between X-ray field & edges of the image receptor:

Left edge deviation	0.64
% of SID (retain sign)	0.97
Right edge deviation	0
% of SID (retain sign)	0
Anterior edge deviation	0.5
% of SID (retain sign)	0.76
Chest edge deviation	0
% of SID (retain sign)	0

Action limit: If x-ray field exceeds image receptor at any side by more than +2% SID or if x-ray field falls within image receptor by more than -2% on the left and right sides, by more than -4% on the anterior side or at all on the chest wall side, seek service department

## Conclusion

The sum of the left plus right edge deviations and anterior plus chest edge deviations are within 2% of SID. The x-ray field does not exceed image receptor at any side by less than 2% of SID. The chest wall edge of compression paddle is within the image receptor.



### **3. Artifact evaluation**

#### **Objective**

To assess the degree and source of artifacts visualized in mammograms or phantom images. This procedure allows the source of artifacts to be isolated to x-ray equipment, or DICOM printer.

**Frequency** Annually

#### **Suggested Equipment**

- Magnification stand.
- Flat Field phantom, 4 cm thick uniform attenuation block of acrylic large enough to cover the digital image receptor. The Flat Field phantom is supplied by the manufacturer.

#### **Regulatory action levels and corrective action**

Artifacts that may interfere with image interpretation must be eliminated before performing clinical imaging

Consult with a radiologist for assistance in evaluating whether artifacts may interfere with image interpretation. A qualified service engineer must eliminate any digital detector artifacts that may be clinically objectionable. The acrylic attenuation block provided by manufacturer and used for detector calibration replaced if it has permanent artifacts that may impact detector calibration.

The recommendations and corrective actions listed in the 1999 ACR Mammography Quality Control Manual should be followed for laser printer and film processor artifacts.

## Result

Type of attenuator:	Acrylic
Thickness of attenuator:	4.0 cm
kVp setting:	28
Density control setting:	N

Image receptor size	18x24	24x30
Cassette #		
Anode	W	W
Filter	Rh	Rh
Focal spot	Large	Large
Emulsion orientation	UP	UP
Resultant film density	-	-
Artifacts visible?	-	-
Processor?		
Acceptable?	Yes	Yes
Describe		
Cassette film screen?	-	-
Acceptable?		
Describe	Yes	Yes
X-ray equipment?		
Acceptable?		
Describe	-	-

จุฬาลงกรณ์มหาวิทยาลัย  
CHULALONGKORN UNIVERSITY

Type of attenuator:	Acrylic
Thickness of attenuator:	4.0 cm
kVp setting:	28
Density control setting:	N

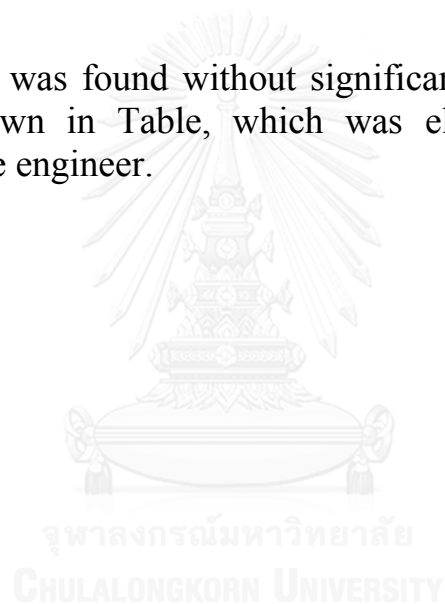
Image receptor size	18x24	24x30
Cassette #		
Anode	W	W
Filter	Ag	Ag
Focal spot	Large	Large
Emulsion orientation	UP	UP
Resultant film density	-	-
Artifacts visible?	-	-
Processor?	-	-
Acceptable?	Yes	Yes
Describe		

Cassette film screen?	-	-
Acceptable?	Yes	Yes
Describe	-	-
X-ray equipment?	-	-
Acceptable?	Yes	Yes
Describe	-	-

---

## Conclusion

The artifact was found without significant artifacts visible. Detail of artifact is shown in Table, which was eliminated before clinical imaging by service engineer.



#### 4. kVp Accuracy/Reproducibility

**Objective** To assure that the selected kVp is accurate within limits and reproducible between exposures.

**Frequency** Annually

##### Suggested Equipment

- Calibrated, non-invasive mammographic kVp meter as per the 1999 ACR Mammography Quality Control Manual, “kVp Accuracy and Reproducibility” section; or invasive kVp divider or similar equipment (see note).
- 0.5 mm or thicker lead or lead equivalent block, wide enough to cover the entire surface of the digital image receptor.

##### Results

Nominal kVp setting	25	26	27	28	29	30
Nominal focal spot size	0.3	0.3	0.3	0.3	0.3	0.3
Target filter combination	W/Rh	W/Rh	W/Rh	W/Rh	W/Rh	W/Rh
Exposure time						
mAs setting	30	30	30	30	30	30
Measured kVp values:						
kVp1	25.94	26.64	27.64	28.84	30.04	31.07
kVp2	26	26.92	27.73	28.89	29.92	31.09
kVp3	25.87	26.61	27.65	28.81	29.99	31.15
kVp4	25.77	26.71	27.66	28.85	29.98	31.12
Mean kVp <kVp>	29.9	26.72	27.66	28.85	29.98	31.12
Standard Deviation	0.09	0.12	0.04	0.03	0.04	0.04
<kVp> - Nominal kVp	0.9	0.72	0.66	0.85	0.98	1.12
0.05 x Nominal kVp	1.25	1.30	1.35	1.40	1.45	1.50
kVp Coefficient of Variation	0.003	0.005	0.001	0.001	0.001	0.001
Exposure in mR						
mR1	3.06	2.81	2.66	2.32	2.2	2.5
mR2	3.01	2.87	2.64	2.36	2.2	2.5
mR3	3.02	2.84	2.63	2.37	2.2	2.5
mR4	3.05	2.84	2.27	2.35	2.2	2.5
Mean Exposure	3.04	2.84	2.55	2.35	2.19	2.50
Standard Deviation	0.022	0.022	0.162	0.020	0.020	0.003
mR Coefficient of Variation	0.007	0.008	0.064	0.008	0.009	0.001

##### Conclusion

The kVp is accurate within limits and reproducible between exposures. The mean kVp differs from the nominal of various kVp of less than  $\pm 5\%$  of nominal kVp. The kVp coefficient of variation is less than 0.02 for all kVp settings.

## 5. Beam quality assessment (Half value layer measurement)

**Objective** To assure that the half-value layer (HVL) of the x-ray beam is adequate to minimize patient dose.

**Frequency** Annually

### Suggested Equipment

- Calibrated mammographic ionization meter and electrometer as per the 1999 ACR Mammography Quality Control Manual, “Beam Quality Assessment” section
- Six to seven aluminum 1145 or 1100 alloy sheets of 0.1 mm thickness as per the 1999 ACR Mammography Quality Control Manual, “Beam Quality Assessment” section
- 0.5 mm or thicker lead or lead equivalent block, wide enough to cover the entire surface of the digital image receptor

### Results

Nominal kVp Setting:	25	26	27	28	29	30
Target/Filter	W/Rh	W/Rh	W/Rh	W/Rh	W/Rh	W/Rh
mAs Setting	30	30	30	30	30	30
<b>Exposure Measurements:</b>						
No Aluminum Filtration, E <sub>0</sub>	308.7	358.9	406.6	454.7	506.1	559.2
0.2 mm of added Aluminum, E <sub>2</sub>	197.8	229.9	262.9	298.2	335.7	375
0.3 mm of added Aluminum, E <sub>3</sub>	160.6	187.4	215.8	245.9	277.9	311.5
0.4 mm of added Aluminum, E <sub>4</sub>	132.5	155	180	206.4	233.1	261.9
(E <sub>0</sub> /2) Value	154.35	179.45	203.3	227.35	253.05	279.6
Record thickness (t <sub>a</sub> <t <sub>b</sub> )	t <sub>a</sub>	t <sub>b</sub>	t <sub>a</sub>	t <sub>b</sub>	t <sub>a</sub>	t <sub>b</sub>
and exposures	0.4	0.4	0.4	0.4	0.4	0.4
that bracket E <sub>0</sub> /2: (E <sub>a</sub> >E <sub>b</sub> )	E <sub>a</sub>	E <sub>b</sub>	E <sub>a</sub>	E <sub>b</sub>	E <sub>a</sub>	E <sub>b</sub>
	0.5	0.5	0.5	0.5	0.5	0.5
Calculated HVL:	0.322	0.325	0.355	0.347	0.355	0.364

### Conclusion

The test result is within the control limits for various kVp and the both W/Rh and W/Ag target filter combination.

## 6. Evaluation of system resolution

**Objective** To evaluate imaging performance, using the system limiting spatial resolution as a performance indicator that may be easily measured in the field.

**Frequency** Annually

### Suggested Equipment

- 18 x 24 cm compression paddle
- High contrast resolution pattern providing a test up to 15 cycle/mm (c/mm, or lp/mm) with 1 c/mm steps in the range 3 – 15 c/mm
- Flat Field phantom

### Results

<b>Nominal focal spot size ( mm )</b>	0.3	0.1
<b>Anode material</b>	W	W
<b>Density control setting</b>	N	N
<b>Limiting resolution in lines-pairs /mm</b>	>7 lp/mm	>7 lp/mm
<b>Bars parallel to A-C axis</b>	14 lp/mm	14 lp/mm
<b>Bars perpendicular to A-C axis</b>	14 lp/mm	14 lp/mm

### Conclusion

The test result was found within the control limits for the anode-cathode and perpendicular axis.

## **7. Breast entrance exposure and average glandular dose (AGD)**

**Objective** To measure the typical entrance exposure and calculate the corresponding glandular dose for an average patient with approximately 4.2 cm compressed breast thickness of 50% adipose, 50% glandular tissue composition, to assess the reproducibility of the automatic exposure control (AEC).

**Frequency** Annually

### **Suggested Equipment**

- 24 x 29 cm compression paddle
- Calibrated mammographic ionization meter and electrometer as per the 1999 ACR Mammography Quality Control Manual, “Breast Entrance Exposure, AEC Reproducibility, Average Glandular Dose, and Radiation Output Rate” section.
- ACR Mammographic Accreditation Phantom (i.e., RMI 156 by Radiation Measurement, Inc.; 18-220 by Nuclear Associates).

## Results

<b>Dosimetry System used:</b>	<b>Victoreen 4000 M</b>		<b>Energy Correction</b>			
<b>Image Receptor:</b>	<b>Film</b>		<b>Factor:</b>	<b>1.00</b>		
<b>Field Restriction:</b>	<b>18x24</b>					
<b>SID (cm):</b>						
<b>Phantom:</b>	<b>ACR/RMI</b>		<b>mR/mAs</b>			
<b>Nominal kVp Setting:</b>	x					
<b>Target/Filtration:</b>						
<b>AEC density control setting:</b>						
<b>mA setting:</b>	66		76		88	
<b>Measured HVL (mm Al):</b>	0.53		0.53		0.53	
<b>Measured Entrance Exposure</b>	<b>R</b>	<b>mAs</b>	<b>R</b>	<b>mAs</b>	<b>R</b>	<b>mAs</b>
<b>Exposure #1</b>	2.1050	66.0	2.4620	76.0	2.8400	88.0
<b>Exposure #2</b>	2.1120	66.0	2.5050	78.0	2.8600	88.0
<b>Exposure #3</b>	2.0960	66.0	2.4660	77.0	2.8640	88.0
<b>Exposure #4</b>	2.1360	67.0	2.5320	78.0	2.9150	89.0
<b>Mean Values</b>						
	2.112	66.2500	2.4913	77.250	2.8698	88.250
<b>Standard Deviations (SD)</b>						
	0.017	0.500	0.033	0.957	0.032	0.500
<b>Coefficients of Variation (CV)</b>						
	0.008	0.008	0.013	0.012	0.011	0.006
<b>Energy-Corrected Exposure:</b>	2.112		2.491		2.870	
<b>Dose conversion factor from table 1-3 (mrad/R):</b>						
<b>Computed average glandular dose (mrad):</b>						

## Conclusion

The test result is within the control limits, the glandular dose was mGy. The coefficient of variation for air kerma does not exceed 0.05.



## 8. Phantom Image Quality Evaluation

**Objective** To assess the quality and consistency of the mammographic image.

**Frequency** Annually

### Suggested Equipment

- 18 x 24 cm compression paddle.
- ACR Mammographic Accreditation Phantom (i.e., RMI 156 by Radiation Measurement, Inc.; 18-220 by Nuclear Associates).
- Acrylic disc, 4.0 mm thick with 1.0 cm diameter, placed on the top of the ACR Mammographic Accreditation Phantom as per the 1999 ACR Mammography Quality Control Manual, “Image Quality Evaluation” section. The ACR mammographic accreditation phantom is used for digital breast tomosynthesis image quality evaluation since it is readily available to medical physicists and radiologic technologists, and to ensure consistent image performance in tomosynthesis imaging over time.

### Results

Date	Fibers	Speck Group	Masses
5/Dec/16	4.5	3.5	4.5
14/Dec/16	5.5	3.5	4.5
22/Dec/16	6	3.5	4.5
26/Dec/16	6	4	4.5
29/Dec/16	6	4	4.5
3/Jan/17	6	3.5	4.5
6/Jan/17	6	3.5	4.5
20/Jan/17	6	3.5	4.5
<b>Mean</b>	<b>5.8</b>	<b>3.6</b>	<b>4.5</b>

### Conclusion

All result recorded from phantom score on print film, SCW and AWS as shown on above table. The numbers of fiber and masses were found within the recommended criteria of the phantom score on diagnostic devices.

## 9. Signal to noise and contrast to noise measurement

**Objective** To assure consistency of the digital image receptor by evaluating the signal-to-noise ratio (SNR) and contrast-to-noise ratio (CNR) of the image receptor.

**Frequency** Annually

### Suggested Equipment

- 18 x 24 cm compression paddle.
- ACR Mammographic Accreditation Phantom (i.e., RMI 156 by Radiation Measurement, Inc.; 18-220 by Nuclear Associates).
- Acrylic disc, 4.0 mm thick with 1.0 cm diameter, placed on the top of the ACR Mammographic Accreditation Phantom as per the 1999 ACR Mammography Quality Control Manual, “Phantom Images” section.

### Data Analysis and Interpretation

The SNR shall be computed using the mean and standard deviation obtained from the ROI next to the acrylic disk.

1. Computed the SNR of the detector according to

$$\text{SNR} = \frac{\text{Mean}_{\text{background}} - \text{DC}_{\text{offset}}}{\text{STD}_{\text{background}}}$$

Where  $\text{Mean}_{\text{background}}$  and  $\text{STD}_{\text{background}}$  are the mean and standard deviation obtained from the ROI Statistics dialog for the ROI next to the acrylic disk and  $\text{DC}_{\text{offset}}$  is a DC offset added to the detector signal and is equal to 50.

2. Compute the CNR of detector according to

$$\text{CNR} = \frac{\text{Mean}_{\text{background}} - \text{Mean}_{\text{disk}}}{\text{STD}_{\text{background}}}$$

Where  $\text{Mean}_{\text{disk}}$  is the mean value obtained from the ROI statistics dialog for ROI on the acrylic disk.

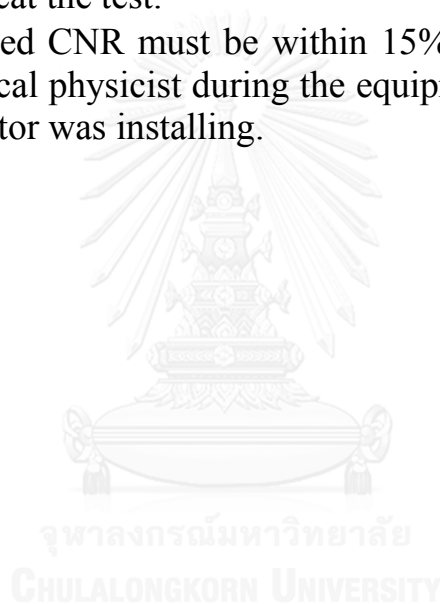
3. Compute the deviation from original CNR measurement according to

$$\text{Diff} = \frac{\text{CNR}_{\text{base}} - \text{CNR}_{\text{measured}}}{\text{CNR}_{\text{base}}} \times 100$$

Where  $\text{CNR}_{\text{base}}$  is the  $\text{CNR}_{\text{base}}$  value established by medical physicist during acceptance testing of digital image detector;  $\text{CNR}_{\text{measured}}$  is new CNR computer in step 2.

Recommended performance criteria and corrective action

- The measured SNR must be equal to or greater than 40. If it is less than 40, repeat the test.
- The computed CNR must be within 15% of the value determined by the medical physicist during the equipment evaluation when the image receptor was installing.



## Results

Date	Mean Value Inside disk	Mean Value Beside disk	Standard Dev. Beside disk	SNR
5/Dec/16	350.3	433.8	8.4	45.7
14/Dec/16	360.7	440.6	8.7	44.9
22/Dec/16	351	431.3	8.6	44.3
26/Dec/16	357.4	445.5	8.6	46
29/Dec/16	354.5	439.6	8.6	45.3
3/Jan/17	365.8	452.3	8.6	46.8
6/Jan/17	361.3	444.9	8.7	45.4
20/Jan/17	367.4	454.9	8.6	47.8
29/Jan/17	365.4	454.6	8.9	45.5

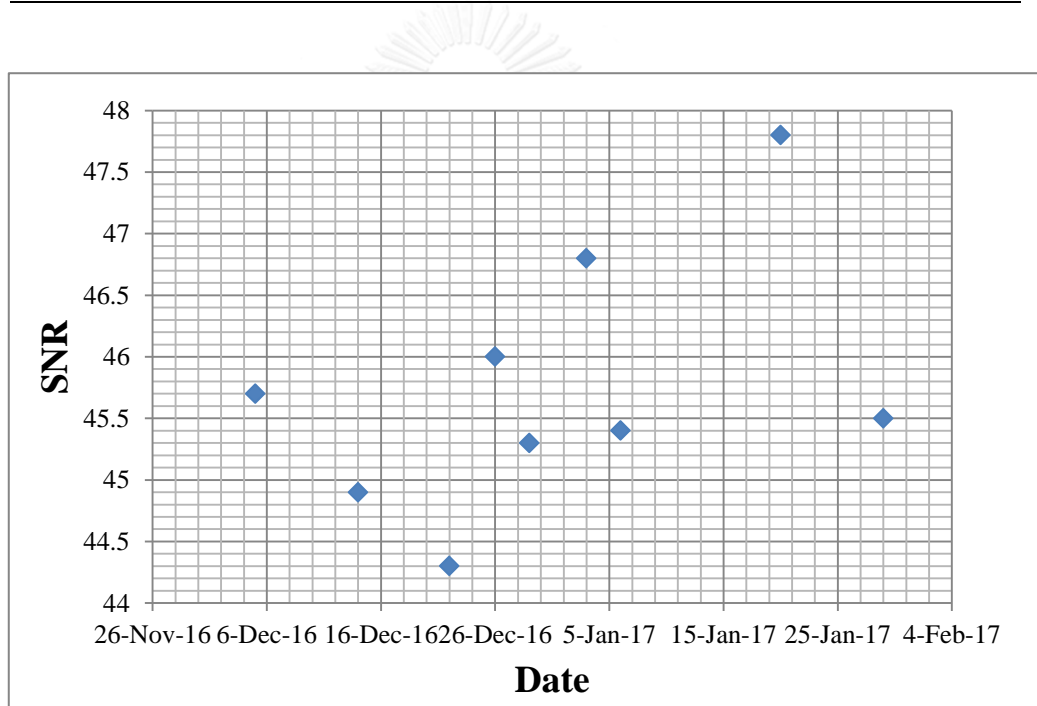


**Figure 1C** SNR control charge 2016-2017

Date	Mean Value Inside disk	Mean Value Beside disk	Standard Dev. Beside disk	CNR	%Diff
5/Dec/16	350.3	433.8	8.4	45.7	-
14/Dec/16	360.7	440.6	8.7	44.9	+7.10
22/Dec/16	351	431.3	8.6	44.3	+5.96
26/Dec/16	357.4	445.5	8.6	46	-3.53
29/Dec/16	354.5	439.6	8.6	45.3	+0.1
3/Jan/17	365.8	452.3	8.6	46.8	-1.61
6/Jan/17	361.3	444.9	8.7	45.4	+2.93
20/Jan/17	367.4	454.9	8.6	47.8	-2.83
29/Jan/17	365.4	454.6	8.9	45.5	-1.31

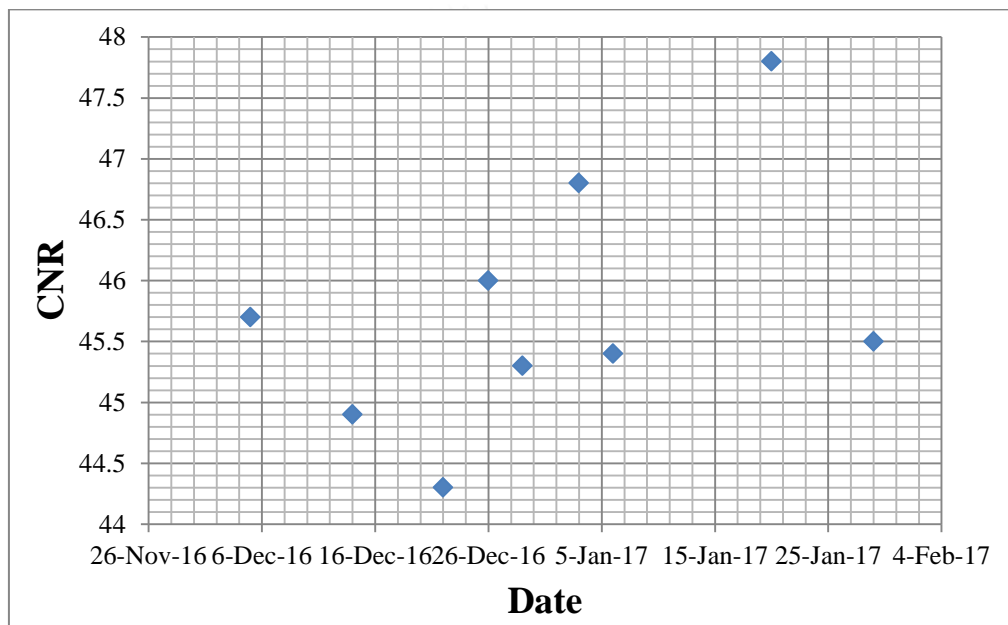


**Figure 2C** CNR control charge 2016-2017

## Conclusion

All result recorded from signal to noise measurement as shown in above table, signal to noise and contrast to noise value are within the recommended performance criteria. The signal to noise and contrast to noise values in 2017 are higher than 2016

## REFERENCES

1. Bushberg J, et al. The Essential Physics of Medical Imaging. 3<sup>rd</sup> ed. California. Lippincott Williams, 2012.
2. Ranger NT, et al. A technique optimization protocol and the potential for dose reduction in digital mammography. Med Phy 2010; 37:962-967.
3. Biegala M, et al. Effect of anode/filter combination on average glandular dose in mammography. Med Phy 2015; 40:45-51.
4. Hermann KP, et al. Average glandular dose with amorphous silicon full-field digital mammography-clinical results. Rofo 2002; 174:696-699.
5. Samei E, et al. To experimentally determine the relationship between radiation dose and observer accuracy in the detection and discrimination of simulated lesions for digital mammography, Radiology 2007; 243:396-404 .
6. Baldelli P, et al. Investigation of the effect of anode/filter materials on the dose and image quality of a digital mammography system based on an amorphous selenium flat panel detector. The British Journal of Radiology 2010; 83:290-295.
7. Emanuelli S, et al. Dosimetric and image quality comparison of two digital mammography units with different target/filter combinations: Mo/Mo, Mo/Rh, W/Rh, W/Ag. Radiol Med 2011; 116:310-318.
8. Dance DR , et al. Breast dosimetry, Applied radiation and isotopes: including data, instrumentation and methods for use in agriculture, industry and medicine. 1999; 50:185.
9. Tavakoli M.B, et al. Evaluation of the relation between breast glandular absorbed dose and radiographic quality in mammography. Iran J 2008; 6:77-82.

10. Izdihar K, et al. Determination of tube output (kVp) and exposure mode for breast phantom of various thickness/glandularity for digital mammography. Malays J 2016; 22:40-47.
11. Uhlenbrock D.F, et al. Comparison of anode/filter combination in digital mammography with respect to average glandular dose. Fortschr Rontgenstr 2009; 181:249-254.
12. Olgar T, et al. Average glandular dose in digital mammography and breast tomosynthesis. Fortschr Rontgenstr 2012; 184: 911-918.
13. Hologic Selenia Dimension. Quality Control Manual Selenia Dimensions 2D FFDM Selenia Dimensions DBT, 2011
14. Mc Gill University Department of Medicine. Mammography Tutorial, 2001.
15. Leed test object medical imaging phantom. Tissue Equivalent Materials, 2001.
16. Maidment AD, et al. A computer workstation for 3-D imaging of the breast. Radiology 1997; 205:741.
17. International Atomic Energy Agency, human health series no 17. Quality Assurance Program for digital mammography, 2011.
18. European Commission. European guidelines for quality assurance in breast cancer screening and diagnosis, 4<sup>th</sup> ed Luxembourg. Office for Official Publications of the European Communities, 2006.
19. American College of Radiology. Mammography Quality Control Manual Mammography Phantom Image Quality Evaluation, 1999.

**VITA**

Name: Chatsuda Songsaeng  
Date of birth: September 17, 1988  
Place of birth: Trang, Thailand  
Qualification: Bachelor of Science Faculty of Medical Technology  
(Radiological Technology) Mahidol University, 2011  
Job experience: Radiological Technologist, Bumrungrad International  
Hospital, mammography specialist for 3 years.

